AD-A207 612 ADVANCED CALCIUM-THIONYL CHLORIDE HIGH-POWER BATTERY (U) RAMAT-TEL-AVIV UNIV AUTHORITY FOR RESEARCH AND INDUSTRIAL DEV. E PELED 08 FEB 89 R/D-5899-CH-01 1/1

UNCLASSIFIED DAJA45-88-C-0012 F/G 10/3 NL

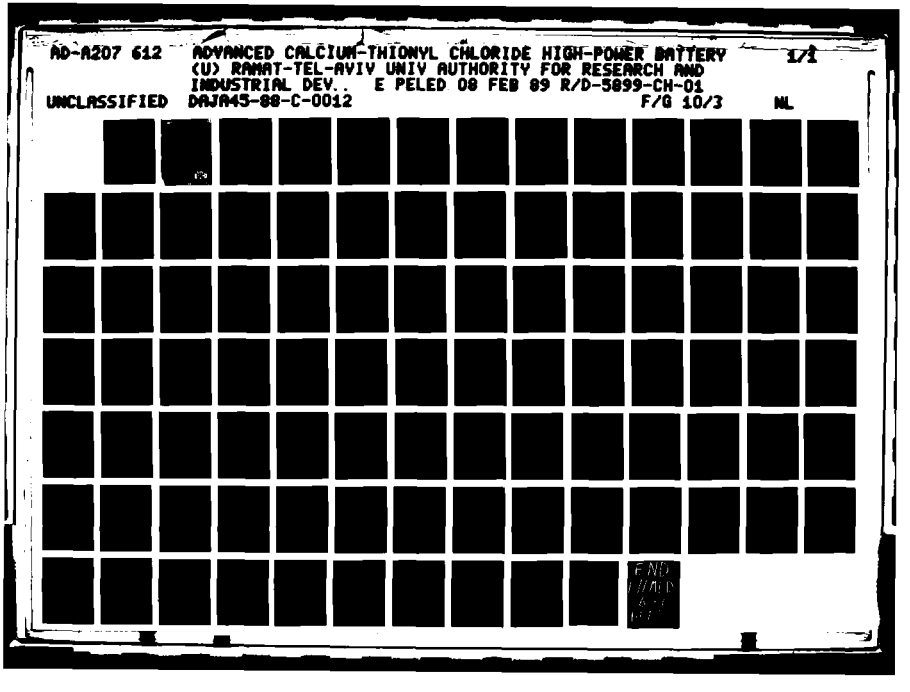

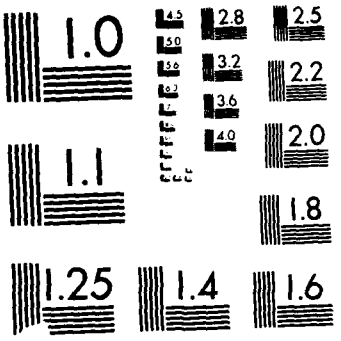

UTION TEST CHART

R/D 5899-C-4-01 (4)

ADVANCED CALCIUM-THIONYL CHLORIDE HIGH-POWER BATTERY

Final Technical Report

by

Prof. E. Peled

Final Report

(December 1987-December 1988)

United States Army

EUROPEAN RESEARCH OFFICE OF THE U.S. ARMY

London England

CONTRACT NUMBER DAJA45-88-C-0012

Ramot, Tel-Aviv University Authority for Research

and Industrial Development Ltd.

Approved for Public Release; distribution unlimited

The research reported in this document has been made possible through the support and sponsorship of the U.S. Government through its European Research Office of the U.S. Army. This report is intended only for the internal management use of the Contractor and the U.S. Government.

ADVANCED CALCIUM-THIONYL CHLORIDE HIGH-POWER BATTERY

Final Technical Report

by

Prof. E. Peled

Final Report

(December 1987-December 1988)

United States Army

EUROPEAN RESEARCH OFFICE OF THE U.S. ARMY

London England

CONTRACT NUMBER DAJA45-88-C-0012

Ramot, Tel-Aviv University Authority for Research

and Industrial Development Ltd.

The research reported in this document has been made possible through the support and sponsorship of the U.S. Government through its European Research Office of the U.S. Army. This report is intended only for the internal management use of the Contractor and the U.S. Government.

SECURITY CLASSIFICATION OF THIS PAGE

REPORT DOCUMENTATION PAGE

Form Approved OMB No. 0704-0188

1a. REPORT SECURITY CLASSIFICATION: Unclassified	1b. RESTRICTIVE MARKINGS
2a. SECURITY CLASSIFICATION AUTHORITY	3. DISTRIBUTION/AVAILABILITY OF REPORT: Approved for Public Release Distribution unlimited
2b. DECLASSIFICATION/DOWNGRADING SCHEDULE	
4. PERFORMING ORGANIZATION REPORT NUMBER(S)	5. MONITORING ORGANIZATION REPORT NUMBER(S)
6a. NAME OF PERFORMING ORGANIZATION: Ramot-TA Univ. Auth. for App. Res. and Ind. Dev. Ltd. / 6b. OFFICE SYMBOL (If applicable)	7a. NAME OF MONITORING ORGANIZATION
6c. ADDRESS (City, State, and ZIP Code): 32 University Street, Ramat Aviv, Tel-Aviv 61392, ISRAEL	7b. ADDRESS (City, State, and ZIP Code)
8a. NAME OF FUNDING/SPONSORING ORGANIZATION: U.S. Army European Research Office / 8b. OFFICE SYMBOL (If applicable)	9. PROCUREMENT INSTRUMENT IDENTIFICATION NUMBER: DAJA45-88-C-0012
8c. ADDRESS (City, State, and ZIP Code): 223/231 Old Marlebone Road London NW1 5th ENGLAND	10. SOURCE OF FUNDING NUMBERS — PROGRAM ELEMENT NO. / PROJECT NO. / TASK NO. / WORK UNIT ACCESSION NO.

11. TITLE (Include Security Classification): Advanced Calcium Thionyl Chloride High Power Battery

12. PERSONAL AUTHOR(S): Prof. Emanuel Peled

13a. TYPE OF REPORT	13b. TIME COVERED	14. DATE OF REPORT (Year, Month, Day)	15. PAGE COUNT
Final Report	FROM 87/12/23 TO 88/12/22	89/2/8	90

16. SUPPLEMENTARY NOTATION

17. COSATI CODES		
FIELD	GROUP	SUB-GROUP

18. SUBJECT TERMS (Continue on reverse if necessary and identify by block number): Calcium battery, thionyl chloride, conductivity. Viscosity Raman spectra, Strontium, Barium, shelf life, High Energy density battery.

19. ABSTRACT (Continue on reverse if necessary and identify by block number)

Calcium Thionyl Chloride Abstract

Recently we, at TAU, have made a breakthrough in the development of two advanced Ca-TC systems which have much better storage properties than the state-of-art Ca-$SOCl_2$ cell. This has been done by replacing the CaX_2 ($X=AlCl_4$) eslectrolyte by SrX_2 (type A), or BaX_2 type B. The project's goals are to gain a better understanding of the electrochemistry of the advanced systems and to establish their safety and performance.

(Cont'd on reverse side)

20. DISTRIBUTION/AVAILABILITY OF ABSTRACT	21. ABSTRACT SECURITY CLASSIFICATION
☒ UNCLASSIFIED/UNLIMITED ☐ SAME AS RPT. ☐ DTIC USERS	
22a. NAME OF RESPONSIBLE INDIVIDUAL	22b. TELEPHONE (Include Area Code) / 22c. OFFICE SYMBOL

This report contains four chapters. The calorimetric study of $Ca/Sr(AlCl_4)_2$-$SOCl_2$+7%(v/v)SO_2 C-size cells during constant-temperature discharge is reported in chapter 1. Fresh and stored (70°C for four weeks) cells were discharged inside a dedicated home-made calorimeter on two loads: 9.4Ω and 4Ω or at 30 and 55°C. The heat flow (W_T) of the cells (termal power) during discharge was measured as a function of discharge time. There was no significant difference between fresh and stored cells with respect to heat generation during discharge.

There was no loss in capacity during four weeks of storage at 70°C.

The following components of W_T were calculated and plotted against discharge capacity: W_S-thermodynamic; W_p-polarization; W_c-chemical. W_p was found to be the largest component of W_T. The maximum corrosion rate (I_c) of the calcium anode during discharge and its minimum Faradaic efficiency (ϵ) were calculated from W_c on the assumption that anodic corrosion is the major component of W_c. At 30°C, ϵ was about 0.9 while at 55° it drops from 0.87 at 2 $mAcm^{-2}$ to 0.84 at 4 $mAcm^{-2}$. At 30°C the value of ϵ, is similar to that of t_1 of the SEI of the calcium, indicating a similar corrosion mechanism for the calcium anode (both under OCV conditions and under load).

Chapter 2 presents a calorimetric study of the baseline cell $Ca/Ca(AlCl_4)_2$-$SOCl_2$ + 7% (V/V)SO_2. The thermal power generated by the Ca/CaX_2 cells is similar to that of the Ca/SrX_2 cells at 30°C. However at 55°C $I_{c,a}$ of the Ca/CaX_2 csells is much higher. As a result the faradaic efficiency of the Ca/CaX_2 cells is similar or lower than that of the Ca/SrX_2 cells.

Chapter 3 presents the performance, safety and storage properties of Ca/CaX_2 and Ca/SrX_2 cells.

The Ca/CaX_2 cell looses most of its capacity after 4 weewks of storage at 70°C. However, the Ca/SrX_2 cell looses only 0-15% of its capacity when discharged over the temperature range -30 to +60°C after being stored for 4 weeks at 70°C. Its voltage delay is 0-100 sec at -20 and -30°C after such storage. It has no voltage delay at room temperature and above. Cells equipped with glass separator and a vent may vent on forced discharge as a result of overheating. The Ca/SrX_2 cell may be made safe and vent-free with the use of a Tefzel separator.

Chapter 4 presents a summary of the results regarding the properties of MX_2-SO_2-TC solutions (M=Ca,Sr,Ba) including Raman spectra, viscosity and conductivity data. We explain the effect of SO_2 and temperature on the conductivity and conduction mechanism.

Table of Contents

CHAPTER 1

Calorimetric Study of the Calcium/$Sr(AlCl_4)_2$-$SOCl_2$ Battery

Abstract

The behavior of $Ca/Sr(AlCl_4)_2$-$SOCl_2$+7%(v/v)SO_2 C-size cells during constant-temperature discharge was studied. Fresh and stored (70°C for four weeks) cells were discharged inside a dedicated home-made calorimeter on two loads: 9.4Ω and 4Ω or at 30 and 55°C. The heat flow (W_T) of the cells (termal power) during discharge was measured as a function of discharge time. There was no significant difference between fresh and stored cells with respect to heat generation during discharge.

There was no loss in capacity during four weeks of storage at 70°C.

The following components of W_T were calculated and plotted against discharge capacity: W_S-thermodynamic; W_p-polarization; W_c-chemical. W_p was found to be the largest component of W_T. The maximum corrosion rate of the calcium anode during discharge and its minimum Faradaic efficiency (ϵ) were calculated from W_c on the assumption that anodic corrosion is the major component of W_c. At 30°C, ϵ was about 0.9 while at 55° it drops from 0.87 at 2 $mAcm^{-2}$ to 0.84 at 4 $mAcm^{-2}$. At 30°C the value of ϵ, is similar to that of t_i of the SEI of the calcium, indicating a similar corrosion mechanism for the calcium anode (both under OCV conditions and under load).

Introduction

The calcium-thionyl chloride battery has recently attracted attention as a safer alternative to high-power lithium batteries[1-15]. The major drawback of this system has been recently solved[10,14] by replacing the $Ca(AlCl_4)_2$ electrolyte by either $Ba(AlCl_4)_2$ or $Sr(AlCl_4)_2$.

The Ca-thionyl chloride (TC) cell is a SEI (solid electrolyte interphase) battery system[4,12]. The calcium anode is always covered by a thin solid electrolyte film, at least a couple of tens of angstroms thick. In most cases this SEI is part of a much thicker porous passivating layer (PL), the thickness of which may reach 50μ.

The morphology and the chemical composition of the PL vary with the electrolyte used, and with the history of both the calcium metal before cell assembly and of the cell[10,14]. The calcium metal as received is covered by an oxide layer up to 50μ thick depending on storage time and conditions. When it is stored in MX_2 (M=Ca,Sr,Ba, X=$AlCl_4$) TC solutions it is slowly converted into MCl_2. The rate of this conversion reaction depends on electrolyte type and on temperature. At room temperature it may take many months to get close to complete conversion while at 70°C storage it may take several weeks. The chemical composition of the PL of calcium stored in MX_2 solutions for long periods of time is: $CaCl_2$ in $Ca(AlCl_4)_2$ solutions; 1-20% $BaCl_2$+80-99% $CaCl_2$ in $Ba(AlCl_4)_2$ solutions, and 20-80% $SrCl_2$ + 80-20% $CaCl_2$ in $Sr(AlCl_4)_2$ solutions.[10,14] In all these cases it is most likely that the SEI is an anionic conductor ($t_- >> t_+$) while t_e is about 0.1 to 0.15[13]. The V_{oc} of the Ca-TC cell is given by:[4] t_i.EMF where t_i is the ionic transference number of the SEI. The EMF was found to be about 3.7V[13].

During discharge the current in the SEI is carried mostly by Cl^- anions. Thus a $CaCl_2$ layer is formed at the Ca/SE interface and Ca^{++} cations move from

the SE/solution interface into the solution[4,12]. During this process it is expected[12,13,14] that the SEI would crack and reheal continuously. The healing process is a precipitation of MCl_2(M=Ca,Sr or Ba), depending on the cation in the electrolyte, which forms as a result of the reduction of TC by the calcium anode in the cracked areas of the SEI (12). It is actually a corrosion reaction of the calcium anode taking place during the discharge of the cell.

$$M^{++} + SOCl_2 + 2e(Ca) \longrightarrow MCl_2 + 1/2S + 1/2SO_2 \qquad (1)$$

(M=Ca,Sr,Ba).

This process is highly exothermic (170 Kcal/mol).

It was indeed noticed that Ca-thionyl chloride batteries heat up significantly during discharge[9,10]. The maximum temperature rise of the can (of a C-size cell) increases with discharge rate from 2-3°C at 50 mA to 100°C at 2400 mA[10]. It was suggested that two main reasons are responsible for this large heating: cell polarization, and corrosion of the calcium anode during discharge. It was previously found that at room temperature and at 1 $mAcm^{-2}$ the utilization of calcium anode in $Ca(AlCl_4)_2$-$SOCl_2$ solution is about 90%[13]. The rest, up to 10% of the calcium metal is probably lost by direct chemical reaction with the thionyl chloride and by disintegration.

The overall thermal power output of a cell during discharge (W_T) is given by

$$W_T = W_s + W_p + W_c \text{ (watts)} \qquad (2)$$

where W_p is the polarization thermal power, overpotential times the current (ηI). W_c is the thermal power which results from chemical reactions in the cell. W_s, which results from entropy changes, can be calculated from

$$W_s = (I/nF).T\Delta S \qquad (3)$$

W_s and W_p can be calculated if the EMF (or ΔG) and the ΔS of the Ca-TC cell

are known. Thus by measuring W_T it is possible to calculate W_c. If it is assumed that the main contribution to W_c is the direct chemical reaction of the calcium anode with TC then it is possible to calculate the corrosion rate (I_c) of calcium from:

$$I_c = W_c/V_H \quad (4)$$

where V_H is the thermoneutral voltage of the Ca-TC cell ($V_H=-\Delta H/nF$), Finally, the differential faradaic efficiency (ϵ) of the calcium anode can be calculated at any DOD (depth of discharge) from:

$$\epsilon = I/(I_c + I) \quad (5)$$

The goal of this work was to study the effect of current density, 70°C storage, and temperature on W_T, W_p, W_c, I_c and ϵ of the $Ca/Sr(AlCl_4)_2$-TC $+SO_2$ cell. The heat generation rates (thermal power) of a C-size Ca-TC cell, at discharge rates of 0.1-1A, were estimated to be in the range 0.1 to 2W. We could not find a commercially available calorimeter for this heat-flow range, (however there are many microcalorimeters available). Thus, our other goal was to design and build a dedicated calorimeter for this purpose.

Experimental

Design considerations

Our goal was to design and build a fast response calorimeter for heat-flow rates of 0.1 to 2W which can accommodate a C-size cell. We chose to build a conduction-type calorimeter as shown in Fig.1. This type of calorimeter is based on Newton's law

$$dq/dt = W = K(T_1 - T_2) \quad (6)$$

where K is the thermal-leakage factor of the calorimeter (i.e. of the thermal conductor around the internal chamber) and T_1 and T_2 are the temperatures of the two surfaces across the thermal conductor - one in contact with the cell

under test and the second in contact with the heat sink.

Equation (6) is valid only for temperature differences smaller than 2-3°C[16]. We found that choosing the heat conductor is not a simple task. In order to measure a heat flow of the order of 2W at a temperature difference of about 2°C it is necessary to use thermal conductor of about 1W/°C.

In order to achieve fast response by the calorimeter the internal testing chamber was made as small as possible. Thus the surface area of the outside cylinder of the internal chamber (facing the cell) is only about 40 cm^2. The thickness of the thermal conductor is about 0.35 cm. Thus it was necessary to find a material whose thermal conductivity is about 0.01 $W°C^{-1}$ cm^{-1}. Metals and also carbon have higher thermal conductivity values and nonmetals (insulators) have much lower values. Therefore we chose a porous nonwoven carbon cloth (RVG 2000) for making this thermal conductor. The use of this material indeed gave the desired calorimeter heat-leakage factor of about 1 W/°C (Fig. 3).

The calorimeter assembly is seen in Fig. 1. It is immersed in a 30 liter water bath whose temperature was controlled by a home made controller to $\pm$ 0.05°C. The C-size Ca-TC cell was introduced into the chamber with the use of a lifter (Fig.2). The temperature difference across the porous carbon cloth, which serves as a thermal conductor, was measured with the use of two K-type thermocouples. These thermocouples were positioned in holes in two centered aluminium cylinders between which the porous carbon cloth was mounted (Fig.1). The differential output of the two thermocouples was amplified 13,300 times with the use of a home-made differential amplifier. The output of this amplifier was recorded with the use of a Yokogawa chart recorder.

The C-size Ca-TC cell or a calibration resistor was introduced into the chamber with the use of a cell lifter shown in Fig. 2. The cell or a

calibration resistor was electrically connected to two leads which were inserted into the chamber through a PVC plug.

The calorimeter was calibrated at 30 and 55°C with the use of 9Ω resistor placed in a dummy C-size can (an empty cell). The current and the voltage across this resistor were measured. The current through this resistor was varied and the amplifier output was recorded vs the input power (Fig.3). It was found that the calorimeter output is a linear function of the input power up to about 2W. Each 1V output is equivalent to a ΔT of about 1.8°C and to 1.08 watts of thermal power input. Thus equation (6) holds for this calorimeter up to a temperature difference of about 3.6°C, where the experimental K value is 0.6 W/°C. At higher temperature differences air convection starts to be appreciable and this leads to non-linearity.

The calorimeter was calibrated either at 30°C or at 55°C before each set of tests. The calibration curves were found to be identical (1.08 ± 0.01 W/V). The response time of the calorimeter is about 30 minutes.

The sensitivity of the calorimeter is limited by electronic noise and by temperature fluctuation of the water bath. The electronic noise was about ±15-20 mV (at the output of the amplifier) which is equivalent to about ±20 mW thermal power (or to about ±0.03°C). The temperature fluctuations of the bath were sometimes reflected in about 50 mV negative output peaks once in several hours. This kind of noise can be reduced by using a better temperature controller for the water bath.

The Ca-TC cell

A hermetically sealed C-size cell was used as a test vehicle. It was assembled with Hudson SS can and cover and Fusite 435 glass to metal seal with an electrolyte-filling tube. The anode was 0.5mm thick 40mm width Pfizer 99.9 calcium foil. The cathode was 0.7mm thick 40mm width teflon-bonded carbon

electrode supported by a nickel Exmet. The separator was 60% porous 50μ thick Tefzel foil (Scimat). The active electrode area was 150 cm^2. The cells were filled with 0.84M $Sr(AlCl_4)_2$ + 7% (V/V)SO_2 TC solution. Cells were discharged inside the calorimeter on a resistive load at either 30 or 55°C. A home-made computerized data-acquisition system based on IMS model 8000 computer was used for these tests.

Results

Two sets of cells were tested; 4 fresh cells and 4 cells which were stored at 70°C for 4 weeks and then at room temperature for 1 to 4 weeks more. Both groups were discharged at 30 and 55°C on two different loads of 4 and 9.4Ω. The average current densities associated with these loads were about 2 and 4 $mAcm^{-2}$.

Figures 4a, 4b, 4c and 4d show the discharge curves together with the associated calorimetric curves (heat flow vs. time) of fresh and stored cells. Each plot presents the discharge curve in two ways; voltage vs. time (line B) and voltage vs. capacity (line C). Each calorimetric curve is plotted on two scales: thermocouple differential amplifier output signal in volts on the left side and thermal power output of the cell on the right side.

All cells, fresh and stored, exhibit a flat discharge curve with no voltage delay (below 2V). Cell-discharge data are summarized in Table 1. In most cases the calorimetric curves (lines A in Figs.4a-4d) exhibit a peak at the start of the discharge and then level off (stay about constant) or decline slightly toward the end of the discharge. The heat-flow (W_T) data at 50% DOD, i.e. in the flat region of the calorimetric curve, are summarized in Table 1. It can be seen that the storage period of four weeks at 70°C does not affect W_T.

Increasing discharge temperature from 30 to 55°C does not seem to affect W_T for 9.4Ω discharge tests (about 2 $mAcm^{-2}$), but may cause up to 10% increase

in W_T for 4Ω (about 4 $mAcm^{-2}$) discharge tests. Increasing the current density (or decreasing the load) by a factor of about 2 increases W_T by a higher factor of 2.2-2.8.

The delivered capacity of the cell at constant temperature discharge was found to increase markedly with increasing the temperature from 30 to 55°C especially for the heavier load discharge tests. It rose from 2.2 Ah to 3.7 Ah for 4Ω discharge and from 3.7 to 4.2 for 9.4Ω discharge (Table 1). When this cell was being discharged in air (and not in a constant temperature water bath) it delivered 3.2 Ah at 4Ω load[17]. This higher capacity was probably due to the fact that in the room temperature discharge test the cell heats up to about 50°C (on 4Ω load) while in the calorimeter its temperature stays about constant.

It is very important to note that these cells lost almost no capacity (less than 5%) during four weeks of storage at 70°C.

Discussions

As mentioned before, our goal was to study the effects of temperature, discharge rate and high-temperature storage on W_T, W_p, W_c, I_c and ϵ. For this purpose we designed and built a dedicated calorimeter for C-size cells. Its noise level, ± 15-20mV, is equivalent to an error of about ±20 mW. Thus we expected an error in W_T of about 1.5-5%. In order to be able to calculate the components of W_T we have to know the ΔG and ΔS values of the cell reaction (7)[2]

$$Ca + SOCl_2 \longrightarrow CaCl_2 + 1/2\ SO_2 + 1/2\ S \qquad (7)$$

By using data from refs.18-20 and thermodynamic cycles it was possible to

calculate the following values for reaction 7:

$\Delta S(298^{o}C) = -52\ J\ mol^{-1}K^{-1}$

$\Delta G(298^{o}C) = -704\ KJ\ mol^{-1}$

$\Delta G(328^{o}C) = -700\ KJ\ mol^{-1}$

$\Delta H(298^{o}C) = \Delta H(328^{o}C) = -720\ KJ\ mol^{-1}$

Using these values, we calculated:

$EMF(298^{o}C) = 3.65\ V$

$EMF(328^{o}C) = 3.63\ V$

$V_H(328^{o}C) = V_H(298^{o}C) = 3.73\ V$

We assumed a constant ΔH for the temperature range 328-303°C.

With the use of these values we calculated the overvoltage (η) of the cell (η = EMF-V(I)) and then W_p. W_s was calculated with the use of Eq.3.

Having W_T, W_s and W_p we calculated W_c - the chemical heat power output by using Eq.2. It is possible that several chemical reactions of unstable discharge intermediates may contribute to W_c. However, there is no solid experimental proof for such reactions and we believe that the largest contribution to it is the corrosion of the calcium anode during discharge. Thus, with the use of Eq.4, we calculated the maximum value for the corrosion current (I_c) of the anode.

With the use of Eq.5 we calculated the minimum value for the faradaic efficiency (ϵ) of the anode. The average values (at 50% DOD) of W_T, W_p, W_c, I_c and ϵ together with the peak values of W_c are summarized in Table 2. Plots of W_T, W_p, W_s, W_c vs. discharge capacity for fresh and stored cells can be found in Figs.5-12. In all cases W_s and W_p are approximately constant during the discharge period. W_c tends to decrease and W_p to increase toward the end of the discharge. In most cases, except Figs.5 and 12, W_c has a peak at the start of the discharge. The W_c peak values are up to 2.5 times larger than its

plateau values. This excessive heat generation may indicate a faster corrosion of calcium at the beginning of the discharge. It may be associated with changes in the composition and properties of the passivating layer of the calcium and with changes in the composition of the electrolyte - i.e. increase of the SO_2 concentration. We found that the calcium anode as received and especially after a long storage period is covered by a thick CaO film. In SrX_2 solutions its conversion into $CaCl_2$ (or $SrCl_2$), although thermodynamically favored, is very slow[21]. Even after one month of storage in SrX_2 - TC solution at 70°C the CaO film is only partially converted into $CaCl_2$ and $SrCl_2$. It is likely that the W_c peak results from a mechanical breakdown of this $CaO-CaCl_2-SrCl_2$ mixed film due to the dissolution of the calcium and formation of a thinner and more protective chloride film. For unknown reasons the W_c peak in Fig.5 appears in the middle of the discharge while in Fig.12 we found no peak at all.

It can be seen (Table 2) that $W_{p,a}$ is always larger by 40-200% than the plateau value of W_c. It means that, at least over the 30-55°C temperature range and upto 4 $mAcm^{-2}$, the corrosion of the anode during discharge is not the predominant factor in cell heating. The one-month storage at 70°C does not seem to affect $W_{c,a}$ and $I_{c,a}$. Raising the discharge temperature from 30 to 55°C increases $W_{c,a}$ by 25% to 90% while the largest effect was for the higher current density. At 30°C $W_{c,a}$ increases linearly with increase in the current density; however, at 55°C, the $W_{c,a}$ increase was larger than the increase in the current density. Thus at the highest temperature and current density, the anode corrosion during discharge is the greatest. It was suggested[22,14] that the combination of high anionic transference number (t_-~1) and the large difference between the equivalent volume of $CaCl_2$ and that of calcium is one of the main reasons for the corrosion of calcium (under OCV conditions) in TC

solutions. The same reasoning holds for its much higher corrosion under discharge. The breakdown and healing process of the SEI during discharge can be described as follows: During discharge (anodic dissolution) new $CaCl_2$ layers are formed in the $Ca/CaCl_2$ interface by migration of Cl^- through the SEI. As the equivalent volume of $CaCl_2$ is twice that of calcium, bulging of the SEI may occur inhomogeneously. In the area of higher local current density this bulging may be more severe and may lead to cracking of the SEI and momentary exposing of fresh calcium surface to the solution. A fast reaction between the exposed calcium and TC immediately begins and this leads to the formation of $CaCl_2$ which precipitates at these areas, reheals the SEI and slows the corrosion reaction. We cannot prove that no other chemical reactions except calcium corrosion contributes to W_c. Thus I_c is the maximum corrosion current of the anode, and ϵ is its minimum Faradaic efficiency. $I_{c,a}$ is affected by temperature and current density in the same way as is W_c. Its calculated values are between 29 and 127 mA. These values are not at all negligible. Therefore ϵ_a varies between 83% and 89%. Storage of one month at 70°C does not seem to affect ϵ_a. However, it decreases with increasing temperature and current density, being the lowest for 55°C and 4 Ω discharge conditions.

It is interesting to note that the value of ϵ is similar to that of t_i[13] - the ionic transference number of the SEI under OCV conditions at room temperature. This means that even at very low discharge rates (close to OCV) the faradaic efficiency of the calcium anode may be only 0.9.

As a result of the disagreement in the literature regarding thermodynamic ΔH, ΔG, and ΔS values there is some uncertainty in the calculation of W_s W_p, W_c, I_c and ϵ. However, we believe that this uncertainty is rather small and is not enough to alter our main conclusions. In addition, we previously found that the EMF of the Ca-TC cell is about 3.7V[13] and that the faradaic

efficiency of the calcium anode at room temperature and 1 $mAcm^{-2}$ is about 90%[13]. Both findings agree well with our calculations.

Conclusions

At temperatures lower than 30°C and current densities 2 mA Cm^{-2} or lower the predominant heat generation factor during discharge of the Ca/SrX_2-TC cell is cell polarization and the faradaic efficiency of the anode is close to 90%. However, on the basis of our results, it is expected that at very high current densities (more than 4mA cm^{-2}) and at discharge temperatures higher than 55°C the predominant heat-generation factor may be anodic corrosion, thus ϵ may be smaller than 80%.

The Ca/SrX_2-TC cell is capable of delivering high rates after four weeks of storage at 70°C with no loss of capacity. In order to be able to increase its continuous discharge rate (sustain power) it is necessary to decrease its polarization and the corrosion rate of the anode during discharge, especially at high temperatures.

References:

1. A. Meitav and E. Peled, Proceedings of the 131st ISE Meeting, Venice, Italy (1980).
2. R.J. Staniewicz, J. Electrochem So. 127, 782 (1980).
3. E. Peled, A. Meitav and M. Brand ibid, 128, 1936 (1981).
4. A. Meitav and E. Peled ibid, 129, 451 (1982).
5. R. Huggins and J.S. Cloyd, Proceedings of the 29th Power Sources Symposium, Atlantic City (1980).
6. C. Walker, Jr., W. Wade, M. Binder and S. Gilman, J. Electrochem. Soc., 133, 1555 (1986).
7. M. Binder, S. Gilman, W. Wade Jr., ibid, 129, 897 (1982).
8. W.K. Behlin, Proceedings of the Symposium on Lithium Batteries, A.N. Dey Ed., Electrochem. Soc., Vol. 84-1 (1984).
9. R.J. Staniewicz, R.A. Dixon and S.J. Hafner, Proceedings of the 33rd International Power Sources Symp., p. 144 (1988) Electrochem Soc. Pub.
10. E. Peled, E. Elster, R. Cohen, J. Kimel and Y. Lavi, ibid p. 136.
11. C.W. Walker Jr., ibid, p. 129.
12. E. Peled in Lithium Batteries, J.P. Gabano Ed., Academic Press, NY (1983).
13. A. Meitav and E. Peled, Electrochemica Acta Vol. 33, 1111 (1988).
14. E. Elster, R. Cohen, M. Brand, Y. Lavi and E. Peled, J. Electrochem. Soc. 135, 1307 (1988).
15. E. Elster, R. Cohen and E. Peled, Proceedings of the 4th International Meeting on Lithium batteries, Vancouver (May 1988).
16. Experimental Thermochemistry Vol. II, H.A. Skinner, Intersclence Publishers, (1974).
17. R. Cohen and E. Peled, unpublished results.

18. Gmelins Handbuch der anorganischen Chemie, System No. 9, Schwefel Teil B Lieferung3, 8th edition 1963 pp. 1793-1802.

19. NBS Tables of Chemical Thermodynamic Properties, Wagman, Evans, Parker, Schumm, Halow, Bailey, Churney, and Nuttal eds.

20. CRC Handbook of Chemistry and Physics 62nd ed (1986).

21. E. Elster and E. Peled, unpublished results.

22. E. Peled, Proceedings of the 32nd International Power Symp., p. 1986, Electrochem. Soc. Pub.

Legends to Figures:

Fig. 1: Calorimeter assembly

Fig. 2: Calorimeter Lifter for a C-size cell.

Fig. 3: A typical calibration curve. A plot of thermocouple differentials amplifier output (v) vs. thermal input power (w).
□ - 30°C; ■ - 55°C.

Fig. 4: Discharge (lines B and C) and calorimetric (line A) curves of C-size Ca/0.84M SrX_2-TC + 7% (v/v) SO_2 cell.
a, Q_{11} fresh, 9.4Ω load 30°C.
b, Q_{12} fresh, 4Ω load 55°C.
c, Q_{20}, stored (70°C, 4 weeks), 9.4Ω load, 30°C.
d, Q_6, stored (70°C, 4 weeks), 4Ω load, 55°C.

Fig. 5: Plots of W_T, W_p, W_c and W_s for cell Q_{13} vs. discharge capacity. Fresh cell 9.4Ω load 55°C.

Fig. 6: Plots of W_T, W_p, W_c and W_s for cell Q_2 vs. discharge capacity. 70°C 4 week storage, 4Ω load, 30°C.

Fig. 7: Plots of W_T, W_p, W_c and W_s for cell Q_{11} vs. discharge capacity. Fresh cell, 9.4Ω load, 30°C.

Fig. 8: Plots of W_T, W_p, W_c and W_s for cell Q_{10} vs. discharge capacity. Fresh cell, 4Ω load, 30°C.

Fig. 9: Plots of W_T, W_p, W_c and W_s for cell Q_{19} vs. discharge capacity. 70°C - 4 week storage, 9.4Ω load, 55°C.

Fig. 10: Plots of W_T, W_p, W_c and W_s for cell Q_6 vs. discharge capacity. 70°C - 4 week storage, 4Ω load, 55°C.

Fig. 11: Plots of W_T, W_p, W_c and W_s for cell Q_{20} vs. discharge capacity. 70°C - 4 week storage, 9.4Ω load, 30°C.

Fig. 12: Plots of W_T, W_p, W_c and W_s for cell Q_{12} vs. discharge capacity. Fresh cell, 4Ω load, 55°C.

Table 1: Discharge Performance of cells.

cell code	discharge temperature (°C)	load (Ω)	Average current (A)	Average Voltage (V)	Capacity (2V cutoff) (Ah)	W_T - Heat flow at 50% DOD (W)
Q_{13}	55	9.4	0.297	2.80	4.2	0.42
Q_{12}	55	4.0	0.620	2.56	3.7	1.2
Q_{11}	30	9.4	0.255	2.39	3.4	0.49
Q_{10}	30	4.0	0.576	2.3	2.2	1.1
Q_{19}*	55	9.4	0.297	2.8	4.0	0.47
Q_6*	55	4.0	0.62	2.56	3.6	1.21
Q_{20}*	30	9.4	0.255	2.39	3.4	0.46
Q_2*	30	4.0	0.576	2.3	2.2	1.1

* Stored cells - 4 weeks at 70°C + 1-4 weeks at RT.

Table 2: Calorimeter test results

cell code	discharge temperature (^{o}C)	Average Voltage (V)	Average discharge current (mA)	Wc,a (W)	Ic,a (mA)	Wc peak (W)	Wp,a (W)	ϵ (%)
Q_{13}	55	2.80	295	0.16	43	-	0.24	87
Q_{12}	55	2.56	620	0.44	118	1.03	0.67	84
Q_{11}	30	2.39	255	0.13	35	0.2	0.32	88
Q_{10}	30	2.3	576	0.28	76	0.4	0.77	88
Q_{19}*	55	2.8	297	0.18	47	0.28	0.25	86
Q_{6}*	55	2.56	620	0.47	127	0.7	0.67	83
Q_{20}*	30	2.39	255	0.11	29	0.2	0.32	89
Q_{2}*	30	2.3	576	0.25	68	0.3	0.67	89

* Stored cells - 4 weeks at 70^{o}C + 1-4 weeks at RT.

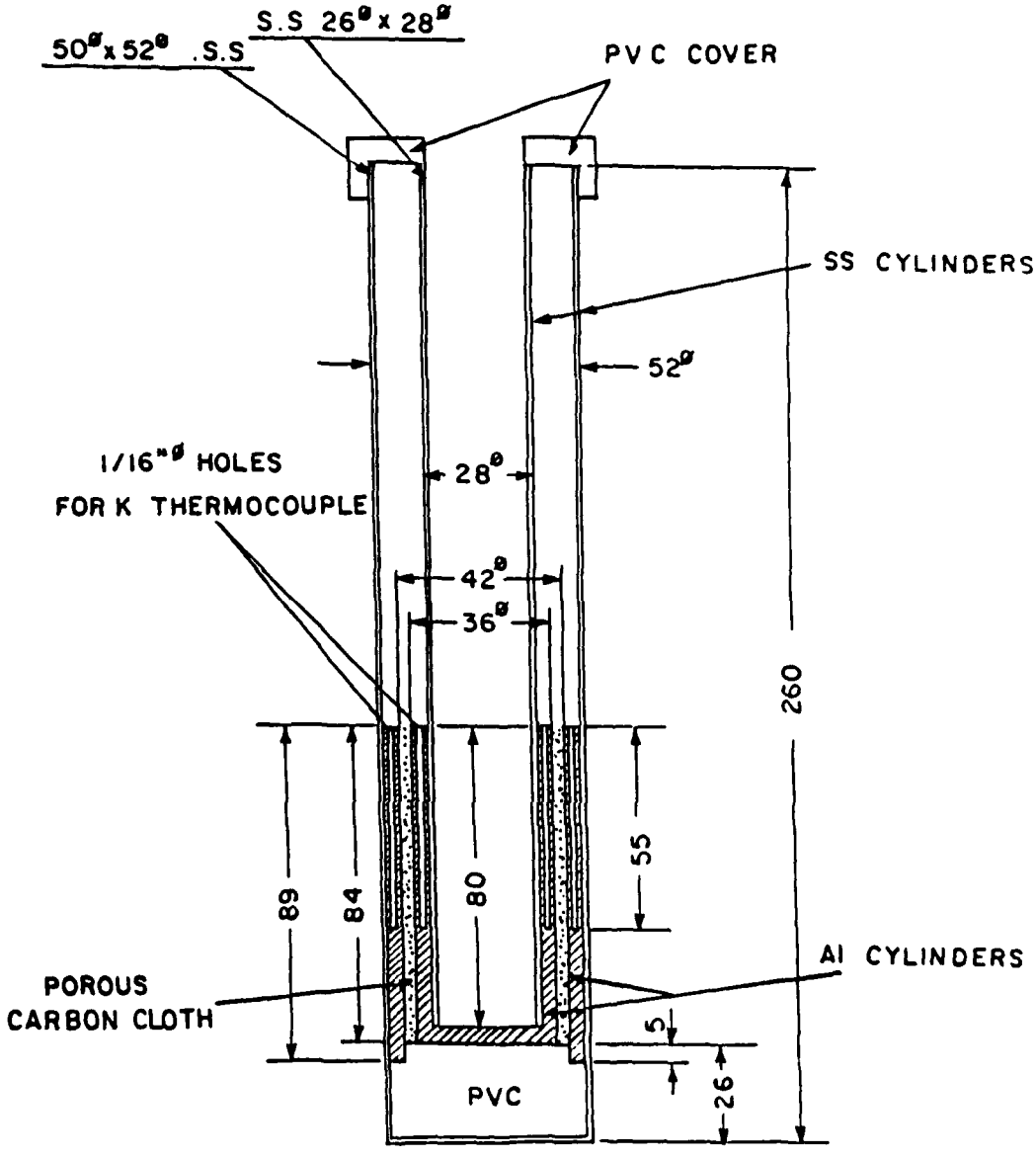
S.S 26ø x 28ø
50ø x 52ø .S.S
PVC COVER
SS CYLINDERS
52ø
1/16"ø HOLES
FOR K THERMOCOUPLE
28ø
42ø
36ø
260
55
89
84
80
AI CYLINDERS
POROUS
CARBON CLOTH
5
26
PVC

Fig. 1

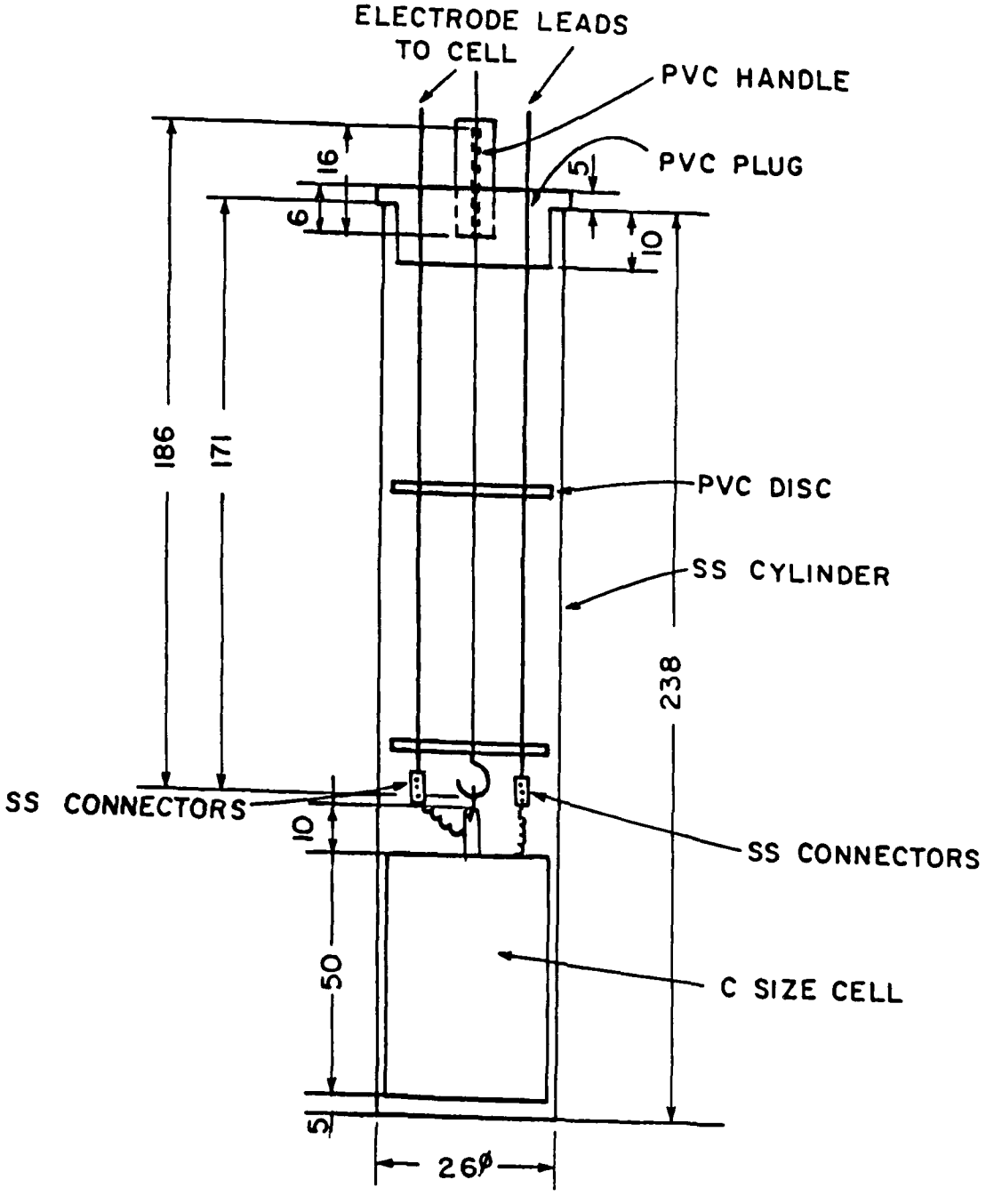
ELECTRODE LEADS
TO CELL
PVC HANDLE
PVC PLUG
16
5
6
10
186
171
PVC DISC
SS CYLINDER
238
SS CONNECTORS
10
SS CONNECTORS
50
C SIZE CELL
5
26ø

Fig. 2

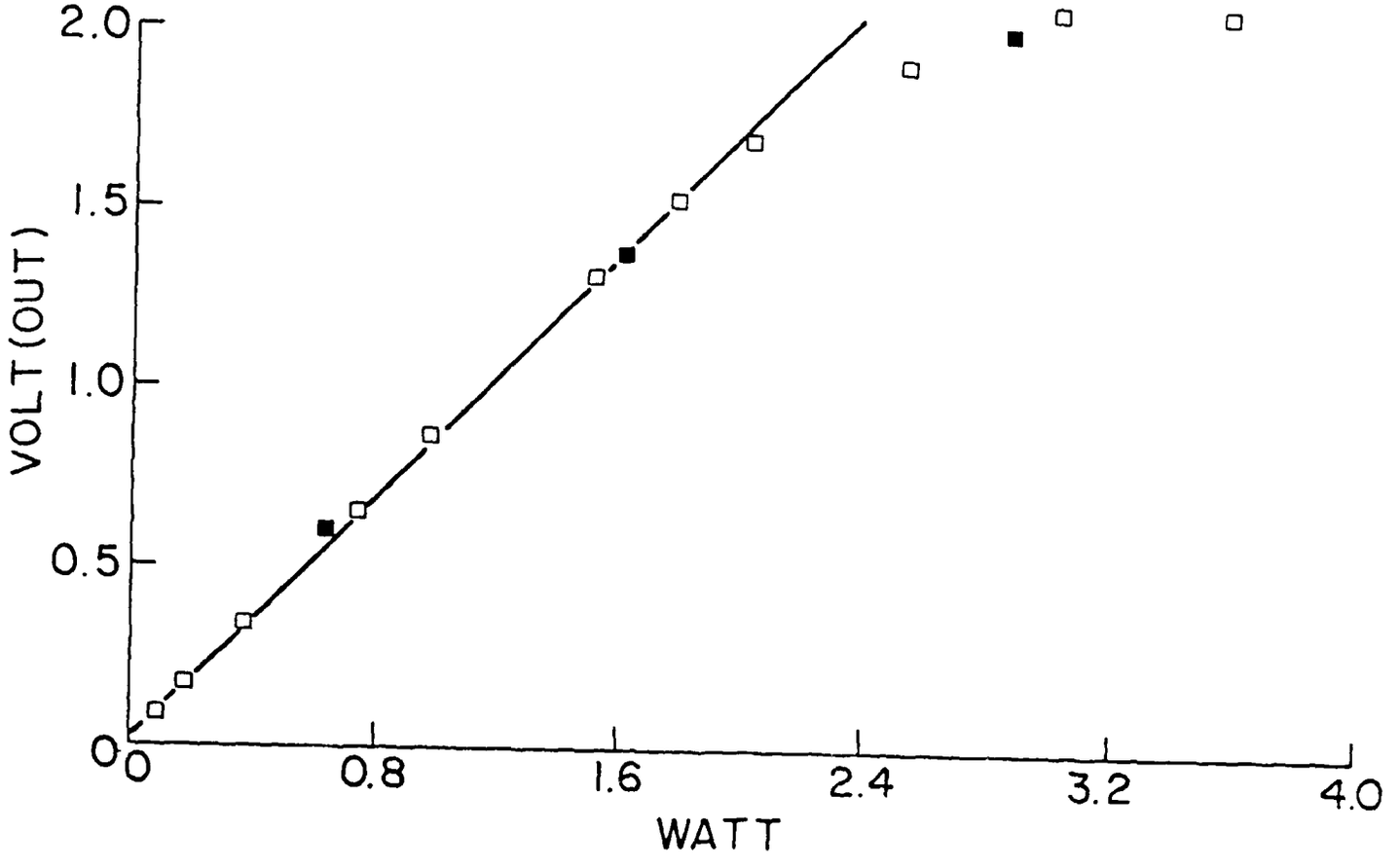

Fig. 3

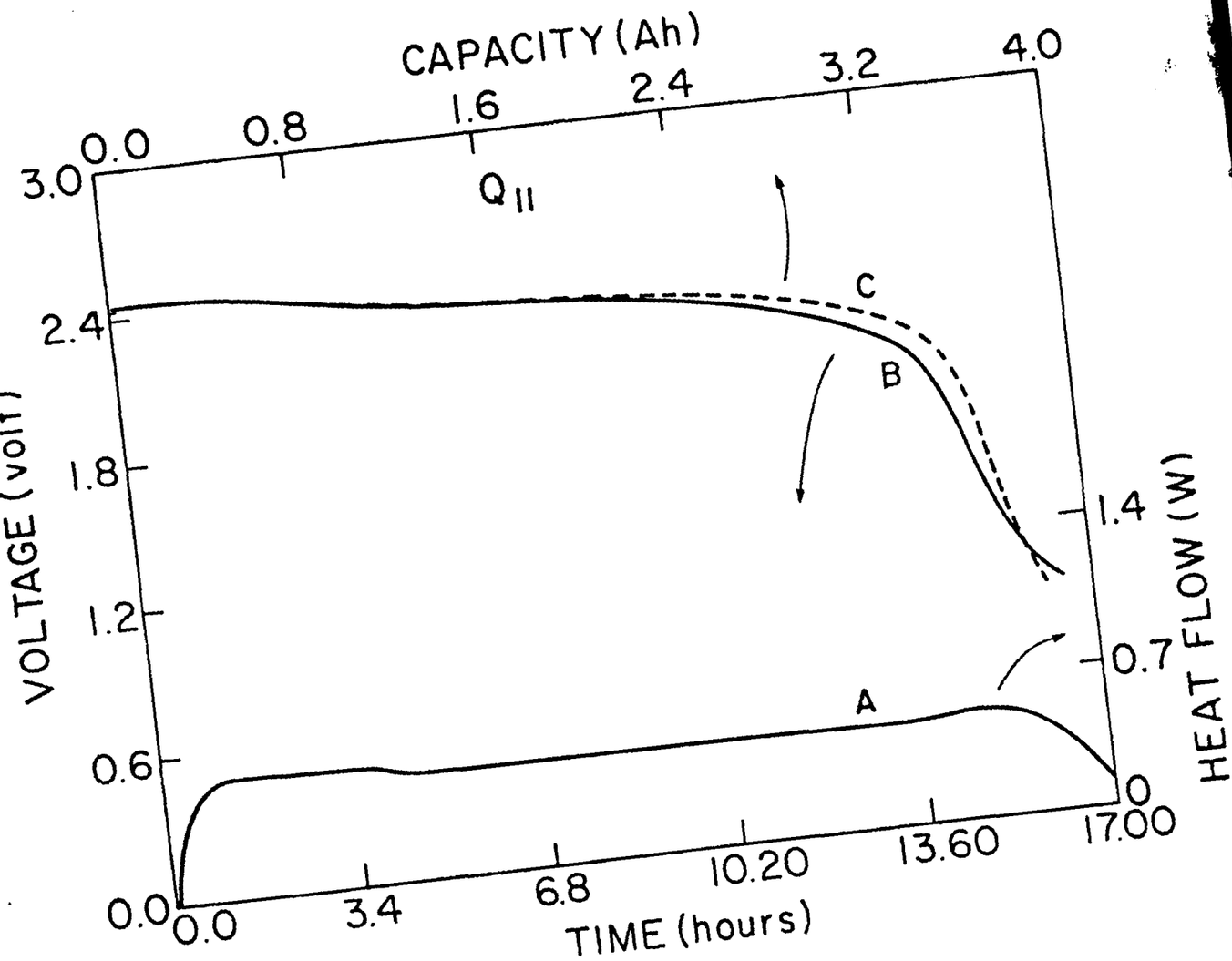
CAPACITY (Ah)
0.0
0.8
1.6
2.4
3.2
4.0
Q_{11}
3.0
2.4
1.8
1.2
0.6
0.0
VOLTAGE (volt)
C
B
A
1.4
0.7
0
HEAT FLOW (W)
0.0
3.4
6.8
10.20
13.60
17.00
TIME (hours)

Fig. 4a

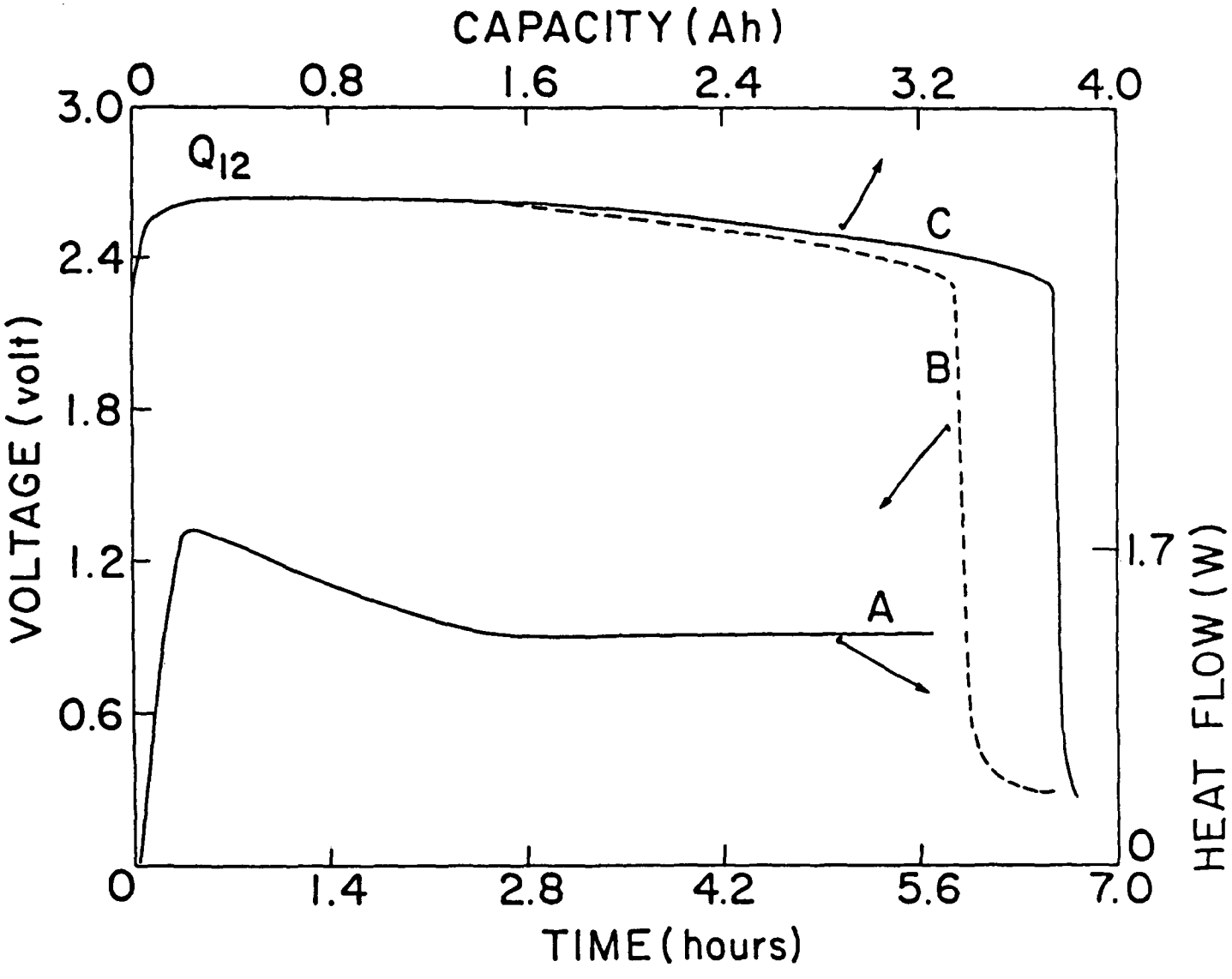
CAPACITY (Ah)
0
0.8
1.6
2.4
3.2
4.0
3.0
2.4
1.8
1.2
0.6
0
Q_{12}
C
B
A
VOLTAGE (volt)
1.7
0
HEAT FLOW (W)
0
1.4
2.8
4.2
5.6
7.0
TIME (hours)

Fig. 4b

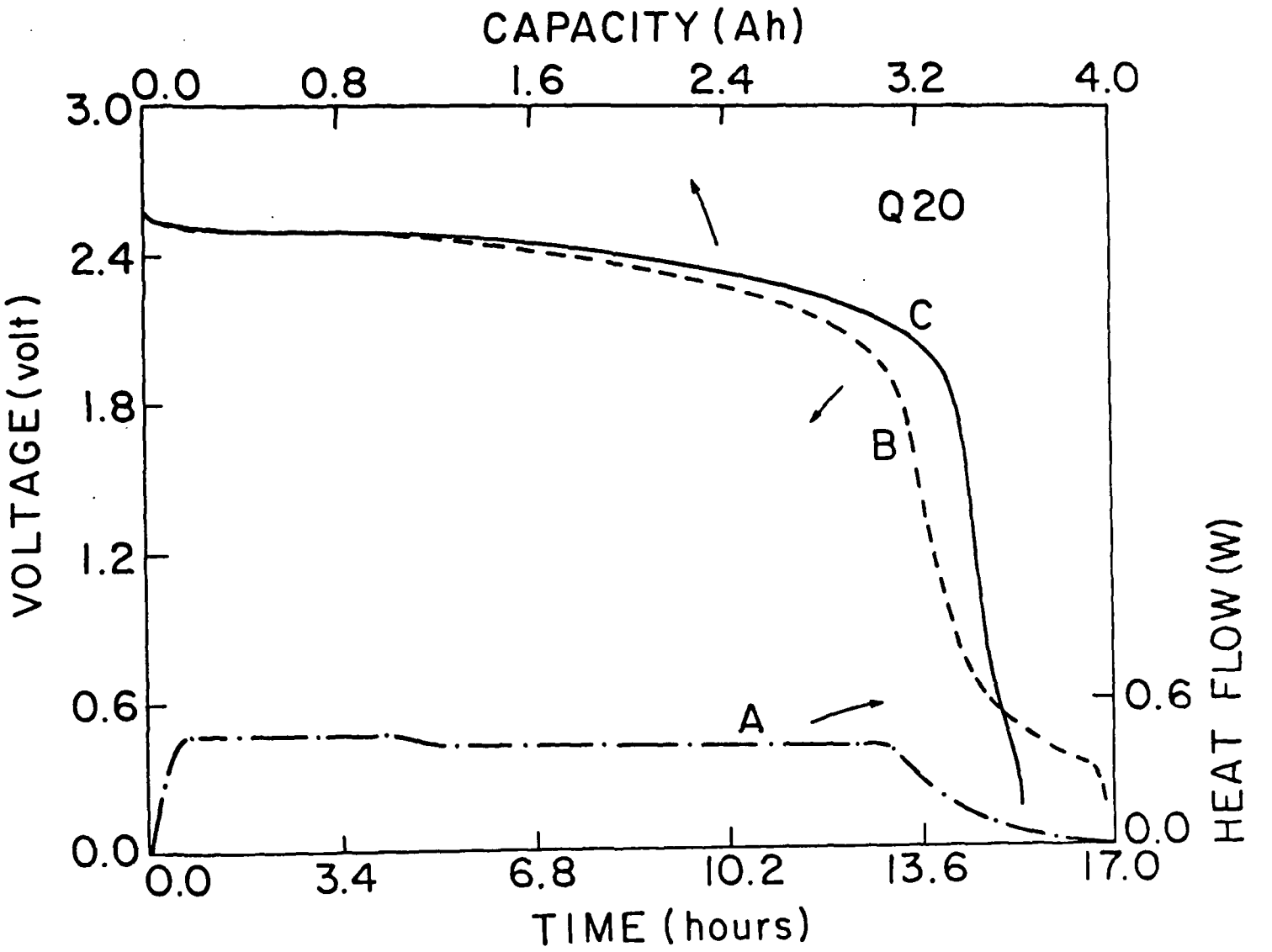
CAPACITY (Ah)
0.0
0.8
1.6
2.4
3.2
4.0
3.0
2.4
1.8
1.2
0.6
0.0
VOLTAGE (volt)
Q20
C
B
A
0.6
0.0
HEAT FLOW (W)
0.0
3.4
6.8
10.2
13.6
17.0
TIME (hours)

Fig. 4c

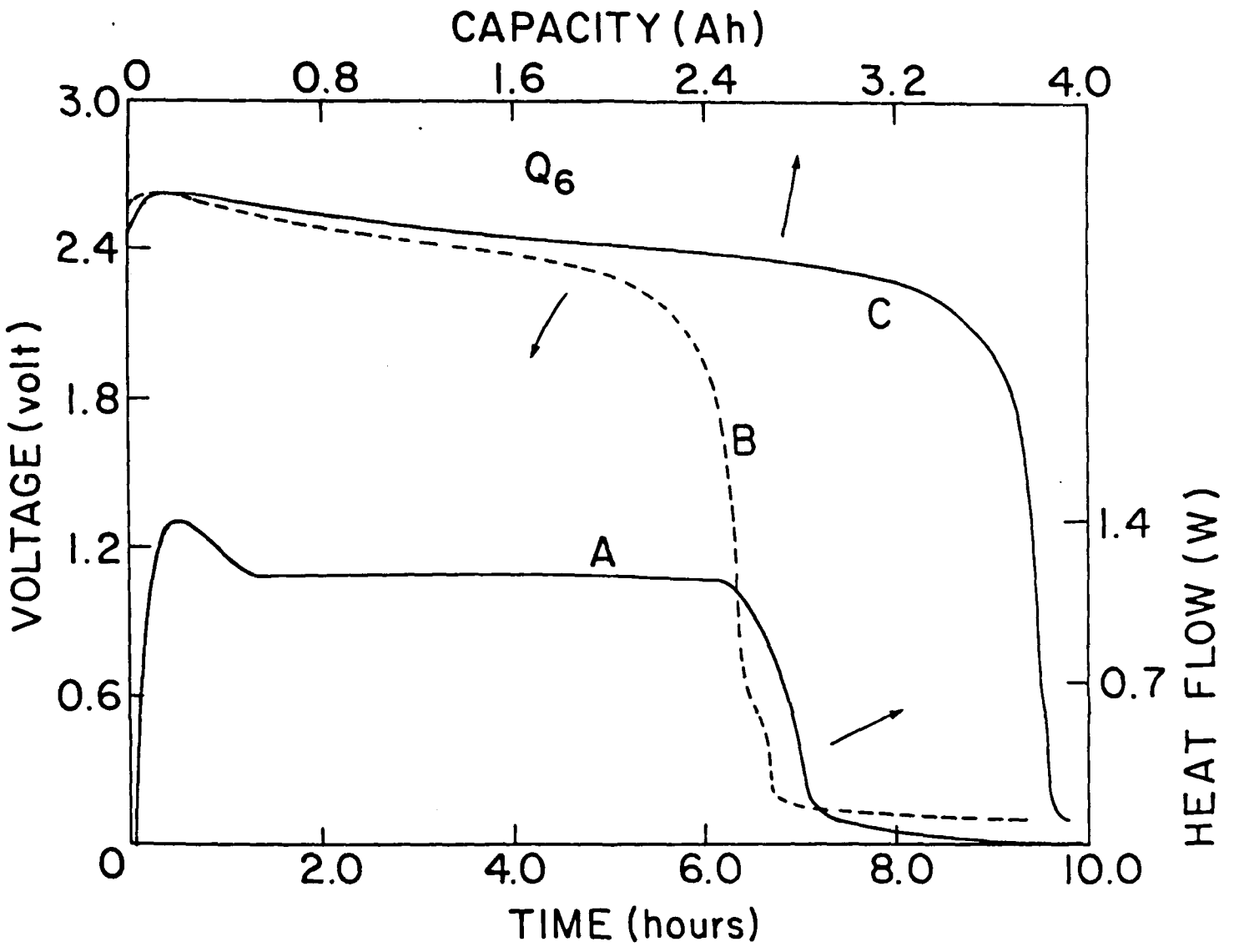
CAPACITY (Ah)
0
0.8
1.6
2.4
3.2
4.0
3.0
2.4
1.8
1.2
0.6
0
Q_6
A
B
C
VOLTAGE (volt)
1.4
0.7
HEAT FLOW (W)
2.0
4.0
6.0
8.0
10.0
TIME (hours)

Fig. 4d

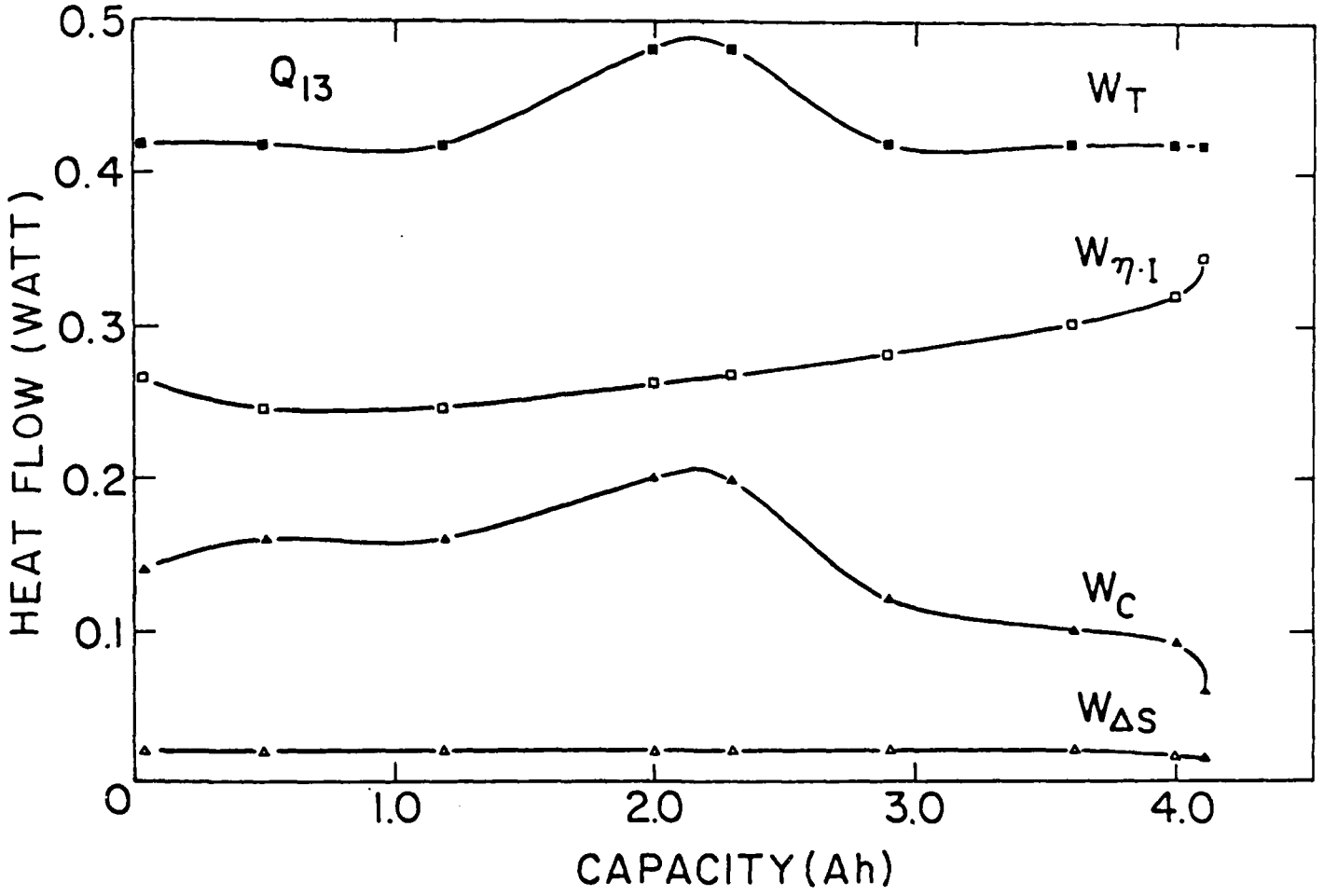
0.5
0.4
0.3
0.2
0.1
0
HEAT FLOW (WATT)
Q_{13}
W_T
$W_{\eta \cdot I}$
W_C
$W_{\Delta S}$
1.0
2.0
3.0
4.0
CAPACITY (Ah)

Fig. 5

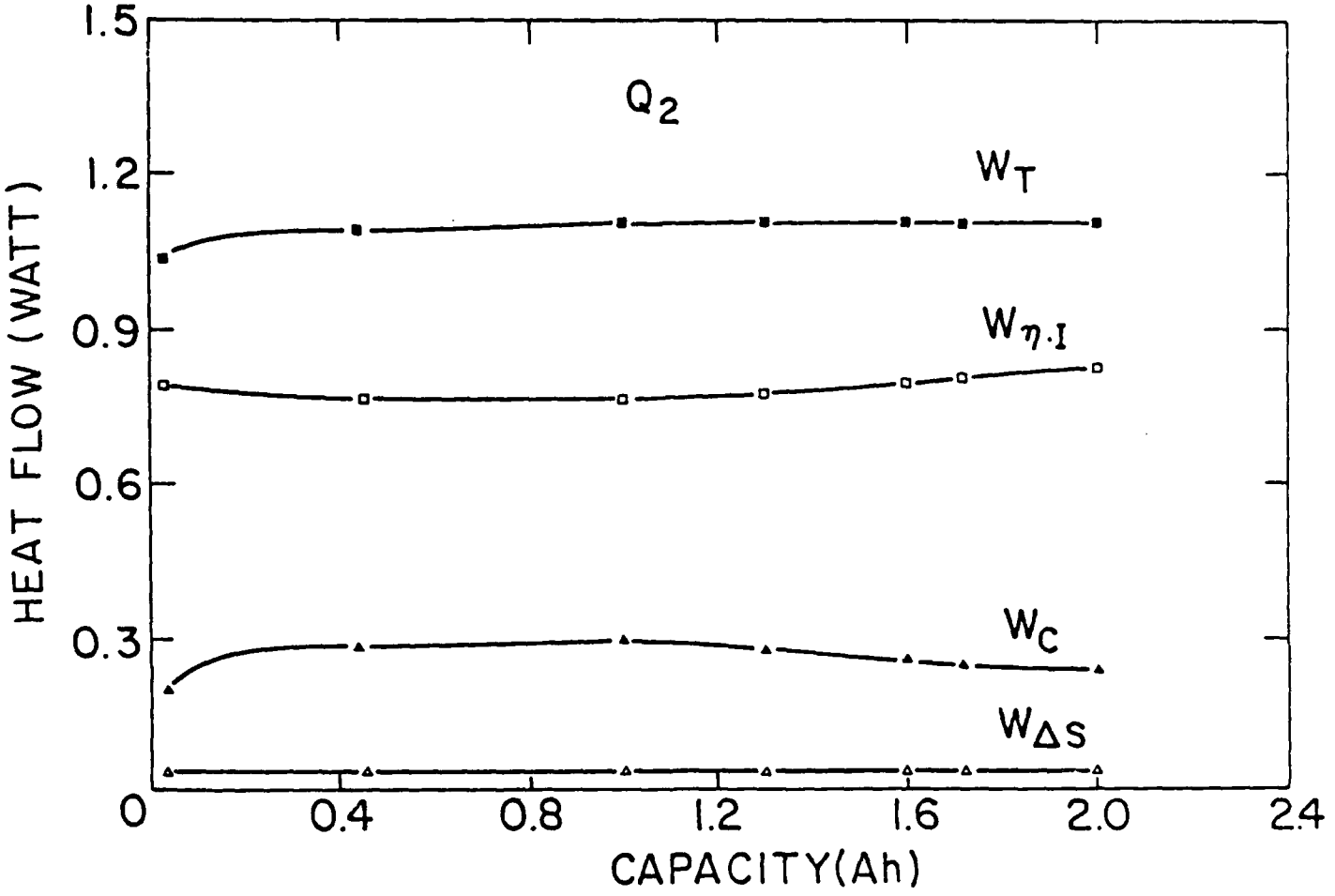
1.5
1.2
0.9
0.6
0.3
0
HEAT FLOW (WATT)
Q2
WT
Wη.I
WC
WΔS
0.4
0.8
1.2
1.6
2.0
2.4
CAPACITY(Ah)

Fig. 6

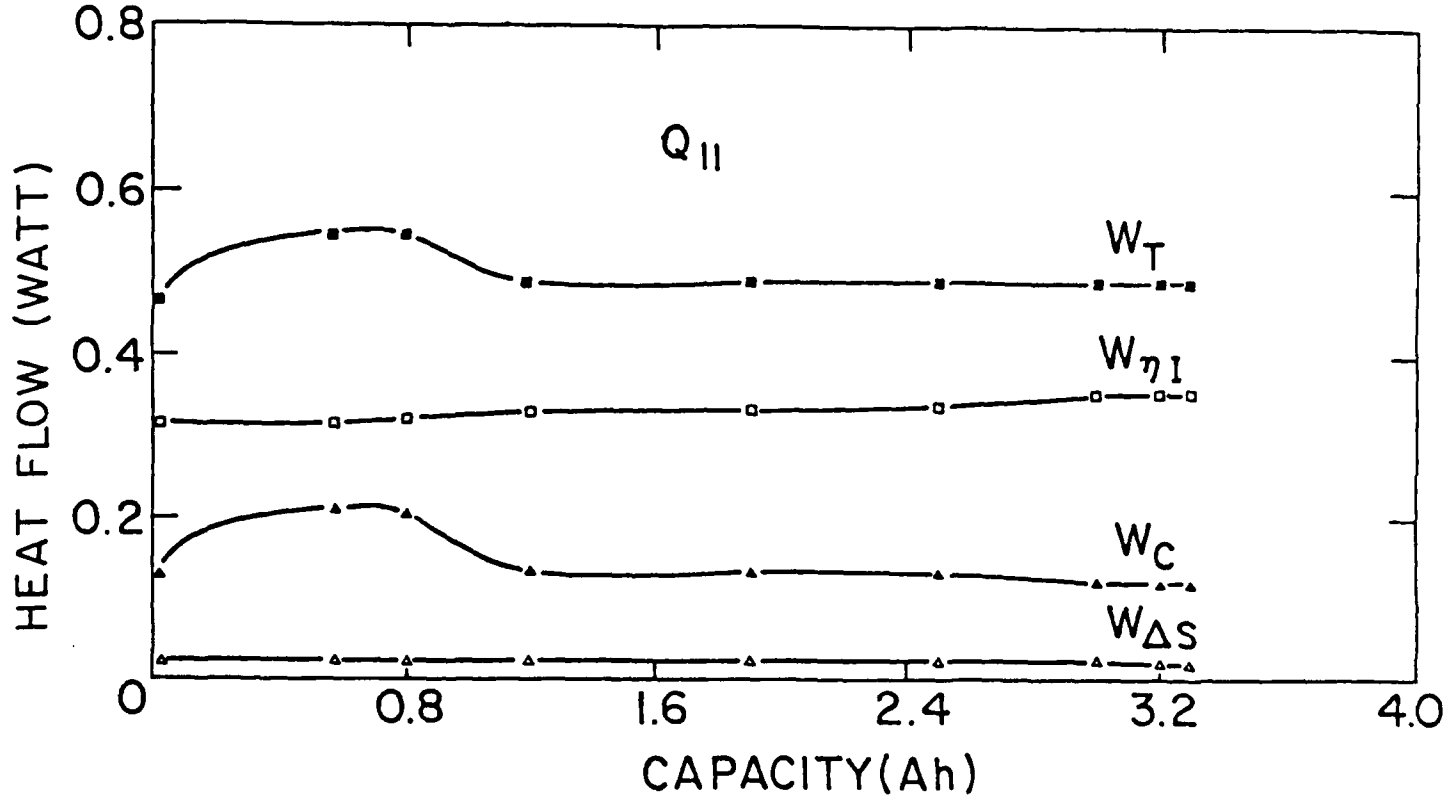
0.8
0.6
0.4
0.2
0
HEAT FLOW (WATT)
Q_{11}
W_T
$W_{\eta I}$
W_C
$W_{\Delta S}$
0.8
1.6
2.4
3.2
4.0
CAPACITY(Ah)

Fig. 7

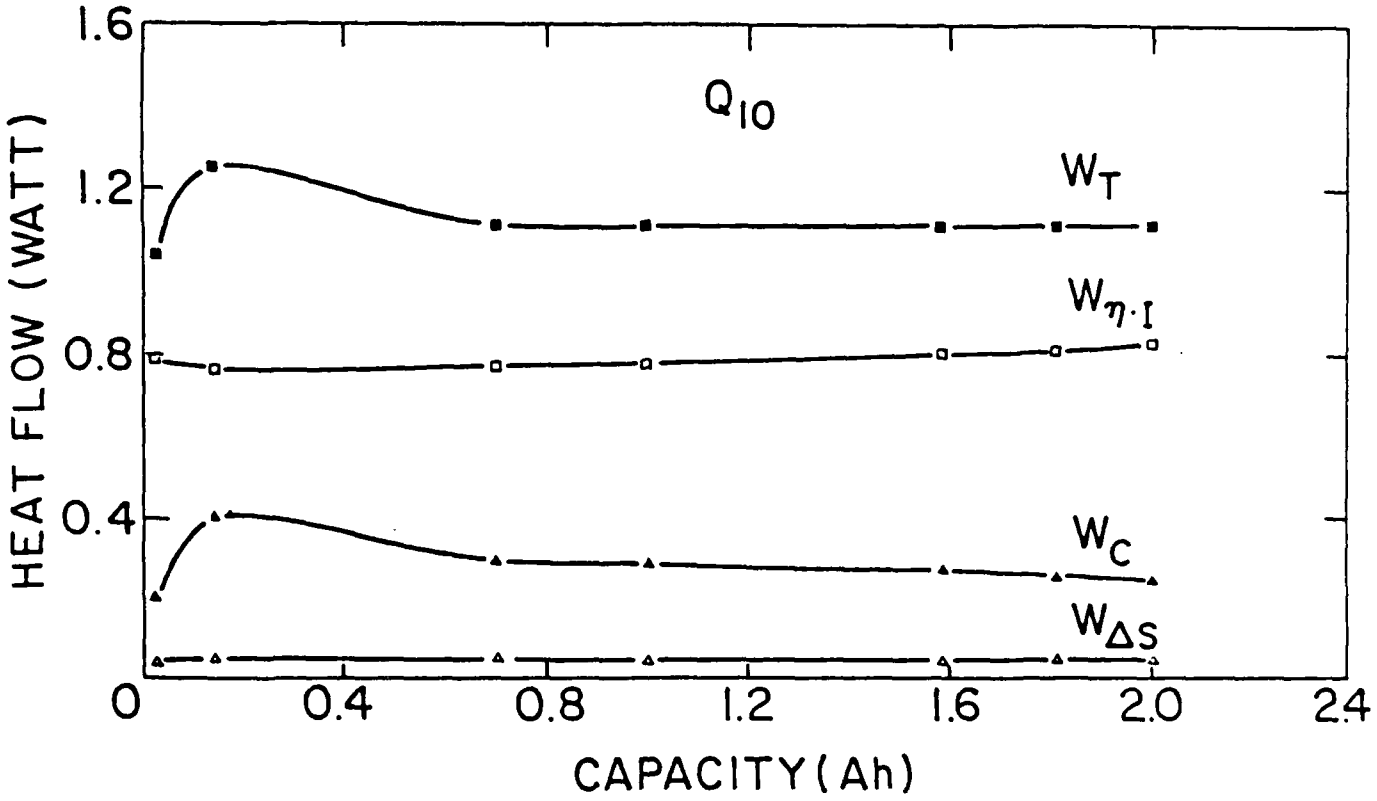
Q10
W_T
W_η·I
W_C
W_ΔS
HEAT FLOW (WATT)
CAPACITY (Ah)
1.6
1.2
0.8
0.4
0
0.4
0.8
1.2
1.6
2.0
2.4

Fig. 8

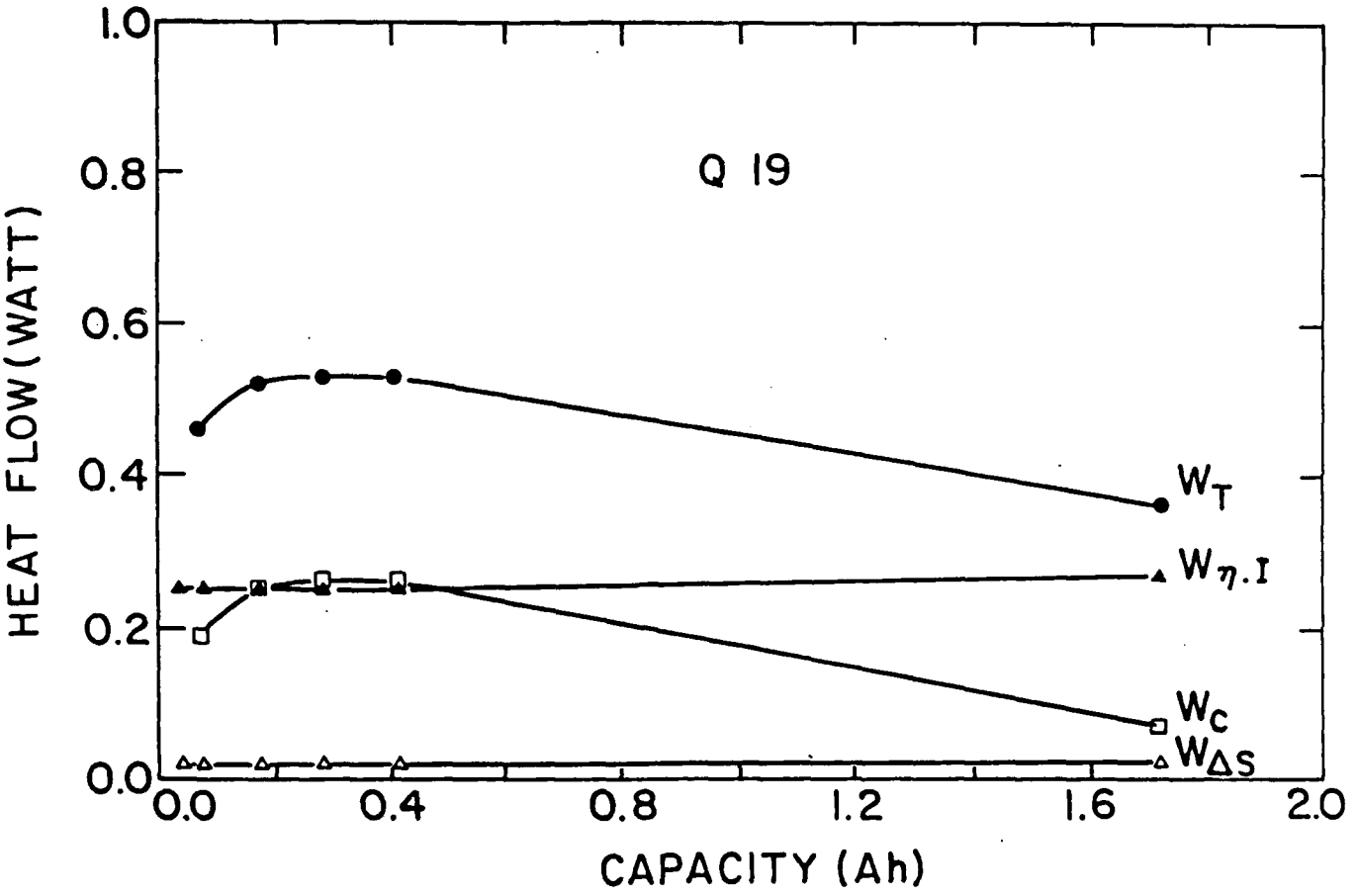
Q 19
HEAT FLOW (WATT)
CAPACITY (Ah)
1.0
0.8
0.6
0.4
0.2
0.0
0.0
0.4
0.8
1.2
1.6
2.0
W_T
$W_{\eta.I}$
W_C
$W_{\Delta S}$

Fig. 9

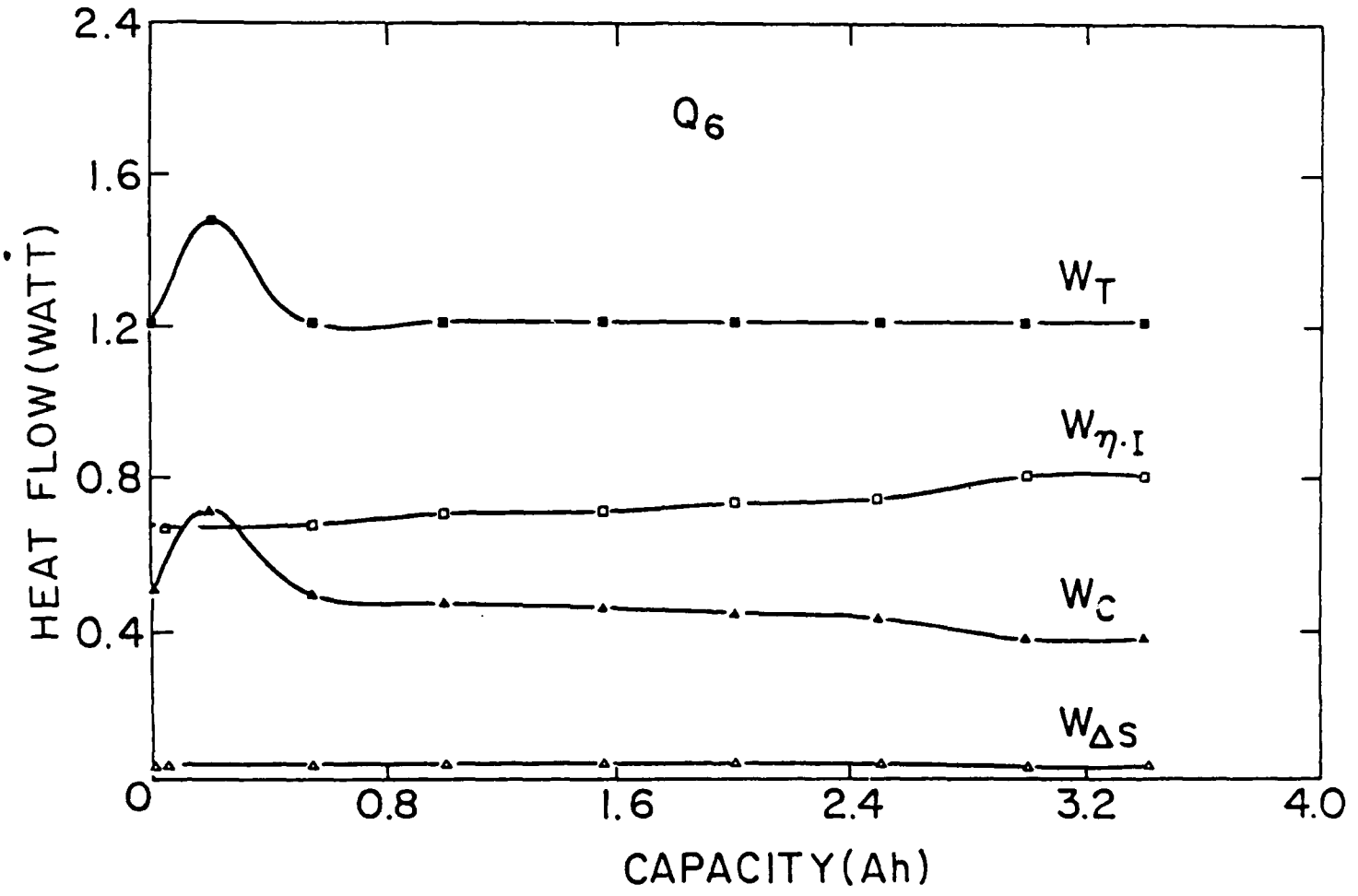
2.4
1.6
1.2
0.8
0.4
0
0.8
1.6
2.4
3.2
4.0
Q_6
W_T
$W_{\eta \cdot I}$
W_C
$W_{\Delta S}$
HEAT FLOW (WATT)
CAPACITY (Ah)

Fig. 10

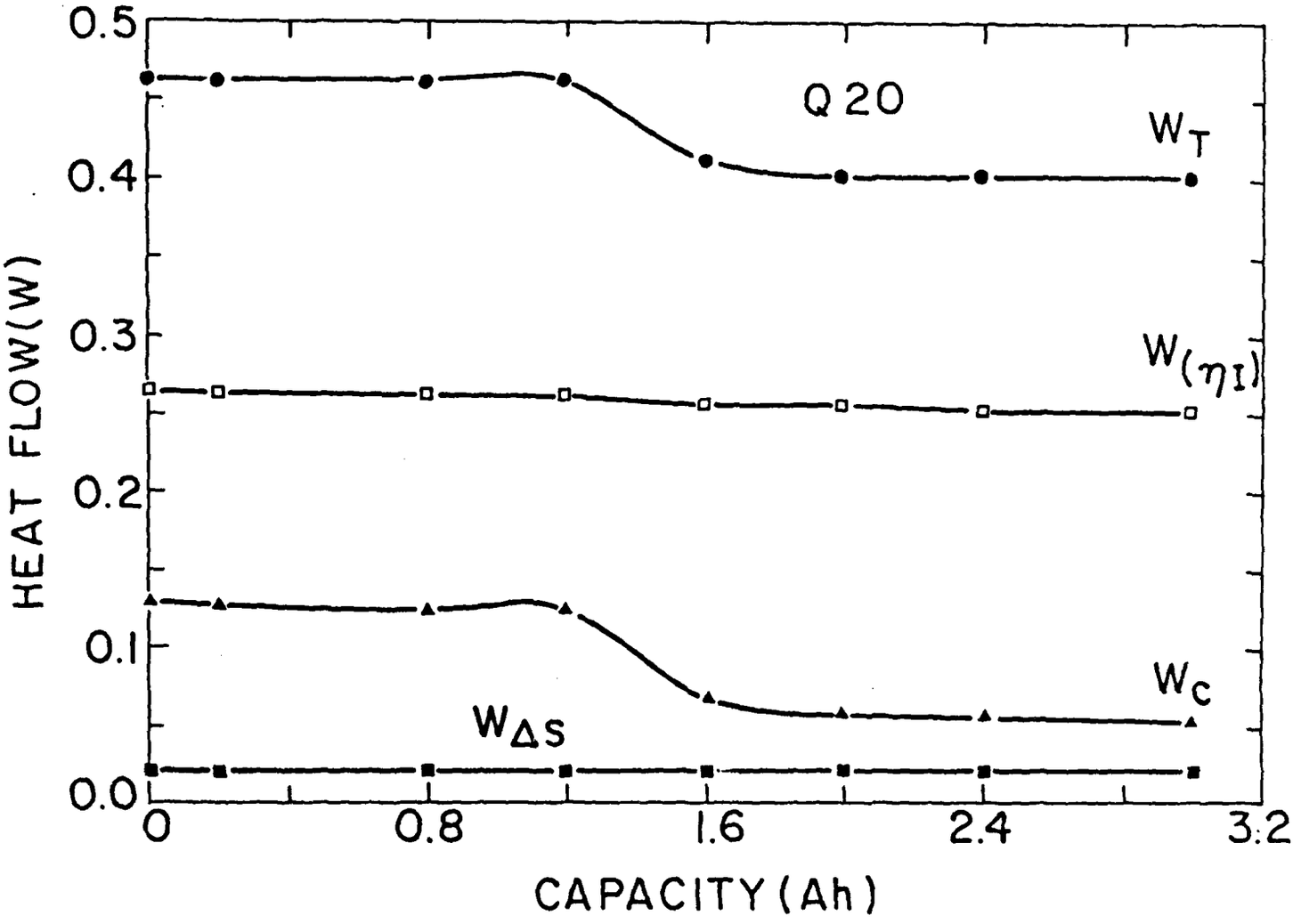
0.5
0.4
0.3
0.2
0.1
0.0
HEAT FLOW(W)
Q 20
W_T
$W_{(\eta I)}$
W_C
$W_{\Delta S}$
0
0.8
1.6
2.4
3.2
CAPACITY (Ah)

Fig. 11

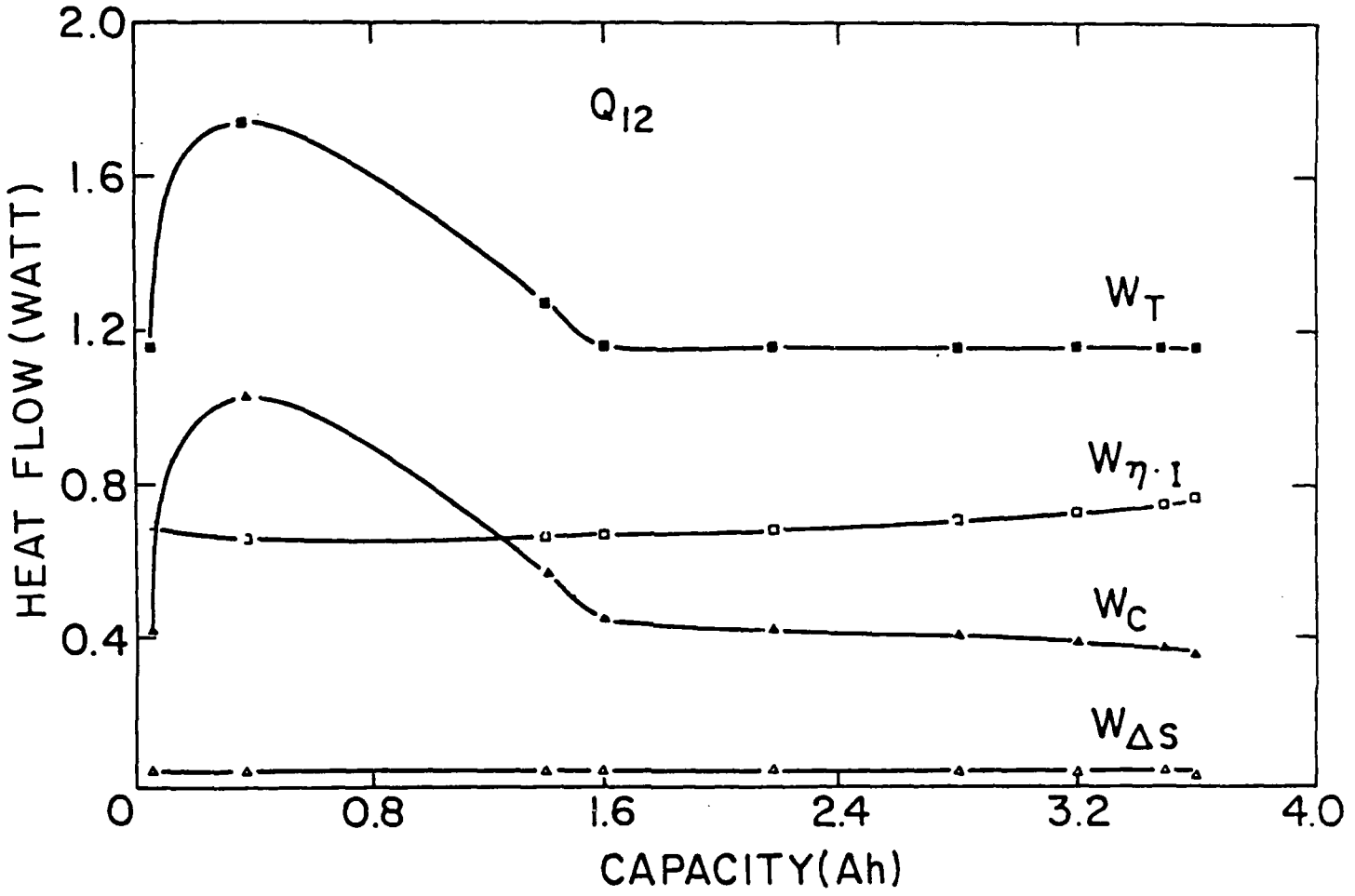
2.0
1.6
1.2
0.8
0.4
0
0.8
1.6
2.4
3.2
4.0
HEAT FLOW (WATT)
CAPACITY(Ah)
Q_{12}
W_T
$W_{\eta \cdot I}$
W_C
$W_{\Delta S}$

Fig. 12

Chapter 2

Calorimetric Study of the $Ca/Ca(AlCl_4)_2$-$SOCl_2$ Battery (baseline system).

Chapter 2:

Calorimetric Study of the Calcium/$Ca(AlCl_4)_2$-$SOCl_2$ Battery (Baseline System)

Introduction

The description of the Ca-TC cell, its properties and the reasons for this calorimetric study can be found in Chapter 1. In addition it contains a description of the calorimeter and the experimental procedures.

The goal of this work was to study the effect of current density, 70°C storage and temperature on: W_T - overall thermal power output of the cell during discharge; W_p - polarization thermal power (overpotential times the current); W_c - thermal power which results from chemical reactions; I_c - the corrosion current of the anode during discharge; ϵ - differential faradaic efficiency of the calcuim anode.

Chapter 1 explains how these parameters were measured and calculated.

Experimental

All experimental procedures have been described in Capter 1, except for the composition of the Ca/Ca^{++} - TC cell and the discharge mode.

The Ca/Ca^{++}-TC cell

A hermetically sealed C-size cell was used as a test vehicle. It was assembled with a Hudson SS can and cover and a Fusite 435 G/M seal with an electrolyte-filling tube. The anode was 0.5mm thick, 40mm width, Pfizer 99.9% calcium foil. The cathode was 0.8mm thick, 40mm width, teflon bonded carbon electrode supported by a nickel Exmet. The separator was 0.12mm thick glass separator. The active electrode area was 130 cm^2. The cells were filled with 0.9M $Ca(AlCl_4)_2$ + 7% (V/V)SO_2 TC solution. Cells were discharged inside the calorimeter at constant current at either 30 or 55°C. A home-made computerized data-acquisition system based on IMS model 8000 computer has been used for these tests.

Results

Two sets of cells have been tested: 4 fresh cells and 4 cells which were stored at 70°C for 2 weeks and then at room temperature for 1-3 weeks. Both groups were discharged at the temperatures of 30°C & 55°C and at constant currents of 285mA and 580mA. The average current densities associated with these currents were about 2.2 and 4.4 $mAcm^{-2}$ respectively.

Figs. 1-7 shows the results of the discharge tests of fresh and stored cells. All cells - fresh and stored - exhibit flat discharge curves with no voltage delay (below 2V).

The calorimetric plots (W_T vs. capacity) of fresh cells have a peak at the beginning of the discharge, then a flat or sloping region and all increase towards the end of the discharge. The calorimetric plots of the stored cells show no initial peak.

Table 1 summarizes the test results. At 55°C the cells had a higher working voltage and produced more heat than at 30°C. At 285mA discharge rate, increasing the discharge temperature from 30 to 55°C resulted in a decrease in the capacity. However at 580mA discharge rate the opposite is true. Two weeks of storage had no significant effect on the thermal power output at 285mA discharge rate but resulted in about 20% increase in $W_{T,a}$* at 580mA discharge rate at 30°C. The average** discharge voltage at 30°C and 285mA discharge rate was not affected by the storage. However, at 55°C the average voltage was 0.25V lower after storage. The average discharge voltage at 30° and 580 mA was also lower after storage. At 55°C the stored cell failed to discharge at all above 1V. Cells lost 25-100% of their capacity after two weeks of storage at 70°C.

* $W_{T,a}$ - total thermal output at 50% DOD (a=average).

** Average - at 50% DOD.

Discussion

As mentioned before our goal was to study the effects of temperature, discharge rate and 70°C storage on W_T, W_p, W_c, I_c and ϵ of the Ca/CaX_2-$SOCl_2$-7% SO_2/C cell ($X=AlCl_4$) and to make a comparison between this cell and the Ca/SrX_2-$SOCl_2$-7% SO_2/C cell presented in Chapter 1. We used the same calorimeter which has a noise level of ± 15-20 mV (~± 20mW). Thus we expected an error in W_T of about 1.5-4%. The components of W_T, I_c and ϵ were calculated as described in Chapter 1 with the use of the same ΔS, ΔG values, and taking the same assumptions. Table 2 summarizes the calorimetric data and Figs. 8-14 show the plots of the components of W_T vs. the discharge capacity of the fresh and stored cells. As the response time of the calorimeter is about 30 minutes the initial portions of the calorimeteric data in all plots were omitted. The cells were discharged at a constant current, thus W_s is constant during the discharge. As the discharge voltage decreases gradually with DOD, W_p increases. At the end of the galvanostatic discharge the discharge voltage drops sharply and W_p rises sharply. Fresh cells discharged at 30°C exhibit more pronounced W_c- peak. In all other cases W_c shows an initial vague peak and decreases with DOD. We think that the initial peak of W_c is associated with the changes of the morphology and the composition of the PL of the calcium.

In fresh cells the composition of this PL is mostly CaO. During storage CaO is converted to $CaCl_2$. This process is accelerated by increasing the temperature. Stored cells show no significant W_c peak at the beginning of the discharge, as most of the CaO in the PL was converted to $CaCl_2$.

At 30°C discharge tests of fresh cells, the contribution of W_p is larger than that of W_c, however at 55°C the opposite is true. The lower discharge voltage (average) of stored cells may result from a partial clogging of the surface of the anode and the separator by the corrosion products of the anode

(i.e. $CaCl_2$ and S). This is why the $W_{c,a}$* of a stored cell (R12) discharged at 55°C is lower and its ϵ is higher than those values of a fresh cell (R11). Increasing the discharge temperature from 30 to 55°C, doubles $W_{c,a}$ and $I_{c,a}$**. It means that the SEI provides less protection against corrosion at 55°C than at 30°C. It seems that for fresh cells $W_{c,a}$ and $I_{c,a}$ increase roughly linearly with the current density. For stored cells $W_{c,a}$ and $I_{c,a}$ increases about 50% more than the increase in the current density. While the current density has a minor effect on ϵ it was found that increasing the temperature from 30 to 55°C has a pronounced effect on it - ϵ droped from 88-90% to 72-75%. It means that at 55°C and 4.4mA/cm^2 28% of the calcium is consumed by corrosion.

Table 3 presents a comparison between the Ca/Sr^{++} and the Ca/Ca^{++} systems. The most pronounced difference between the two systems is expressed in their storage ability. The Ca/Ca^{++} cells lost 25-100% of its capacity after two weeks of storage at 70°C while the Ca/Sr^{++} cells lost almost no capacity after four weeks of storage at this temperature. The thermal power generated by the Ca/Sr^{++} cell is similar or smaller than that produced by the Ca/Ca^{++} cell.

The corrosion current (at 50% DOD) of the calcuim anode ($I_{c,a}$) during discharge is similar to that of Ca/Sr^{++} cells at 30°C. However, at 55°C $I_{c,a}$ of the Ca/Sr^{++} cells is much smaller than that of the Ca/Ca^{++} cells. As a result the faradaic efficiency of the Ca/Sr^{++} cell is similar or higher than that of the Ca/Ca^{++} cell. The lower ϵ values obtained for the Ca/Ca^{++} cell at 55°C are in agreement with its lower delivered capacity at this temperature.

* $W_{c,a}$ = at 50% DOD.

** $I_{c,a}$ = at 50% DOD.

TABLE 1 : Discharge data

Fig. No.	Cell Code	Discharge Temp. [°C]	Discharge Current [mA]	Average# Voltage [V]	Capacity 2V Cutoff [Ah]	$W_{T,a}$# Heat Flow [W]
1	R_9*	30	285	2.56	3.44	0.46
2	R_{11}*	55	285	2.88	3.05	0.58
3	R_6*	30	580	2.44	2.60	1.03
4	R_5*	55	580	2.79	2.73	1.36
5	R_3**	30	285	2.52	2.45	0.48
6	R_{12}**	55	285	2.66	2.34	0.56
7	R_4**	30	580	2.28	1.67	1.21
	R_{10}**	55	580	<1	-	-

* Fresh Cells.

** Stored Cells - 14 days at 70°C and 1-3 weeks at R.T.

at 50% DOD.

TABLE 2: Calorimetric test results

Cell Code	Discharge Temp. (°C)	Average# Voltage (V)	Discharge Current (mA)	$W_{p,a}$# (W)	$W_{c,a}$# (W)	I_c# mA	W_c Peak (W)	ϵ# (%)
R_9*	30	2.56	285	0.31	0.12	32	0.27	90
R_6*	30	2.44	580	0.71	0.28	75	0.51	88
R_{11}*	55	2.88	285	0.21	0.35	93	0.40	75
R_5*	55	2.79	580	0.49	0.83	222	0.96	72
R_3**	30	2.52	285	0.32	0.13	35	0.22	89
R_4**	30	2.28	580	0.80	0.37	99	0.42	85
R_{12}**	55	2.66	285	0.28	0.26	69	0.36	80

* Fresh cells.

** Stored cells - 14 days at 70°C and 1-3 weeks at R.T.

at 50% DOD.

TABLE 3 - Comparison between Ca/Sr^{++} and Ca/Ca^{++} systems

Temp. (°C)	Av.c.d.$^{\Delta}$ ($mAcm^{-2}$)	Ca/Sr^{++} Systems				Ca/Ca^{++} system			
		Capacity (Ah)	$W_{T,a}$# (W)	$I_{c,a}$# (mA)	ϵ# (%)	Capacity (Ah)	$W_{T,a}$# (W)	$I_{c,a}$# (mA)	ϵ# %
55*	2	4.2	0.42	43	87	3.05	0.58	93	75
55*	4	3.7	1.20	118	84	2.73	1.36	222	72
30*	2	3.4	0.49	35	88	3.44	0.46	32	90
30*	4	2.2	1.10	76	88	2.60	1.03	75	88
55**	2	4.0	0.47	47	86	2.34	0.56	69	80
55**	4	3.6	1.21	127	83	0			
30**	2	3.4	0.46	29	89	2.45	0.48	35	89
30**	4	2.2	1.10	68	89	1.67	1.21	99	85

* Fresh cells.

** Stored cells: Ca/Ca^{++} - 2 weeks at 70°C and 1-3 weeks at R.T.
Ca/Sr^{++} - 4 weeks at 70°C and 1-4 weeks at R.T.

Δ The actual values varied between 1.7 to 2.2 and 3.5 to 4.4 mA.

\# at 50% DOD.

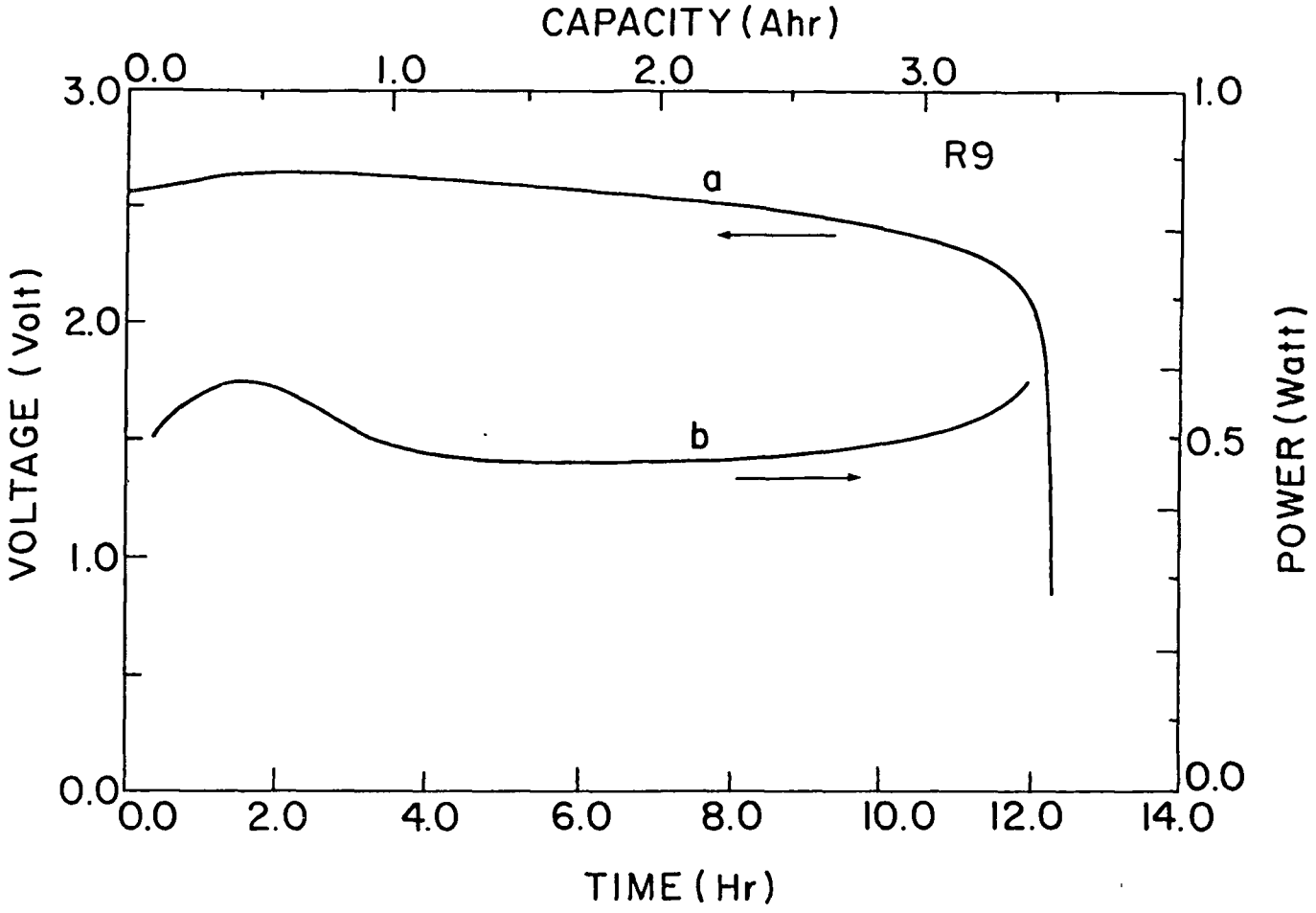

Fig.1: Discharge (line a) and calorimetric(line b)curves of C-size Ca/0.9M CaX_2-TC +7% (V/V) SO_2cell; a fresh cell, 285mA, 30°C.

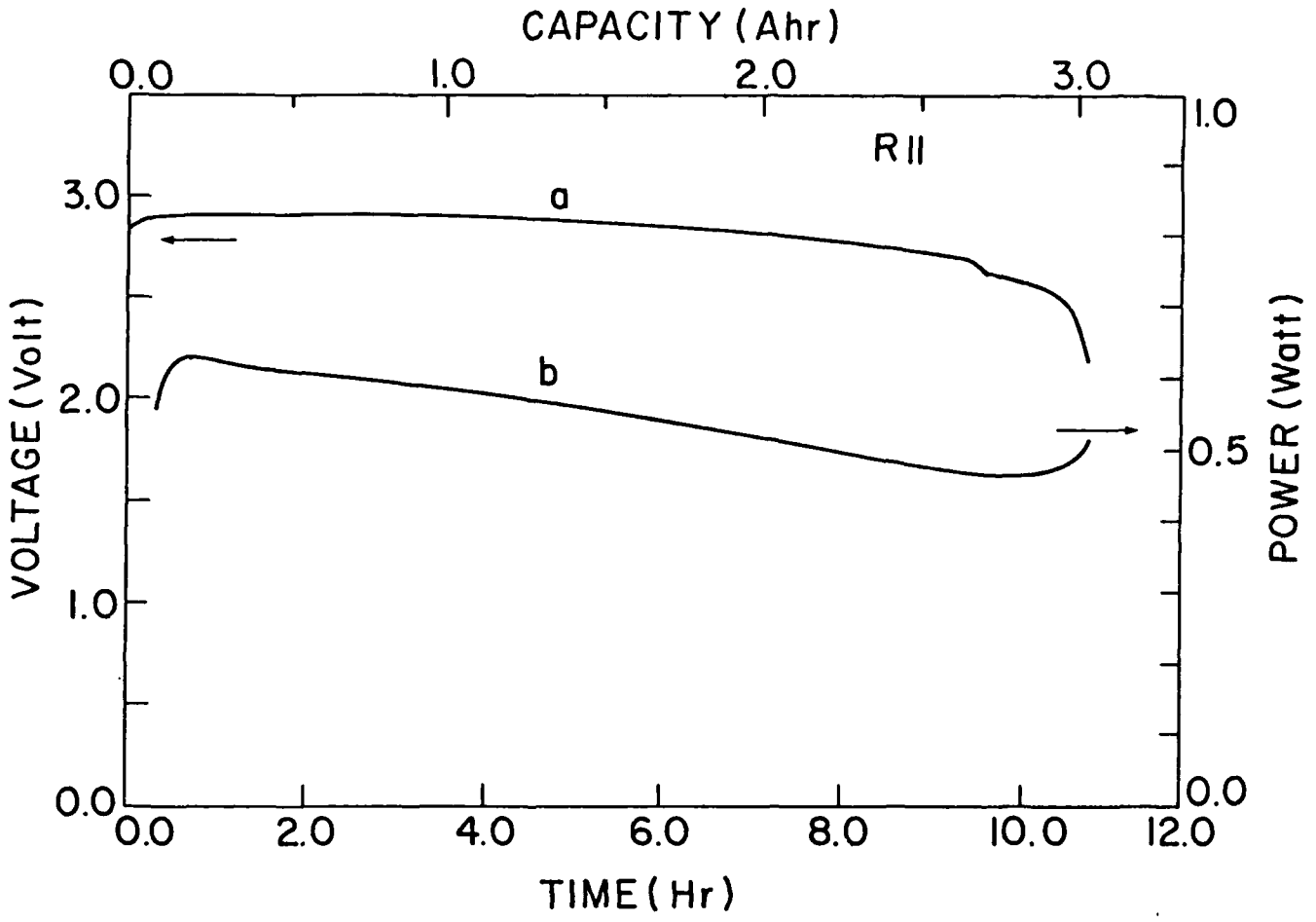

Fig. 2: Discharge (a) and calorimetric (b) curves of a fresh cell, 285mA, 55°C.

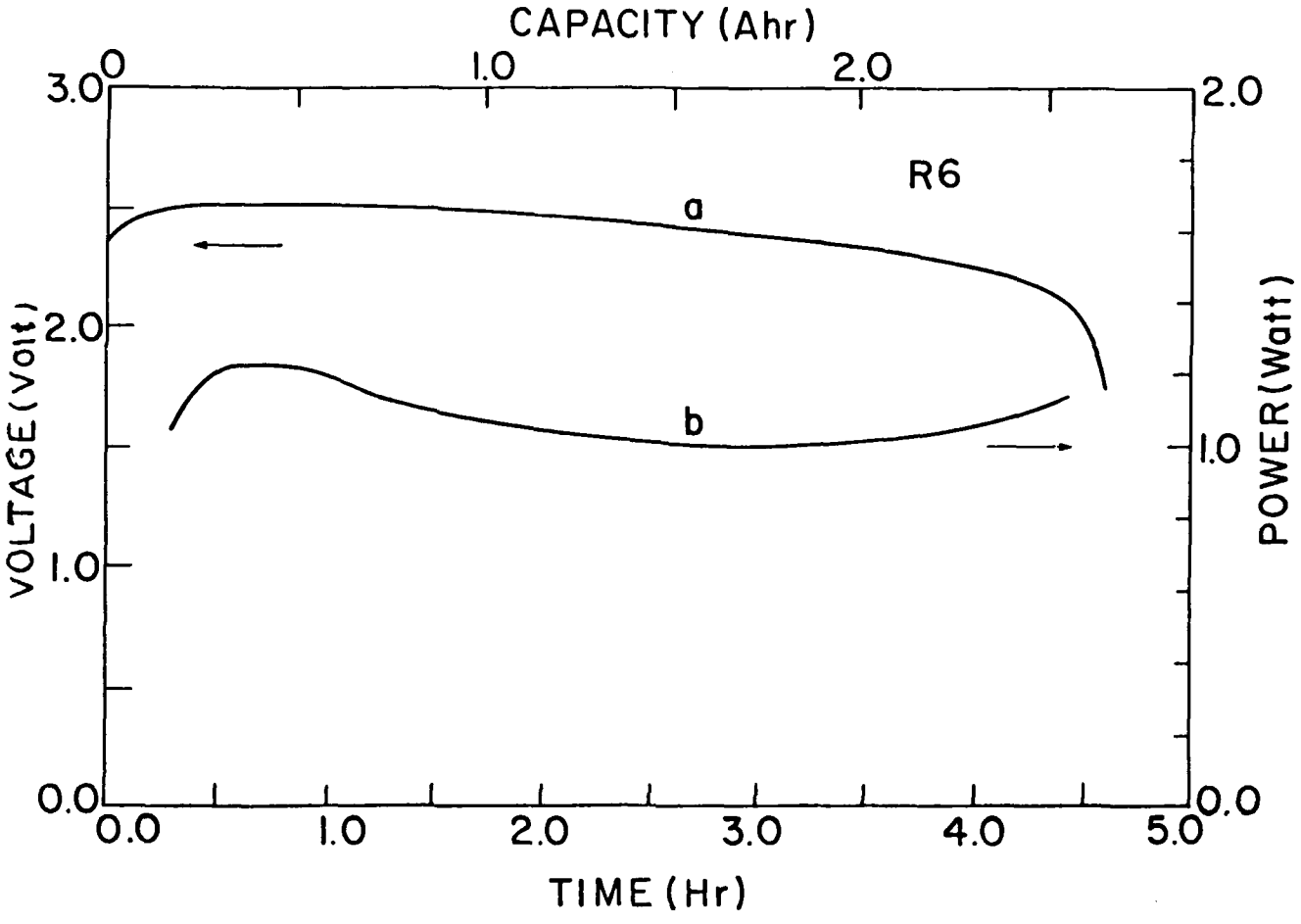

Fig.3: Discharge (a) and calorimetric (b) curves of a fresh cell, 580mA, 30°C.

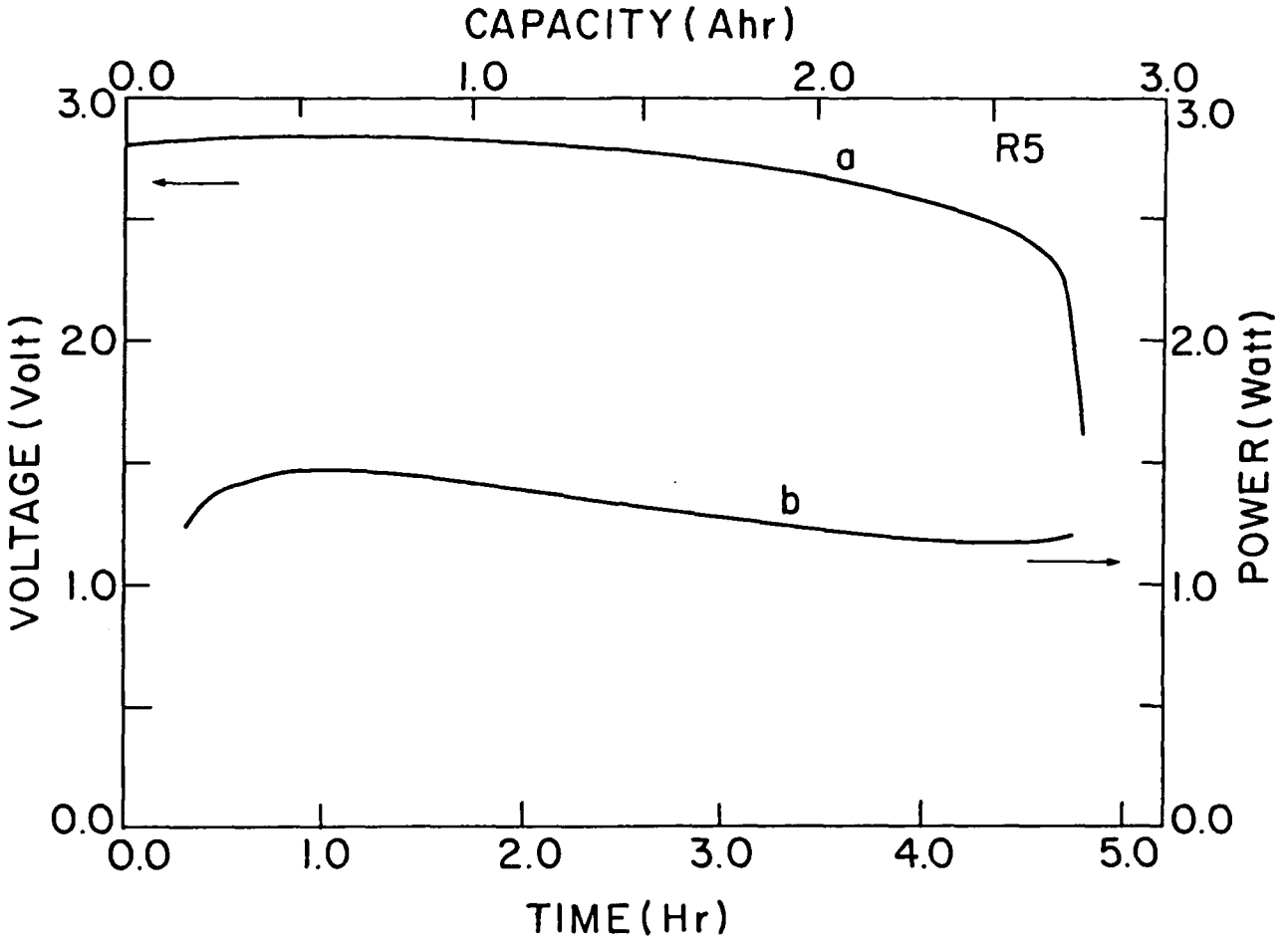

Fig.4: Discharge (a) and calorimetric (b) curves of a fresh cell, 580mA, 55°C.

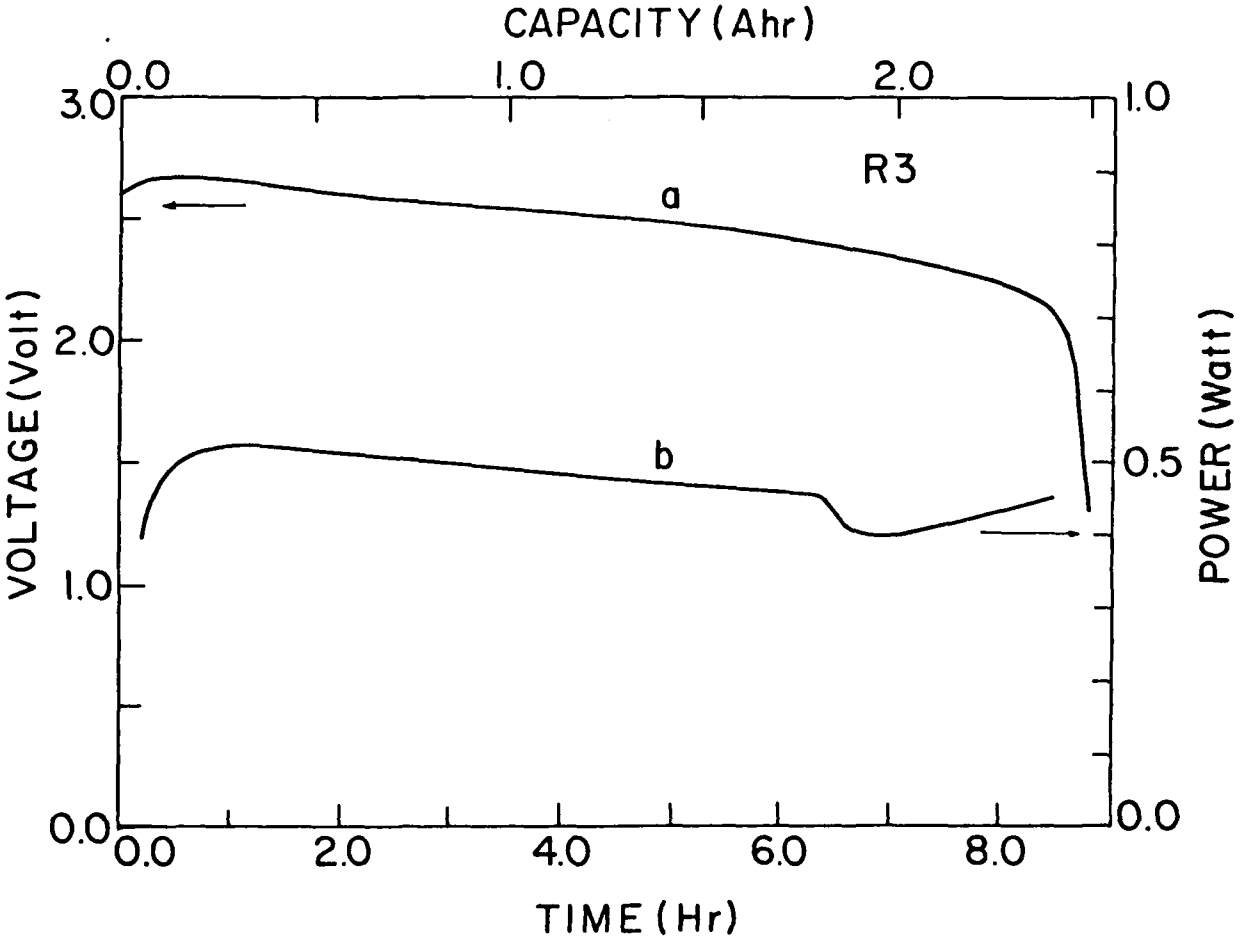

Fig.5: Discharge (a) and calorimetric (b) curves of a stored cell (70°C, 2 weeks) 285mA, 30°C.

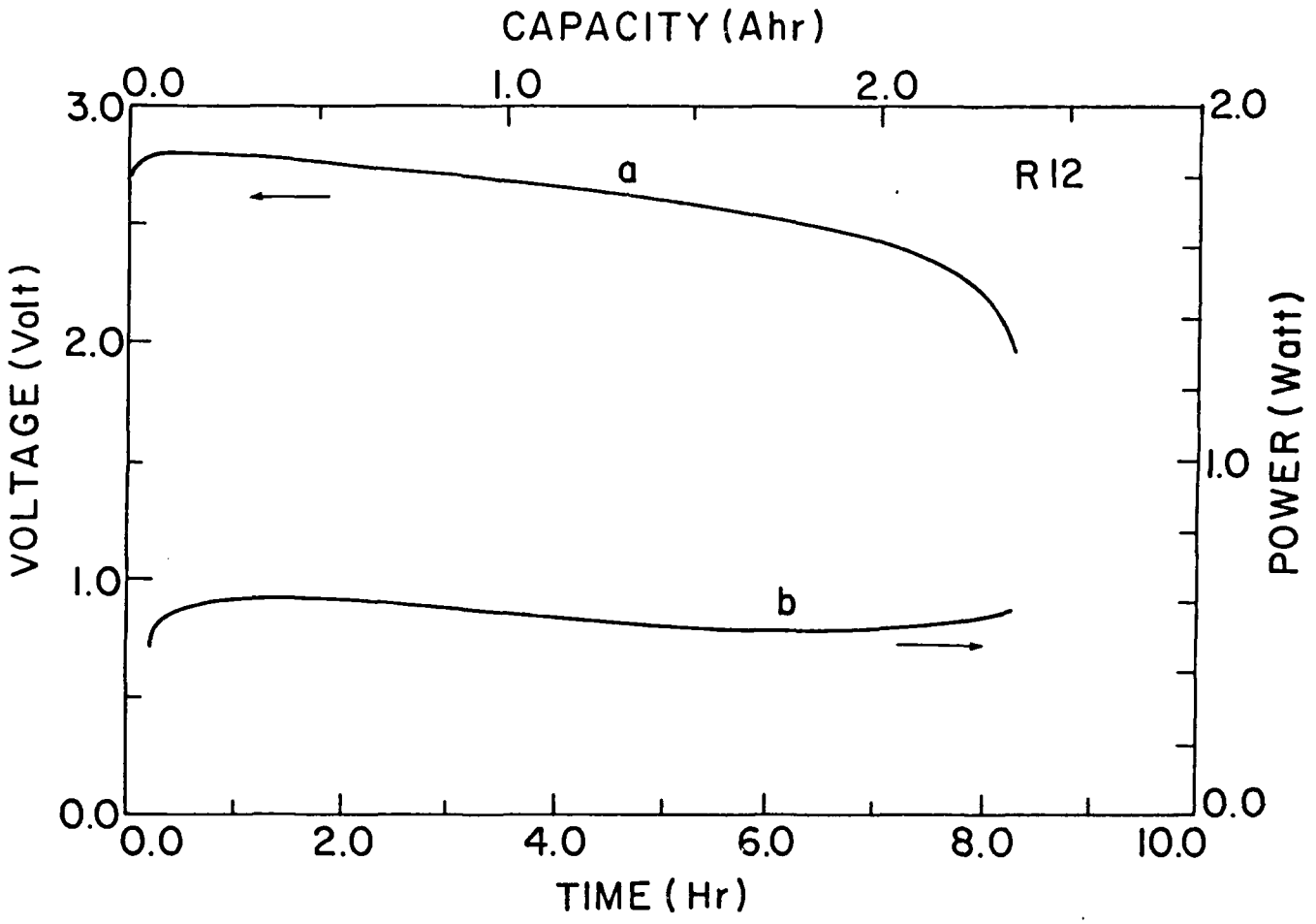

Fig.6: Discharge (a) and calorimetric (b) curves of a stored cell (70°C, 2 weeks), 285mA, 55°C.

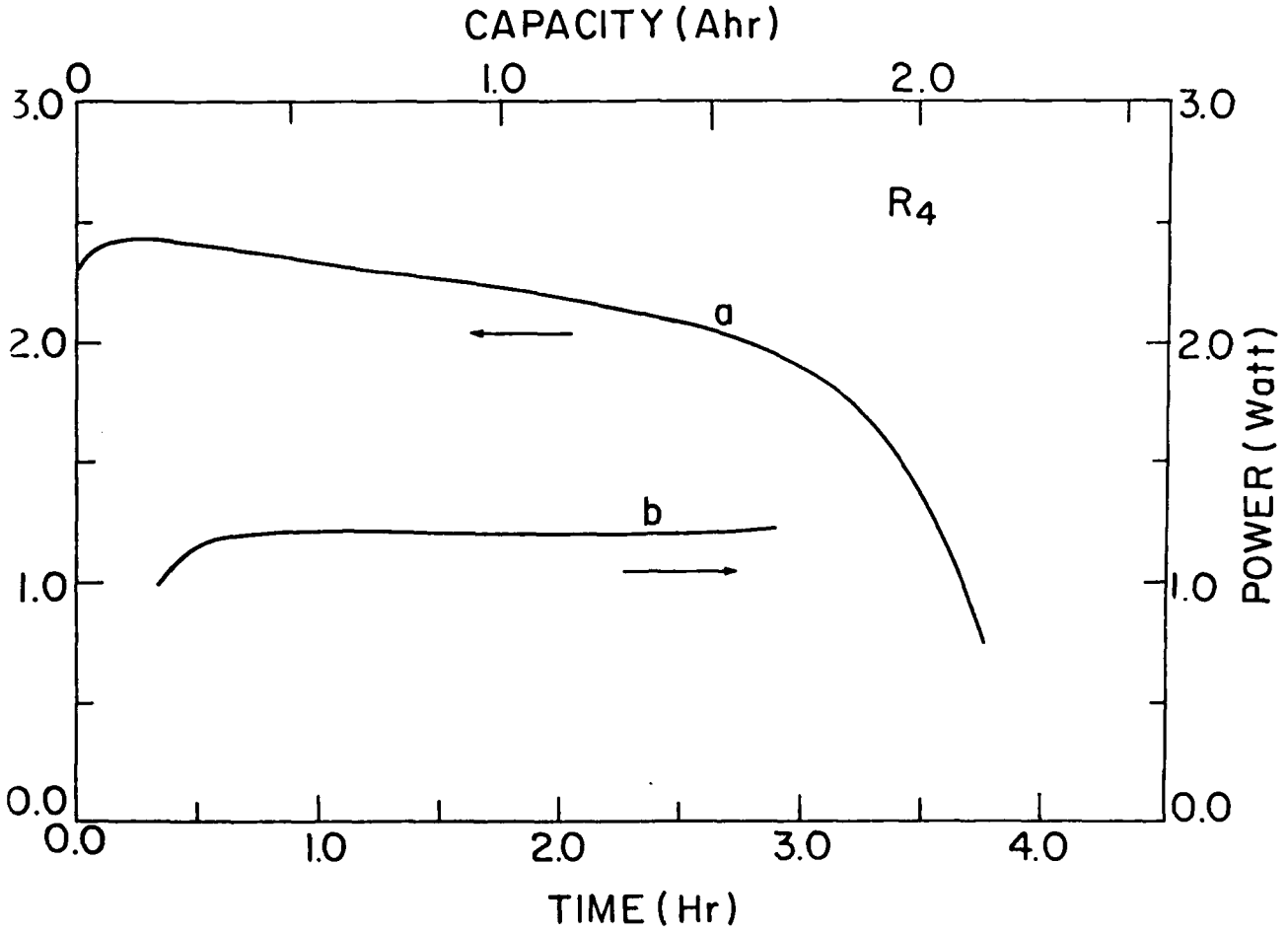

Fig.7: Discharge (a) and calorimetric (b) curves of a stored cell (70°C, 2 weeks), 580mA, 30°C.

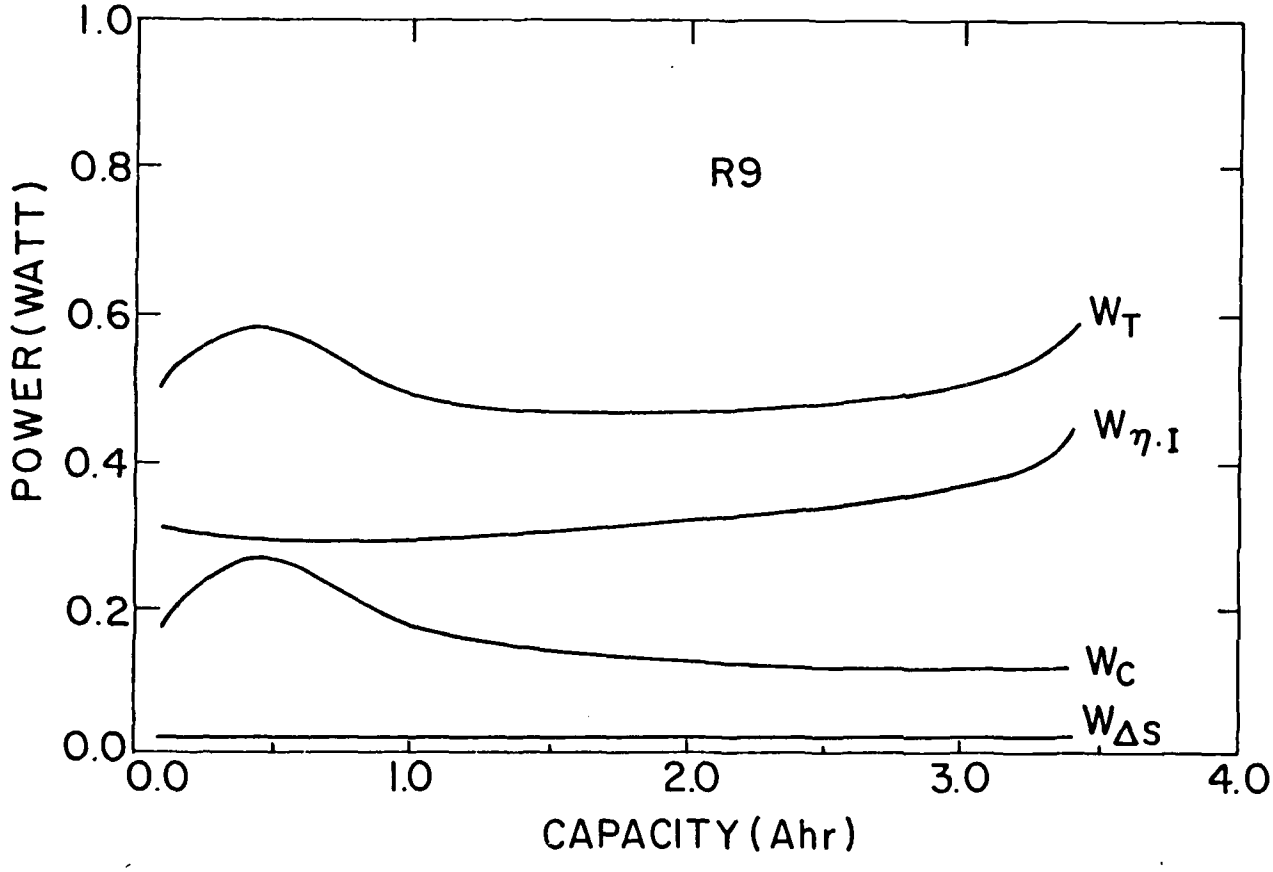

Fig.8: Plots of W_T, W_p, W_c and W_s vs. discharge capacity; a fresh cell, 285 mA, 30°C.

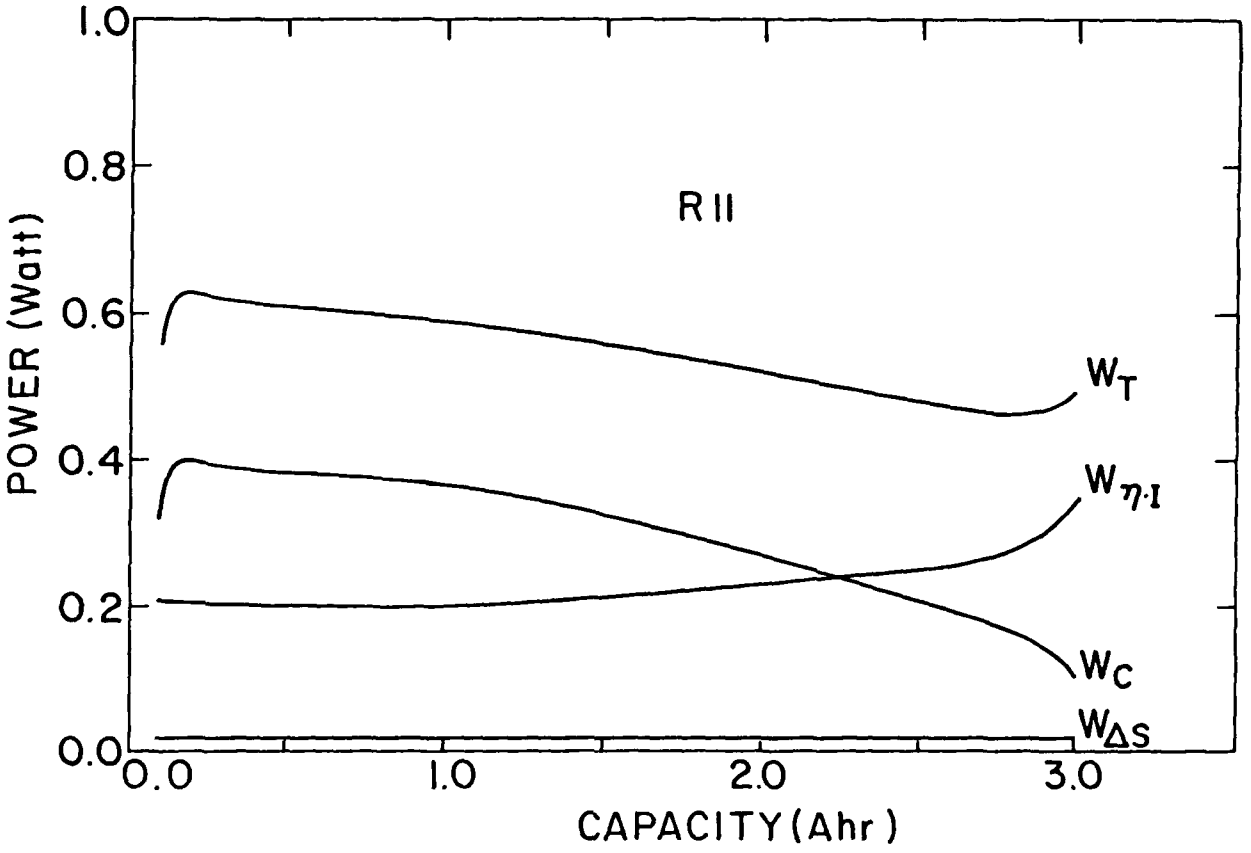

Fig.9: Plots of W_T, W_p, W_c and W_s vs. discharge capacity; a fresh cell, 285mA, 55°C.

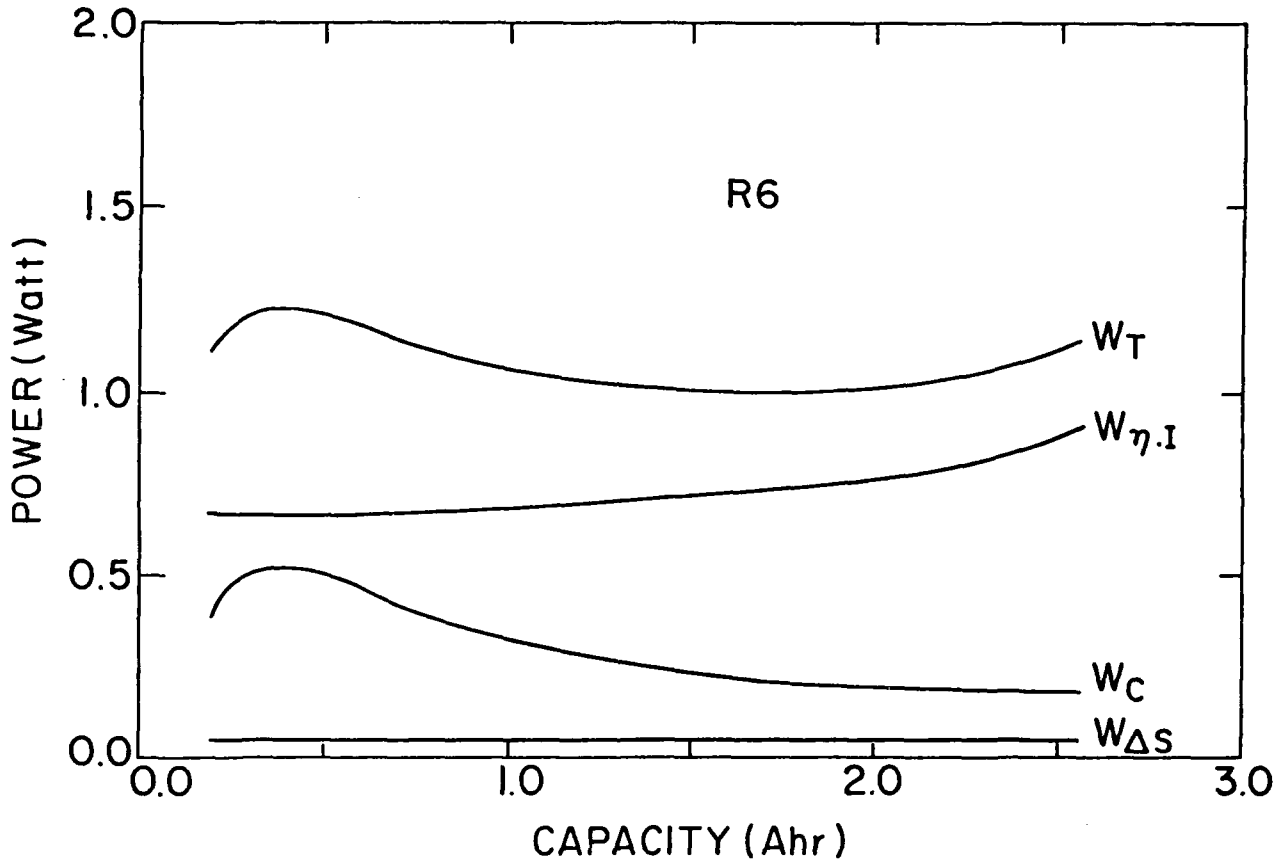

Fig.10: Plots of W_T, W_p, W_c and W_s vs. discharge capacity; a fresh cell, 580mA, 30°C.

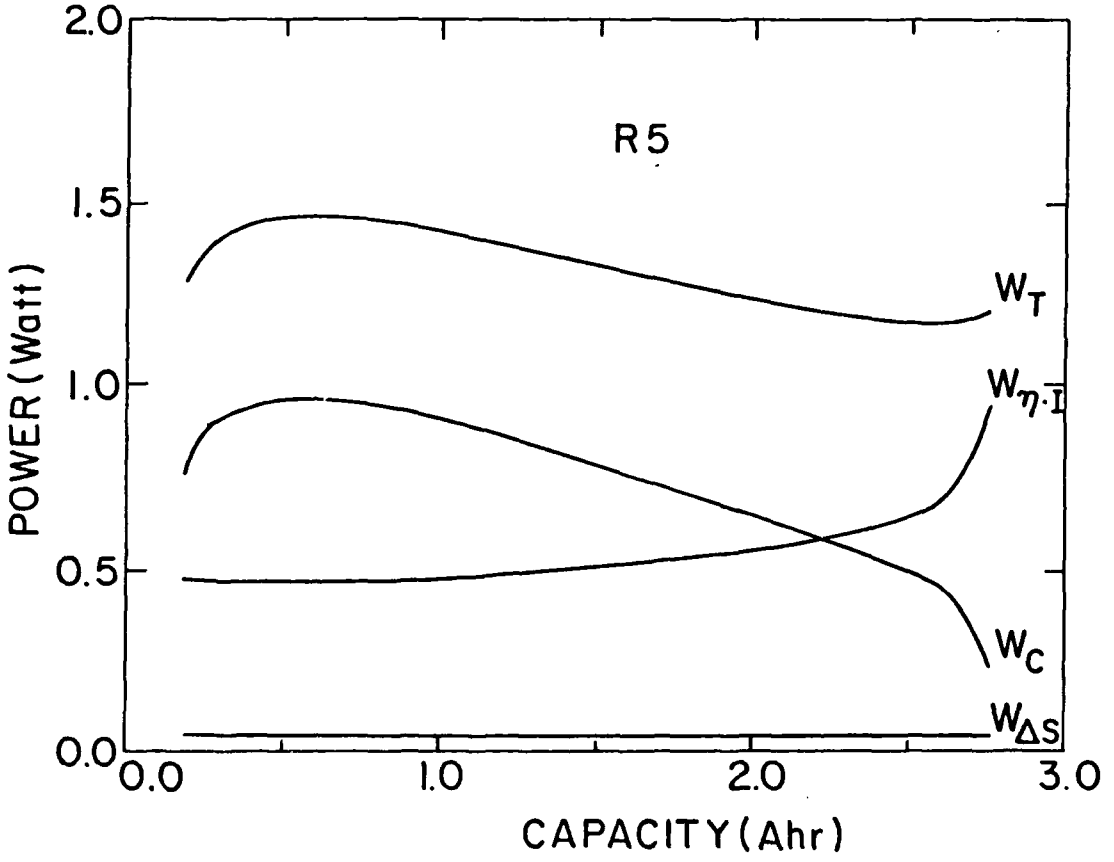

Fig.11: Plots of W_T, W_p, W_c and W_s vs. discharge capacity; a fresh cell, 580mA, 55°C.

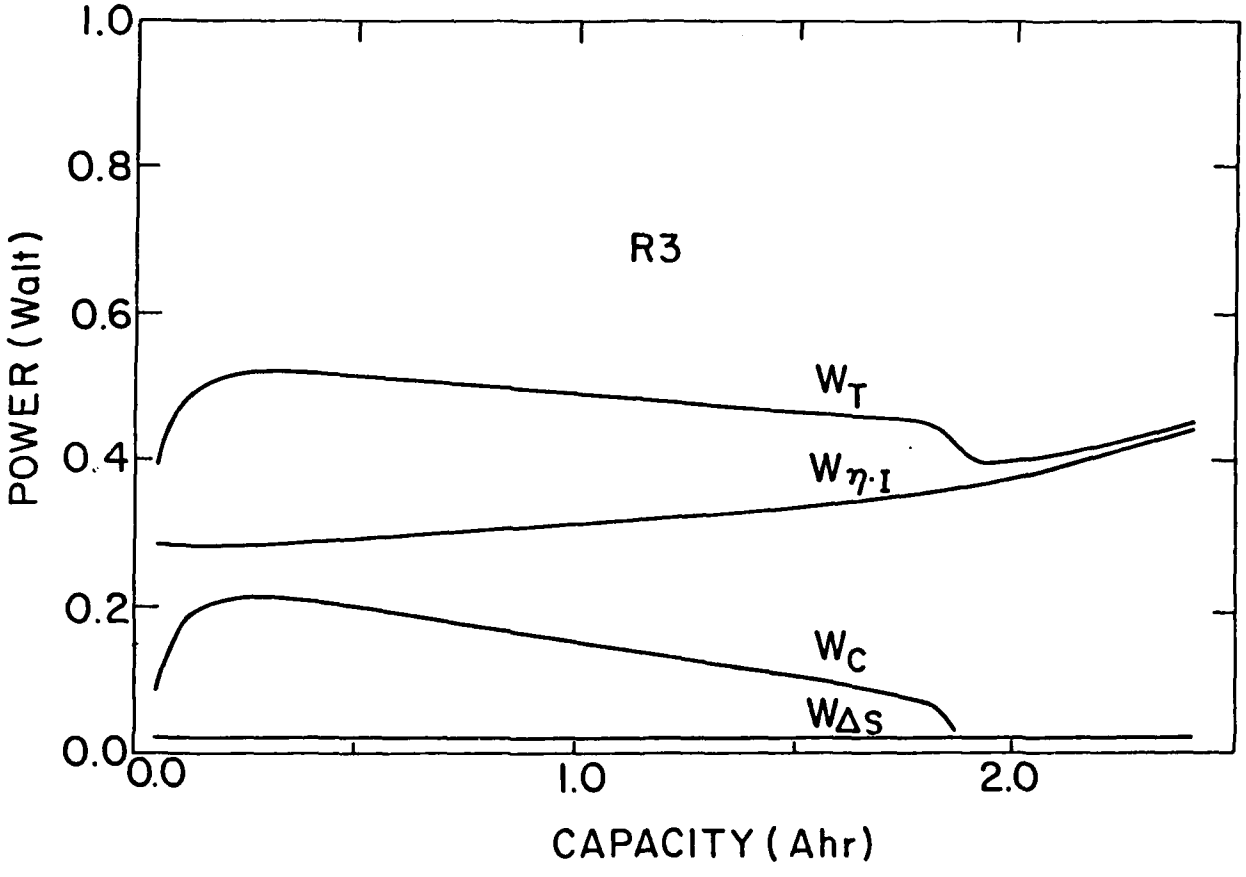

Fig.12: Plots of W_T, W_p, W_c and W_s vs. discharge capacity; a stored cell (70°C, 2 weeks), 285mA, 30°C.

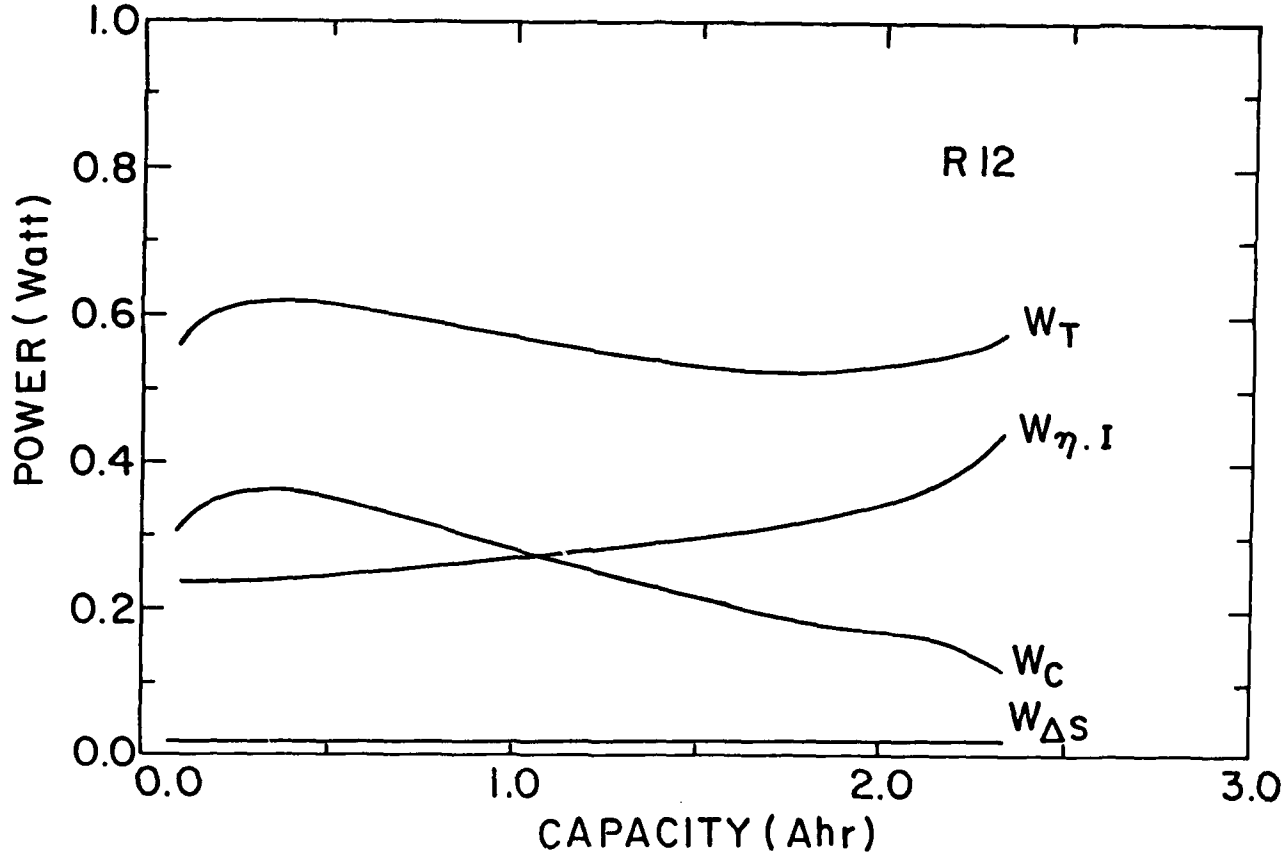

Fig.13: Plots of W_T, W_p, W_c and W_s vs. discharge capacity; a stored cell (70°C, 2 weeks), 285mA, 55°C.

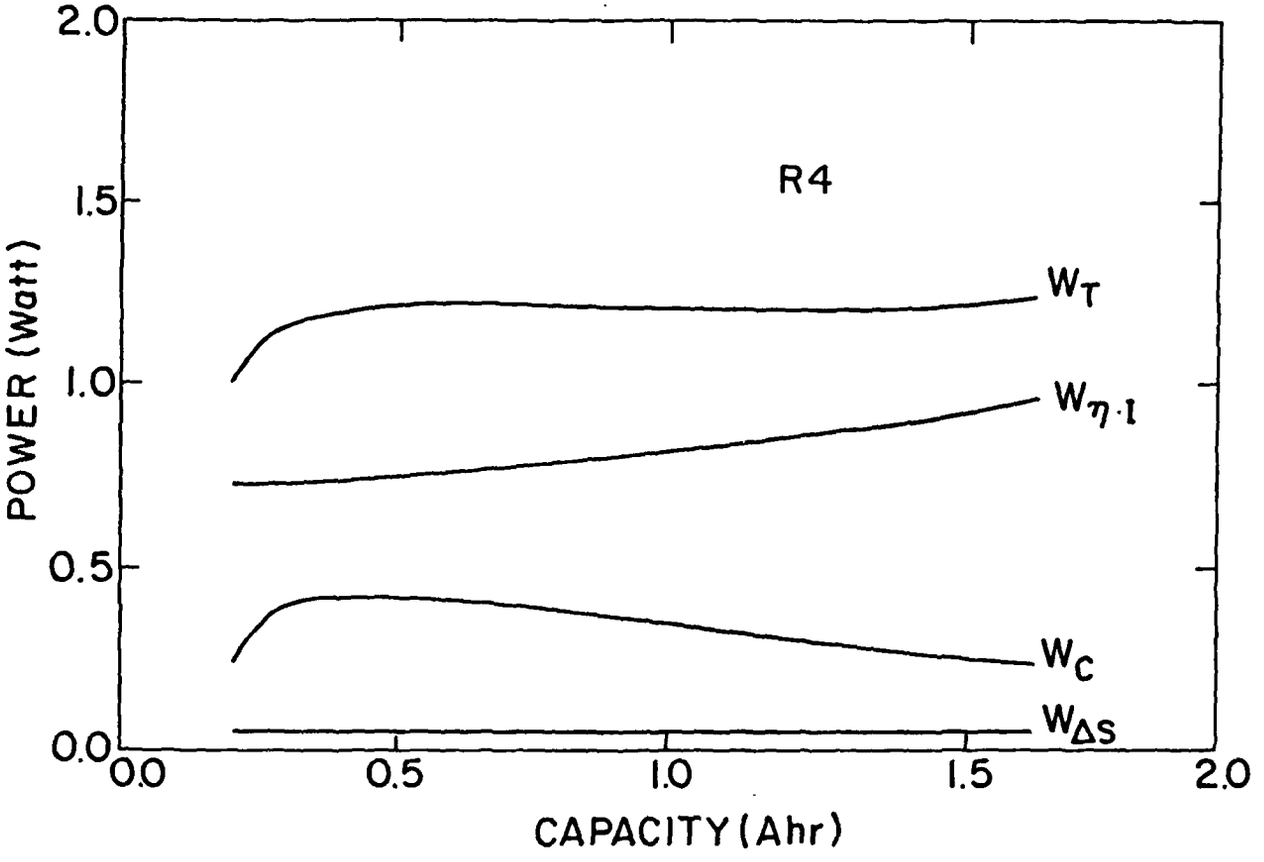

Fig.14: Plots of W_T, W_p, W_c and W_s vs. discharge capacity; a stored cell (70°C, 2 weeks), 580mA, 30°C.

Chapter 3

Storage Properties, Performance and Safety of C-size Calcium-TC Cells.

This report has been presented at the 33rd Power Sources Conference, June 1988.

Chapter 3

Storage Properties, Performance and Safety of C-size Calcium-TC Cells

Introduction

After being fully developed the calcium-thionyl chloride battery should have up to 50% higher volumetric energy density that the Li-SO_2 battery. Thus, per unit of energy, it should be more economical. The calcium-thionyl chloride cell can be produced as a safe vent-free cell which will not rupture or leak over a wide range of abusive conditions including: short-circuit, partial mechanical compression (internal short-circuit), forced discharge and charging.

Its major drawback has been rapid corrosion of the calcium anode (i.e. too short a shelf life). This high rate of corrosion in the CaX_2 ($X=AlCl_4$) electrolyte results from the fact that the $CaCl_2$ SEI does not provide the calcium anode with sufficient corrosion protection (1,2,3). In order to improve the SEI properties the CaX_2 electrolyte has been replaced by SrX_2 or BaX_2 electrolytes (2,3). As a result, both the morphology and the chemical composition of the passivating layer were changed. In both electrolytes the corrosion rate of calcium is slower than in the CaX_2 electrolyte. C-size laboratory stainless-steel cells employing these electrolytes successfully underwent a four weeks storage test with minimal loss of capacity (2).

In this paper we compare the storage ability of the Ca/CaX_2-TC cell with that of the Ca/SrX_2-TC cell and evaluate the safety and the performance of the latter.

Experimental

A hermetically sealed C-size cell was used as a test vehicle. In the past it was found that the G/M seal leaked and so it was replaced by a Fusite G/M seal which contains an electrolyte-filling port. This change solved the leakage problem. The cell has a stainless-steel can and cover. Two versions of cells have been used: one with a 0.15mm thick nonwoven glass separator and 130 cm^2 electrode area and the other with a 50 M thick Tefzel separator and 150 cm^2 electrode area. The electrolytes used were: 0.9M CaX_2 + 7% (V/V) SO_2, 0.84M SrX_2 + 7% SO_2 and 0.75 M SrX_2 in TC. Some of the storage, discharge and safety tests were carried out at Tadiran.

Results and discussion

This paper should be treated as an interim report since the research is in progress and not all tests have been completed. In order to demonstrate the better storage properties of the Ca/SrX_2-TC cell we built and tested base-line cells with the state-of-the-art CaX_2 electrolyte. We previously found (1,2,4,5) that SO_2 increases the conductivity of the MX_2 (M=Ca,Ba,Sr) electrolytes and decreases its viscosity; thus it should improve cell performance. The optimal SO_2 and electrolyte concentration have yet to be found. Filling cells with electrolytes having SO_2 concentration higher than 10% seems to have two disadvantages: it may decrease the working voltage of the cell and it requires a positive pressure for filling. Thus, as a first choice, we decided on only 7% (V/V) SO_2 concentration. For a comparison we also discharged cells with no SO_2 added.

Table I summarizes the results of the discharge tests of fresh and stored cells. Cells were discharged at several rates over a temperature range of -30 to +60°C.

Properties of Ca/0.9M CaX_2 + 7% SO_2 cells

At 25°C fresh cells delivered 3.4Ah and 3.2Ah across 10 and 4.6 respectively. Cells which were stored for 2 weeks at 70°C lost 30% or 20% of their capacity when discharged at RmT across 4.6 or 10 respectively. After 4 weeks of storage the cell discharged at 25°C across 10 lost 55% of its capacity (Fig.1), while another cell failed to discharge at all.

Properties of Ca/SrX_2 cells

A fresh Ca/SrX_2 cell has a RmT capacity across a 10 load (or 0.25A) similar to that of a Ca/CaX_2 cell (see Table I). However, while the best Ca/CaX_2 cell lost 55% of its capacity after 4 weeks of storage at 70°C the Ca/SrX_2 cell seemed to lose no capacity when discharged at RmT across a 10 load (Fig.1 and Table I). An addition of 7% SO_2 does not seem to affect capacity loss at 70°C storage. One cell which was stored for four weeks at 70°C and discharged at 0.25A at RmT showed a lower discharge voltage (only 2.1V) with oscillations. Similar voltage oscillations were found previously for cells which contained the BaX_2 electrolyte (2). In the case of the SrX_2 electrolyte, tests on about forty cells, showed only two cases of voltage oscillations. At -20°C and 100 mA discharge rate the Ca/SrX_2 cell delivered the same capacity (3.2Ah) as at RmT across a 10 load (Table 1). In addition, 4 weeks of storage at 70°C resulted in minimal capacity loss (6%) and no voltage penalty (Table 1).

At -30°C and 10 load the fresh Ca/CaX_2 cell delivered 2.3Ah (to 1.5V cut-off voltage) while fresh or stored Ca/SrX_2 cells delivered only 1.5Ah. The use of a slighly higher concentration of SrX_2 together

with 7% SO_2 increased capacity at -30°C by 0.5Ah to 1.9-2Ah (across a 10 load) and average discharge voltage by about 100 mV (Fig.2). Both cells, (with or without SO_2), showed no capacity loss when discharged at -30°C across a 10 load. The voltage delay measured for fresh and stored cells at -20°C and -30°C varied between 0 and 100 sec (Table 1).

Cells discharged at 60°C showed 30% less capacity than those discharged at RmT while their discharge voltage was about 0.3V higher. Storage of a cell at 70°C for 4 weeks caused a 15% loss of capacity when it was discharged at 60°C. The lower capacity of 60°C seems to be associated with a high rate of corrosion of the anode during medium to high rates of discharge. This hypothesis has still to be proved. However we found that even at RmT, cells heated up significantly at high discharge rates. The maximum temperature rise of the cell can at RmT discharge was about 2-3°C 10-15°C, 25°C, 45°C and more than 100°C for discharges at about 50mA, 250mA, 500mA, 900mA and 2400mA respectively. Preliminary calorimetric measurements indicated that the heat output of the cell during discharge is more than twice its "internal resistive heat" (overvoltage times the discharge current).

Safety tests of Ca/SrX_2 cells

Safety tests included charge, forced discharge, short circuit, high discharge rate and nail penetration. The results are summarized in Table II. Most of the cells contained a rupture disc type vent in the bottom of the cell; this disc ruptures at 120 to 150°C. Cells with no vent can be safely heated to 250°C. At above 300°C the G/M seal starts to leak. In order to avoid a possible break of the cover-to-can weld we carried out most of the tests with cells which contained the abovementioned vent mechanism. Except for venting, no other hazardous results were experienced. Nail penentration resulted only in electrolyte leakage. Several forced discharge tests were carried out for cells which were discharged under a variety of conditions with current limitation of 0.25A and voltage limitation of 15V. It was found that when some time elapsed between the discharge test and the forced discharge test, the cell did not vent and its temperature rise was 20 to 60°C. In two cases the cell did vent; once when the forced discharge test immediately followed the discharge test and in another case when the cell was forced discharged at 60°C following a -20°C discharge test. The plots of voltage, current and temperature during -10V forced discharge test of a cell that was previously discharged at 0.9A to a cut off voltage of 2V can be seen in Fig.3. This cell rested for two weeks between these two tests. It took about 40 minutes before the cell reached reversal and another 60 minutes before the forced voltage reached -10V and the forced current started to drop. Maximum can temperature reached 80°C. After 320 minutes the forced current decreased below 30mA. It seems that this transition time (the time elapsed between reversal and beginning of current decrease) will decrease if the forced discharge voltage and current decrease. We believe that cell venting was due solely to the pressure rise in the cell as a result of overheating.

It seems that an excellent way to make this cell safe and vent-free is to use a Tefzel separator. In this case it is also possible to increase the electrode area by 15% without changing the electrode thickness. When such a cell is shorted (Fig.4) its short-circuit current reached a maximum value of 8.5A after 4 minutes and then it sharply decreased to less than 0.2A after about 20 minutes. The maximum can temperature was 120°C while the inside cell temperature may be several tens of degrees higher. In this temperature range the Tefzel separator starts to melt and this results in the closing of its pores and an increase in its resistance. When this cell was discharged across a heavy load of 1 , it delivered 0.9Ah at an average current of 2.4A. Cell temperature rose to 125°C and the current dropped to less than 0.2A after 20 minutes from the time the maximum temperature was reached.

Summary

The Ca/CaX_2 cell loses most of its capacity after 4 weeks of storage at 70°C. However the Ca/SrX_2 cell loses only/0-15% of its capacity when discharged over the temperature range -30 to +60°C after being stored for 4 weeks at 70°C. Its voltage delay is 0-100 sec. at -20 and -30°C after such storage. Cells may vent on forced discharge as a result of overheating. The Ca/SrX_2 cell may be made safe and vent-free with the use of a Tefzel separator. On high-rate discharge these cells overheat, possibly as a result of the corrosion of the calcium anode covered by a thin, fresh and disordered SEI.

References

1. E. Peled, Proceedings of the 32nd Power Sources Symposium Cherry Hill, June 1986, p. 445.
2. E. Elster, R. Cohen, M. Brand, Y. Lavi and E. Peled
   a) Electrochemical Society Meeting, Honolulu, Osctober 1987,
   b) J. Electrochem. Soc., in press.
3. E. Elster, R. Cohen and E. Peled
   4th International Meeting on Lithium Batteries
   Vancouver, Canada, May 1988.
4. E. Peled, E. Elster, J. Kimel, R. Cohen and M. Brand
   3rd International Meeting on Lithium Batteries,
   Kyoto, May 1986.
5. R. Cohen, J. Kimel, E. Elster, E. Peled
   4th International Meeting on Lithium Batteries,
   Vancouver, Canada, May 1988.

TABLE I: SUMMARY OF PERFORMANCE

Discharge rate or Load [Ω]	Discharge Temp.	Electrolyte **	Storage 70°C	Ave.cell Voltage	V.D. sec to 2V	Capacity [Ah] to 2V	Remarks
11.2 (240mA)	RmT	A	-	2.7 V	0	3.2	-
*250mA	RmT	A	-	2.8 V	0	2.85	-
10 (280mA)	RmT	A	4 weeks	2.8 V	0	3.2	-
*250mA	RmT	A	4 weeks	2.1 V	0	2.6	Oscill.
10 (270mA)	RmT	A1	4 weeks	2.7 V	0	3.2	-
*(250 mA)	60°C	A	-	3.1 V	0	2.3	-
*(250 mA)	60°C	A	4 weeks	3.05 V	0	2.0	-
*100 mA	-20°C	A	-	2.5 V	42	3.2	-
*100 mA	-20°C	A	4 weeks	2.55 V	0	3	-
10 (180 mA)	-30°C	A	-	1.8 V	10	1.4	(1.5 V)*
10 (190 mA)	-30°C	A	4 weeks	1.9 V	100	1.5	(1.5 V)*
10.3 (200 mA)	-30°C	A1	-	2.0 V	0	1.9	(1.5 V)*
10 (180 mA)	-30°C	A	4 weeks	2.0 V	NA	2	(1.5 V)*
10 (260 mA)	RmT	C	-	2.6 V	0	3.5	
4.6 (570 mA)	RmT	C	-	2.6 V	0	3.2	-
4.1 (560 mA)	RmT	C	2 weeks	2.3 V	0	2.2	-
10.1 (250 mA)	RmT	C	-	2.5 V	0	2.9	-
10.1 (230 mA)	RmT	C	4 weeks	2.3 V	0	1.5	-
10.1 (180 mA)	-30°C	C	-	1.8 V	9	2.4	(1.5 V)*
3 (0.9 A)	RmT	A1	-	2.8 V	0	3.2	Tefzel Sep.
55 (50 mA)	RmT	A1	-	2.7 V	0	4	Tefzel Sep.
1 (2.4 A)	RmT	A1		2.4 V	0	9	Tefzel Sep.

* Tested by Dr. A. Meitav at Tadiran
$ Cut off voltage
** Electrolytes A - 0.75M SrX_2, A1 - 0.84M SrX_2 + 7% SO_2, C - 0.9M CaX_2 + 7% SO_2

TABLE II

SUMMARY OF SAFETY TESTS

Type of test	Previous discharge	Max. cell temp.	Remarks
Forced discharge	RmT, 0.9 A	80°C	2 weeks rest at RmT voltage limit 10 V
Forced discharge*$	RmT, 250 mA	-	Vented after 20 min
Forced discharge*$ 60°C	RmT, 250 mA	78°C	Cell voltage -15 V
Charge*$	RmT, 250 mA	37°C	" " +15 V
Forced discharge*$ 60°C	-20°C,100 mA		Vented at -12.9 V
Forced discharge*$	60°C,250 mA	37°C	-
Forced discharge*$	-20°C,100 mA	48°C	-
Nail penetration*	-	-	-
Short circuit (0.1)	-	120°C	Tefzel separator
Heavy load (1)	-	125°C	" "

---

* Tested by Dr. A. Meitav at Tadiran

$ Current limit 250 mA, voltage limit 15 V

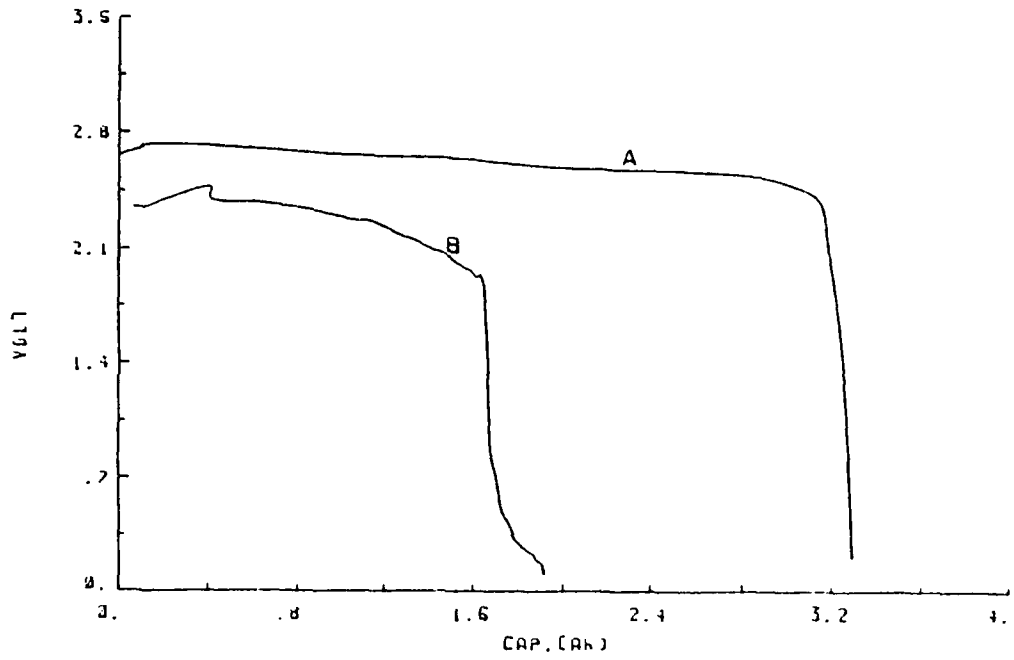

Fig. 1. Discharge curves at RT, after 4 weeks storage at 70°C, 10Ω Load. A: 0.84 M $Sr(AlCl_4)_2$ + 7% SO_2
B: 0.9 M $Ca(AlCl_4)_2$ + 7% SO_2

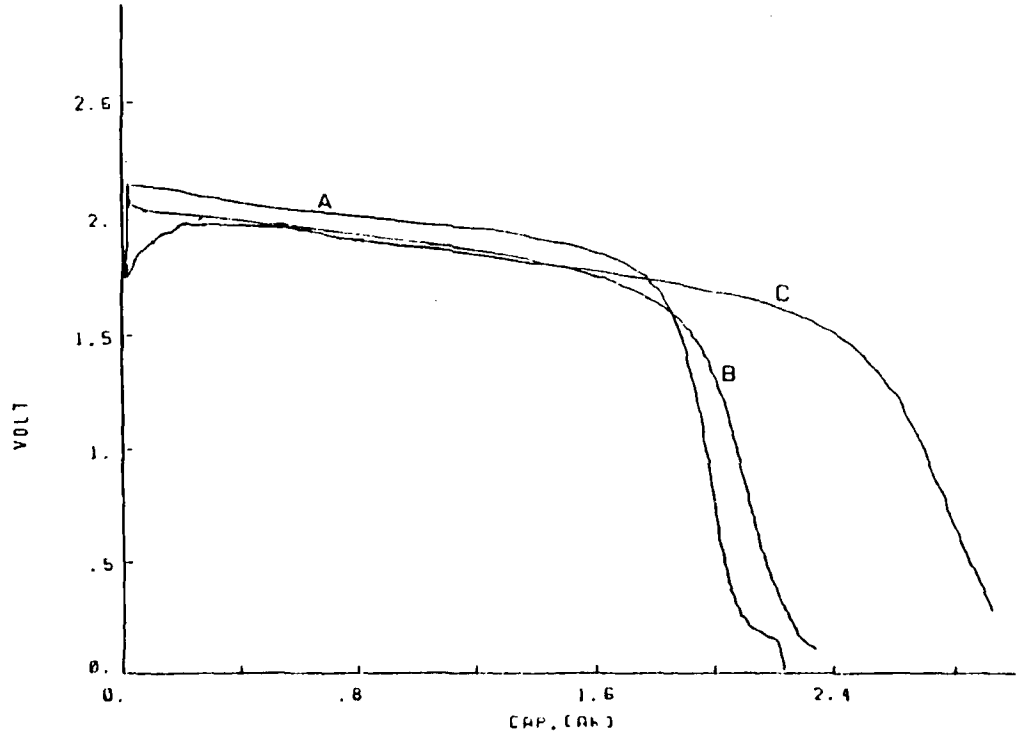

Fig. 2. Discharge curves at -30°C, 10Ω Load. A,B: 0.84 M $Sr(AlCl_4)_2$ +7% SO_2; A-fresh; B-stored cell. C: 0.9 M $Ca(AlCl_4)_2$ + 7% SO_2

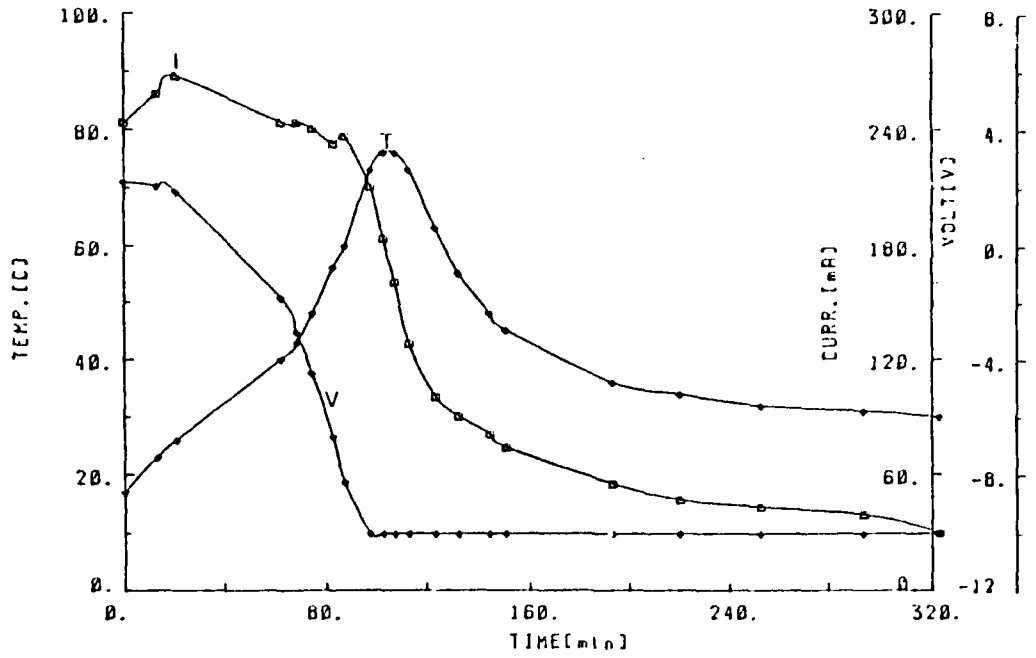

Fig. 3. Forced discharge test of 0.84 M $Sr(AlCl_4)_2$ + 7% SO_2 C-cell

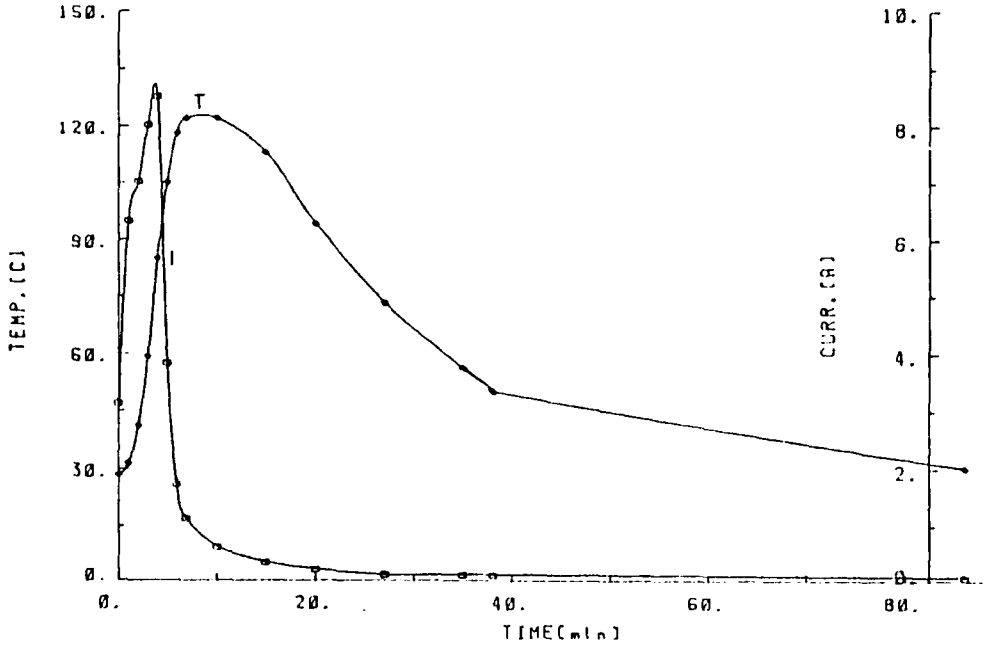

Fig. 4. Short circuit test of 0.84 M $Sr(AlCl_4)_2$ + 7% SO_2 C-cell, 0.1Ω Load.

Chapter 4

Properties of Ca, Sr and Ba Tetrachloroaluminate-SO_2-TC Solutions.

This report has been presented at the 4th IMLB,

Vancouver, May 1988

Chapter 4

Properties of Thionyl Chloride Solutions

Solutions of alkali-metals tetrachloroaluminates in thionyl chloride (TC) exhibit very interesting physicochemical properties [1-3]. They have been studied mainly in connection with the development of the Ca-TC battery. It was recently found [4,5] that replacing the $Ca(AlCl_4)_2$ electrolyte in the Ca-TC battery by either $Ba(AlCl_4)_2$ or $Sr(AlCl_4)_2$ resulted in a battery with a much longer shelf life. This is due to slower calcium corrosion. In these two electrolytes the chemical composition and properties of the SEI which cover the calcium anode are different from that of the SEI in calcium tetrachloroaluminate. These modified SEIs provide better corrosion protection for the calcium anode than does the $CaCl_2$ SEI in the $Ca(AlCl_4)_2$ electrolyte.

The purpose of this paper is to describe the physicochemical properties of TC solutions of calcium, strontium and barium tetrachloroaluminates with emphasis on the effect of SO_2 on the solution properties.

At high salt concentrations in solvents of low dielectric constant like TC (E ~ 9), the predominant species are ionic aggregates [6]. In concentrated MX_2-type solutions in TC ($X=AlCl_4^-$, $M^{++}= Ca^{++}, Sr^{++}, Ba^{++}$) the smallest and most likely predominant charged ionic aggregates are MX^+ MX_3^- formed in the following reaction:

$$2MX_2 \qquad MX^+ + MX_3^- \qquad [1]$$

Accordingly the equivalent conductivity is twice the molar conductivity. These ionic aggregates may be separated by molecules of the solvent (Y), (MYX^+ and $XYMYX^0$ etc) in equilibrium with ionic aggregates with no solvent molecules between the ions.

Density, viscosity (Figs.1-4) and conductivity (Figs.5-10) measurements were made at different SO_2 concentrations in the range 0-50% (V) over a temperature range of 10 to 70°C, and in some cases -30 to 230°C. Over the range -30 to +70°C for MX_2-TC solutions containing little or no SO_2 and low salt concentrations, the conductivity increases in the order Ca > Ba > Sr. At low temperature and high SO_2 and MX_2 concentrations the conductivity increases in the order Ca > Sr > Ba. In CaX_2 [2] and SrX_2 solutions the conductivity increases monotonously with SO_2 concentrations (Figs.5-8). In most cases, the conductivity temperature plot has a peak near room temperature [2] whose location depends on SO_2 and MX_2 concentrations. This means that at higher temperatures the conductivity decreases with temperature. In BaX_2 solutions the effect of SO_2 is more complex (Figs.9,10). Increasing the concentration of SO_2 to 50% (V) results in an increase in conductivity of up to a factor of 8. The density and viscosity of these solutions increase in the order Ba < Sr ~ Ca. It is of interest to note that increasing the concentration of SO_2 to 10% (V) increases the density of 0.8 - 1.3M MX_2 solutions but does not significantly alter their viscosity. However, raising the concentration of SO_2 to more than 20% (V) results in a decrease of both viscosity and

density. The equivalent conductivity (Eq.1) corrected for the change in the viscosity of MX_2-TC-SO_2 solutions can be as high as 100 Ω^{-1} cm^2eq^{-1} (Figs.17-19). The apparent energy of activation for viscosity can be found in Table 1.

Raman spectra measurements, taken at room temperature (Figs.11-14 and 4) indicated the formation of a complex between SO_2 and M^{++}. The $M(SO_2)^{++}$ peak height increases with SO_2 concentration. It seems that for SrX_2 the maximum value of n is three (Fig.15). A smaller n value is estimated for BaX_2 solutions. Our results can be interpreted as follows. The ionic migration in MX_2-TC-SO_2 solutions takes place by two parallel mechanisms, a Stokesian and a non-Stokesian relay-type mechanism. The apparent negative energy of activation for conduction at high temperatures results from the breaking of ionic aggregates and shifting from solvent-separated ionic aggregates to intimate ionic aggregates (Fig.16). This should reduce the dissociation constants of the uncharged ionic aggregates (Eq.1), and in addition, it should shorten the hopping range. The enhancement of conductivity by SO_2 at low concentration is predominantly due to the formation of a larger SO_2-M^{++} complex ion (or aggregate of such ions) and at high concentration is due to the decrease in the viscosity of the electrolytes.

References

1. A. Meitav and E. Peled. J. Electrochem. Soc. 129, 451 (1982).
2. E. Peled, Proceedings of the 32nd Power Sources Symposium, Cherry Hill, N.J. P.445 1986.
3. E. Peled in "Lithium Batteries" J.P. Gabano Ed. AP 1983.
4. E. Elster, R. Cohen, M. Brand, Y. Lavi and E. Peled. J. Electrochem Soc. Submitted for publication.
5. E. Elster, R. Cohen, M. Brand, Y. Lavi and E. Peled. Proceedings of the 172nd Electrochemical Soc. Meeting, Honolulu 1987.
6. R.M. Fuoss and F. Accascima "Electrolytic Conductance" Interscience, New York (1959).

TABLE 1

APPARENT ENERGY OF ACTIVATION FOR VISCOSITY ($X = AlCl_4$)

SOLUTION	Ea kcal/mol
1.2M CaX_2, 0-30% SO_2	4.6
1.3M SrX_2, 0-30% SO_2	5.4
1.3M BaX_2, 0-30% SO_2	3.2
1 M CaX_2, 0-30% SO_2	3.8
0.84M SrX_2, 0-30% SO_2	2.7
0.84M BaX_2, 0-30% SO_2	3.0

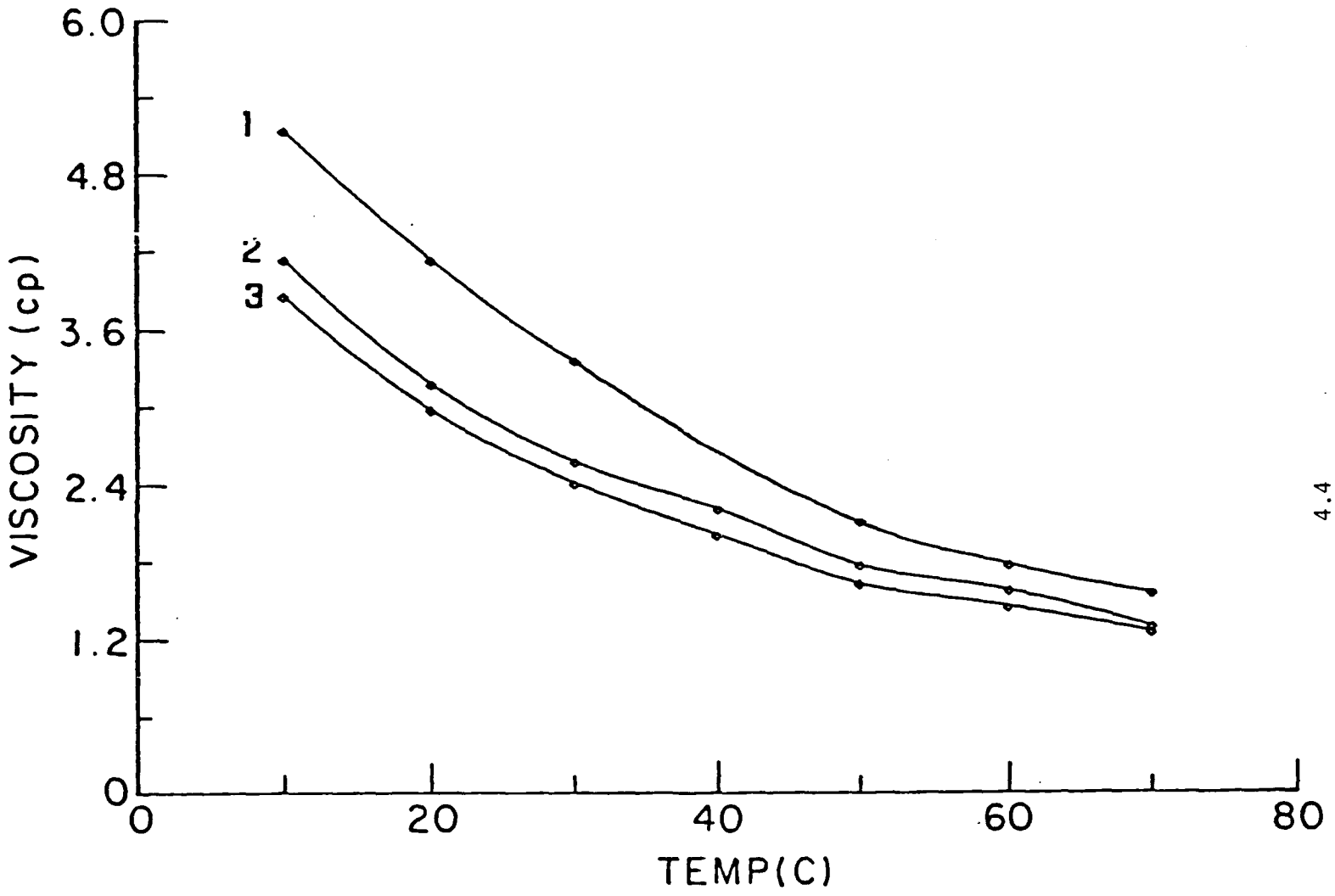

4.4

Fig. 1 . Viscosity of 1M CaX_2-TC-SO_2 solutions vs temperature.

SO_2 volume percent: 1-0; 2-20; 3-30.

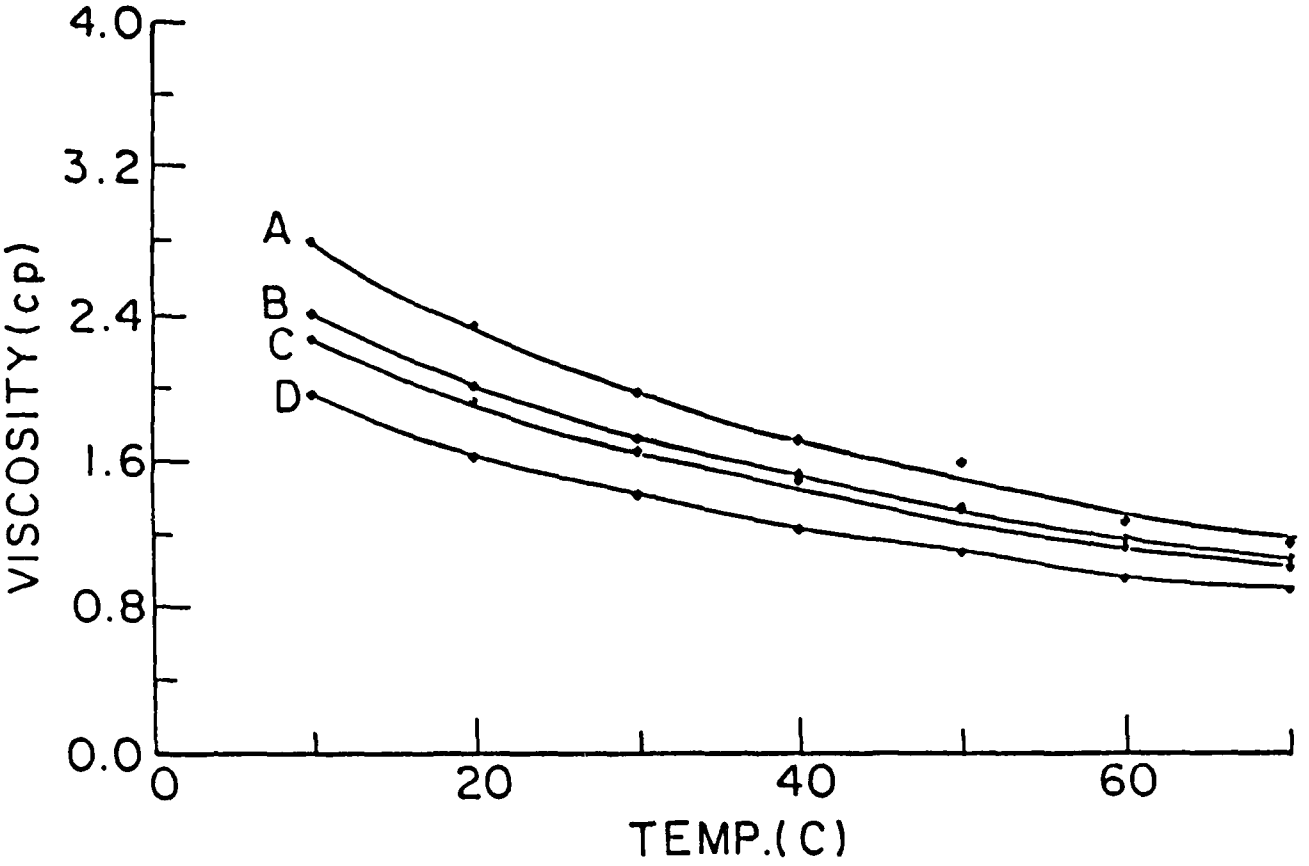

Fig. 2. Viscosity of 0.84M BaX_2-TC-SO_2 solutions vs temperature. SO_2 volume percent: A-0; B-10; C-20; D-30.

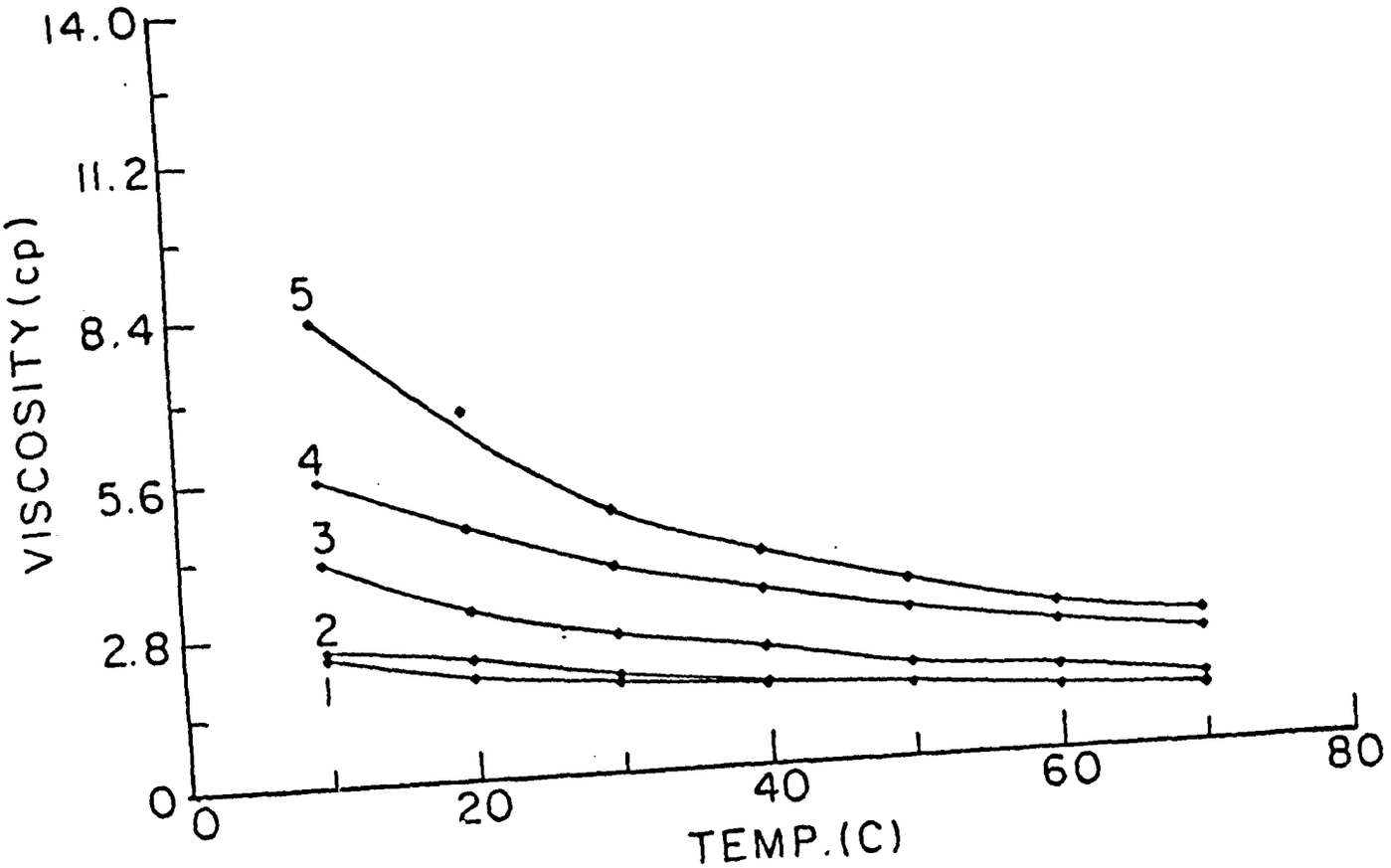

Fig. 3. Viscosity of MX_2-TC+20% SO_2 (v/v) solutions vs temperature.
1-0.84M BaX_2; 2-0.84M SrX_2; 3-1M CaX_2;
4-1.3M BaX_2; 5-1.3M SrX_2.

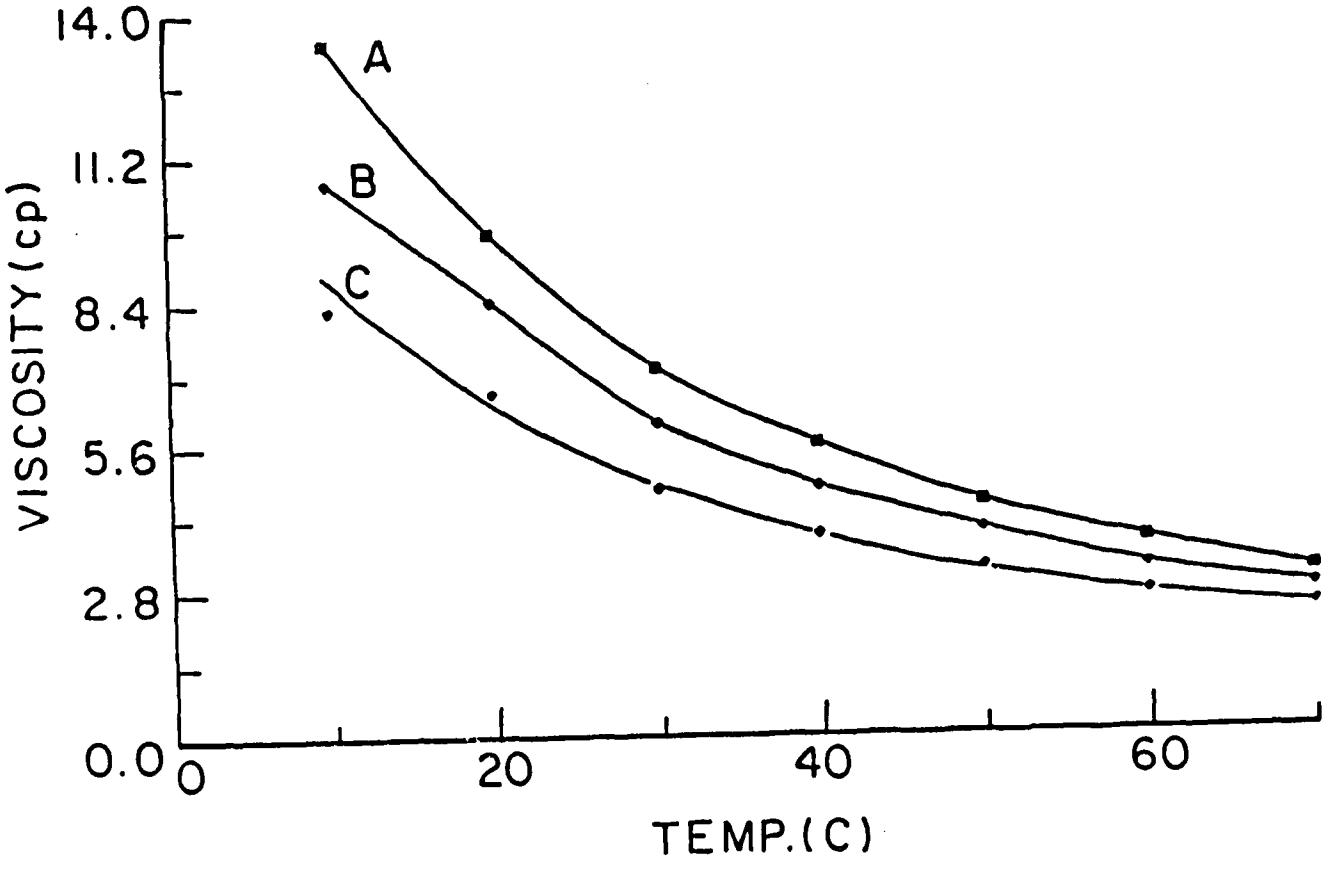

Fig. 4. Viscosity of 1.3M SrX_2-TC-SO_2 solutions vs temperature. SO_2 volume percent: A-0; B-10; C-20.

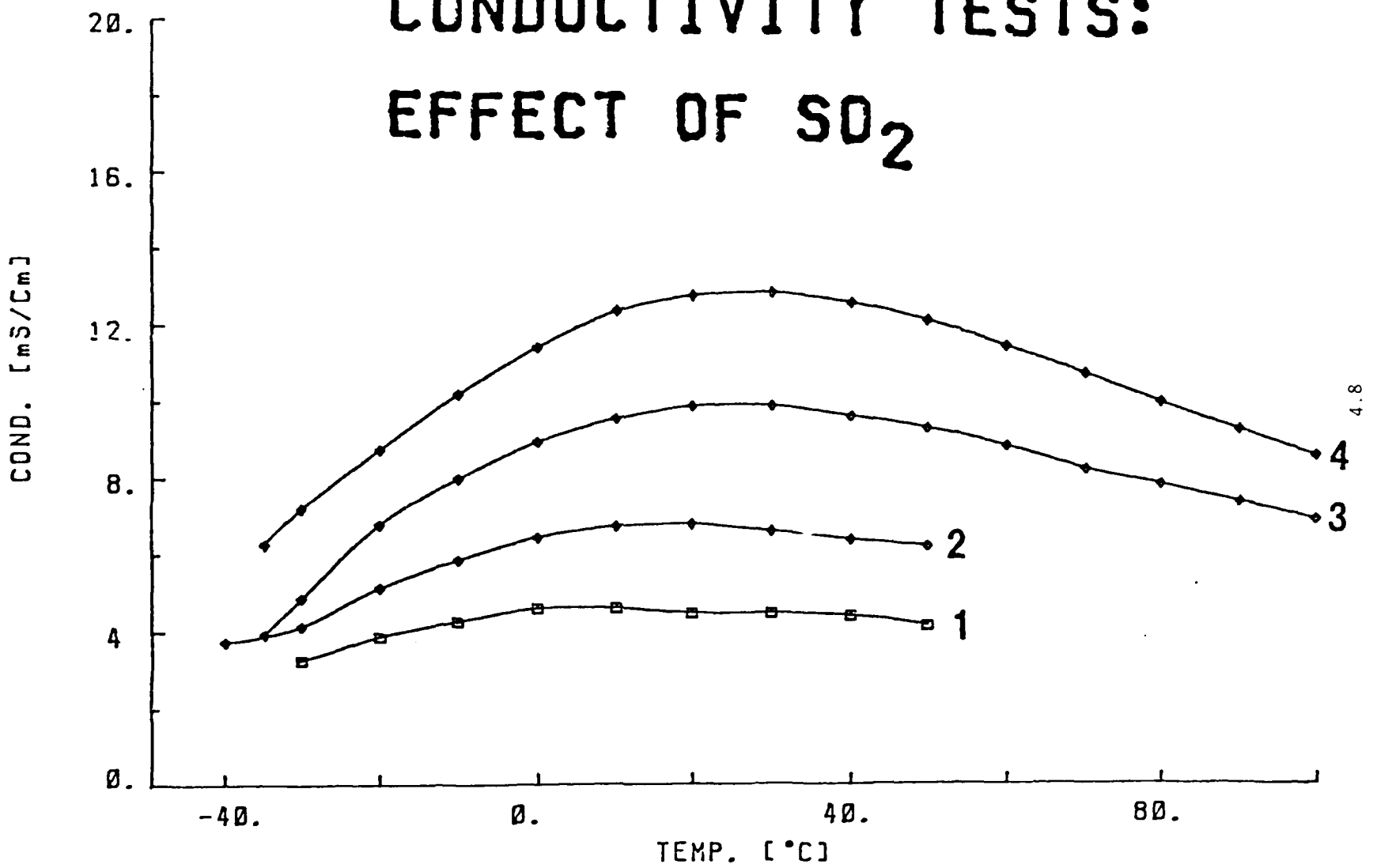

Fig. 5. The effect of SO_2, and temperature on the conductivity of 0.7M $Ca(AlCl_4)_2$-TC solution.
1-0%; 2-10%; 3-20%; 4-30% (V/V) SO_2.

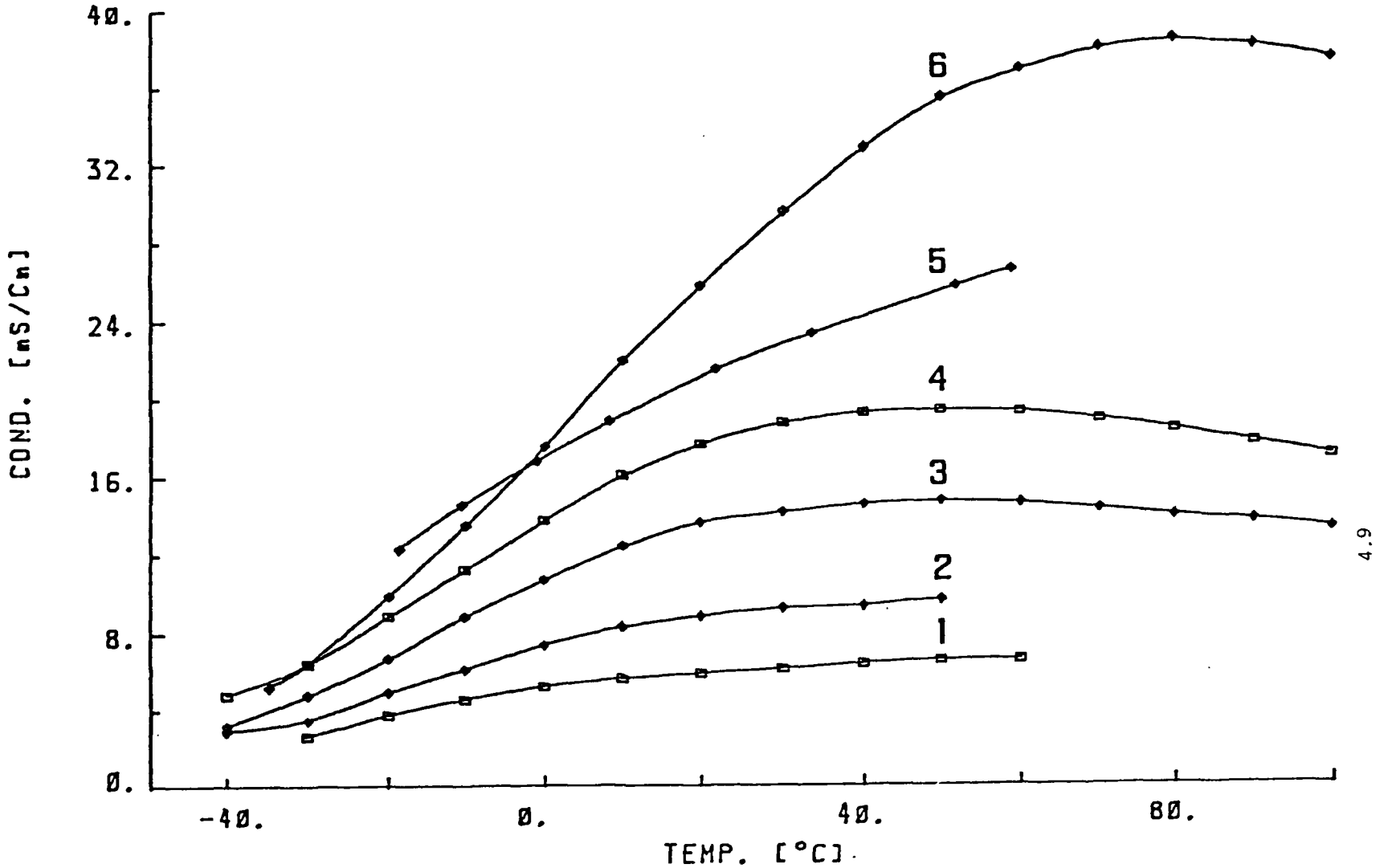

Fig. 6. The effect of SO_2, and temperature on the conductivity of 1M $Ca(AlCl_4)_2$-TC solution.
1-0%; 2-10%; 3-20%; 4-30% (V/V) SO_2;
5-1.8M $LiAlCl_4$-TC, 0% SO_2;
6-1.3M $Ca(AlCl_4)_2$, 50% SO_2.

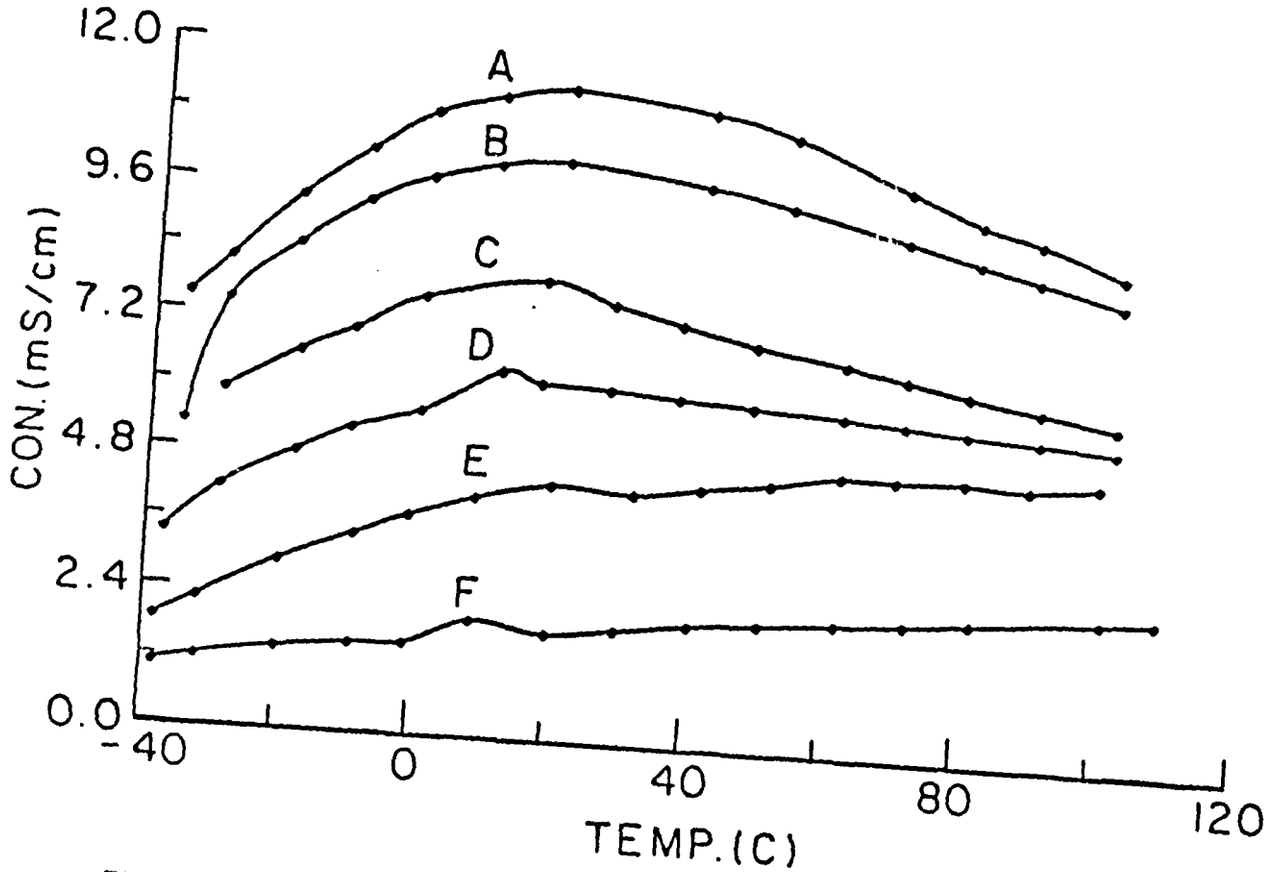

Fig. 7. Conductivity of 0.84M SrX_2-TC-SO_2 solutions vs temperature. SO_2 volume percent: A-50; B-40; C-30; D-20; E-10; F-0.

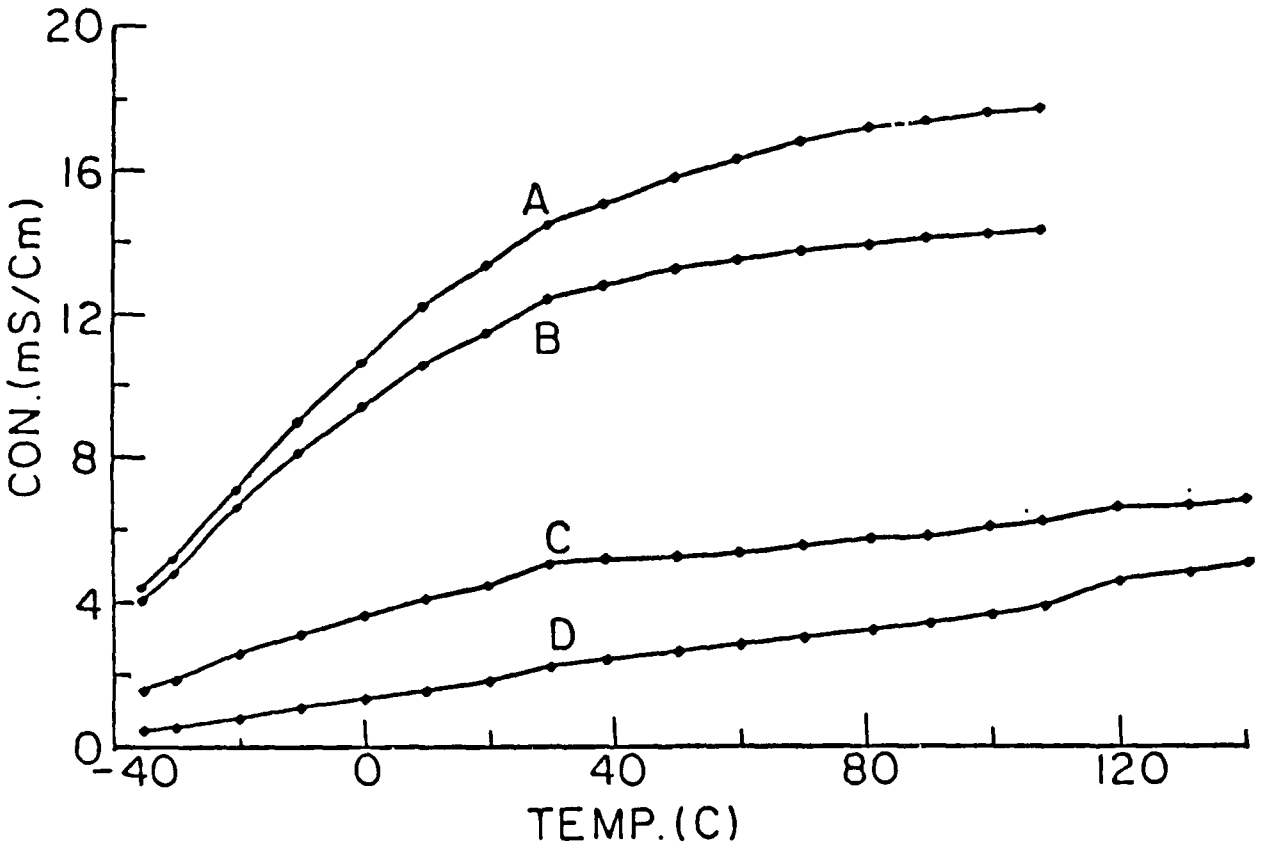

Fig. 8. Conductivity of 1.3M SrX_2-TC-SO_2 solutions vs temperature. SO_2 volume percent: A-30; B-20; C-10; D-0.

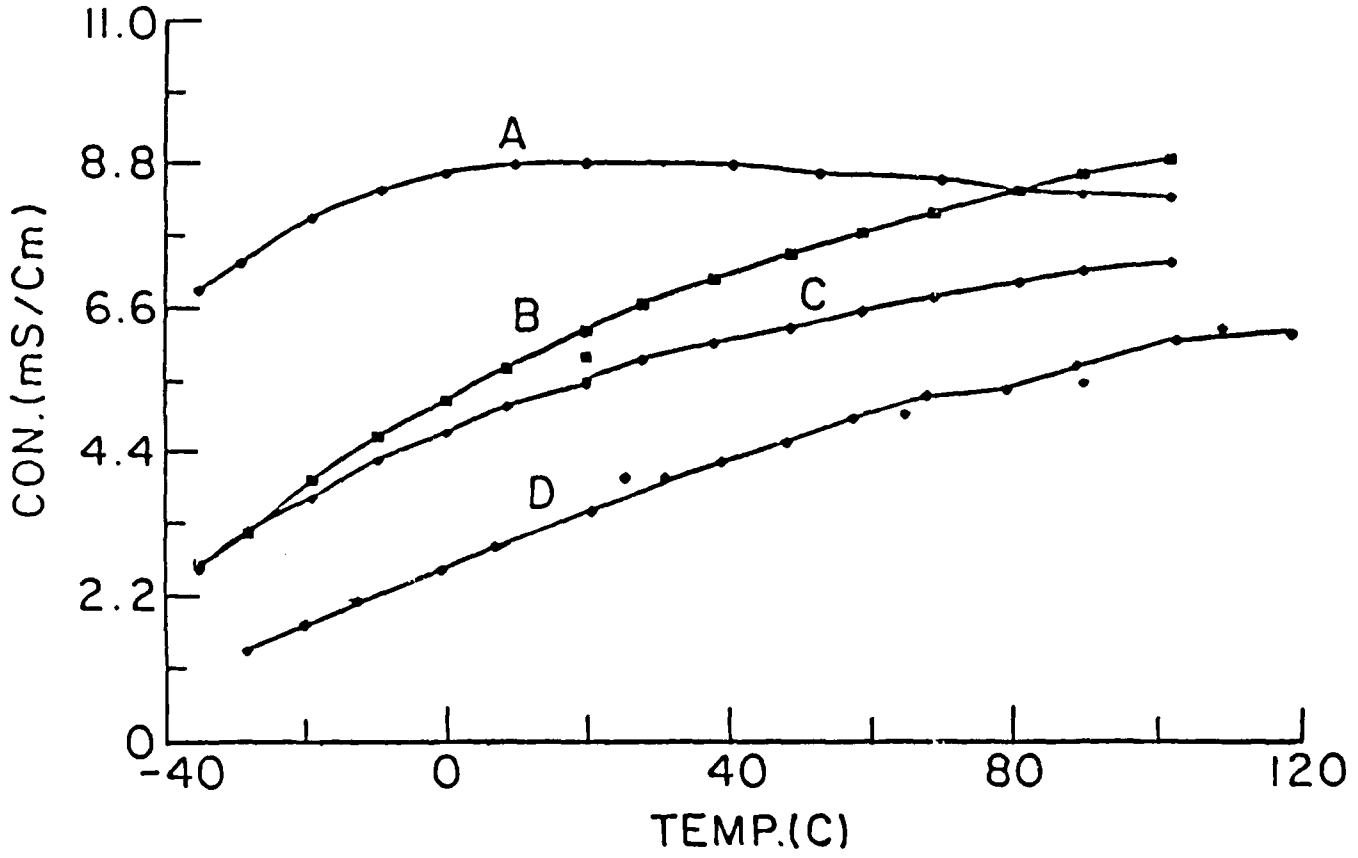

Fig. 9. Conductivity of 0.84M BaX_2-TC-SO_2 solutions vs temperature. SO_2 volume percent: A-40; B-20; C-10; D-0.

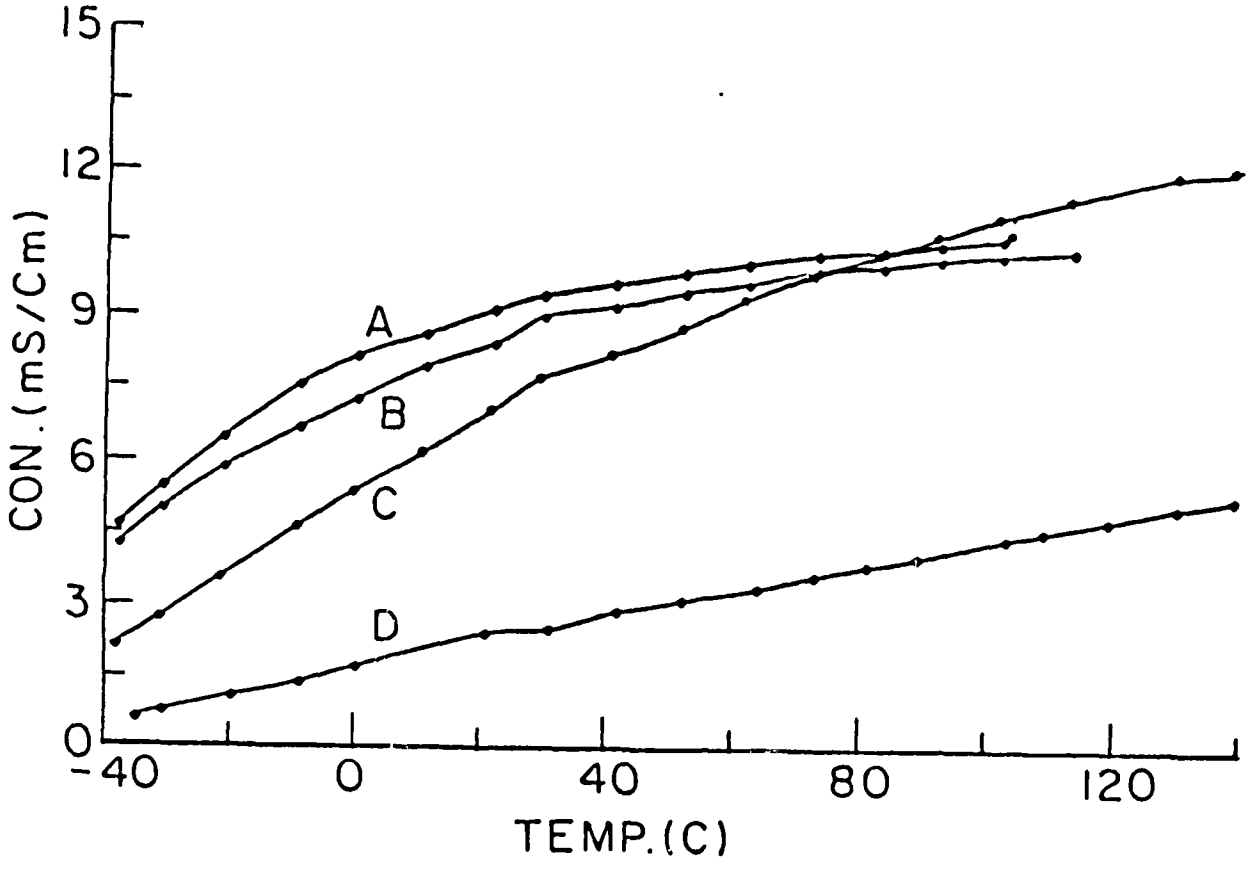

Fig. 10. Conductivity of 1.3M BaX_2-TC-SO_2 solutions vs temperature. SO_2 volume percent: A-30; B-20; C-10; D-0.

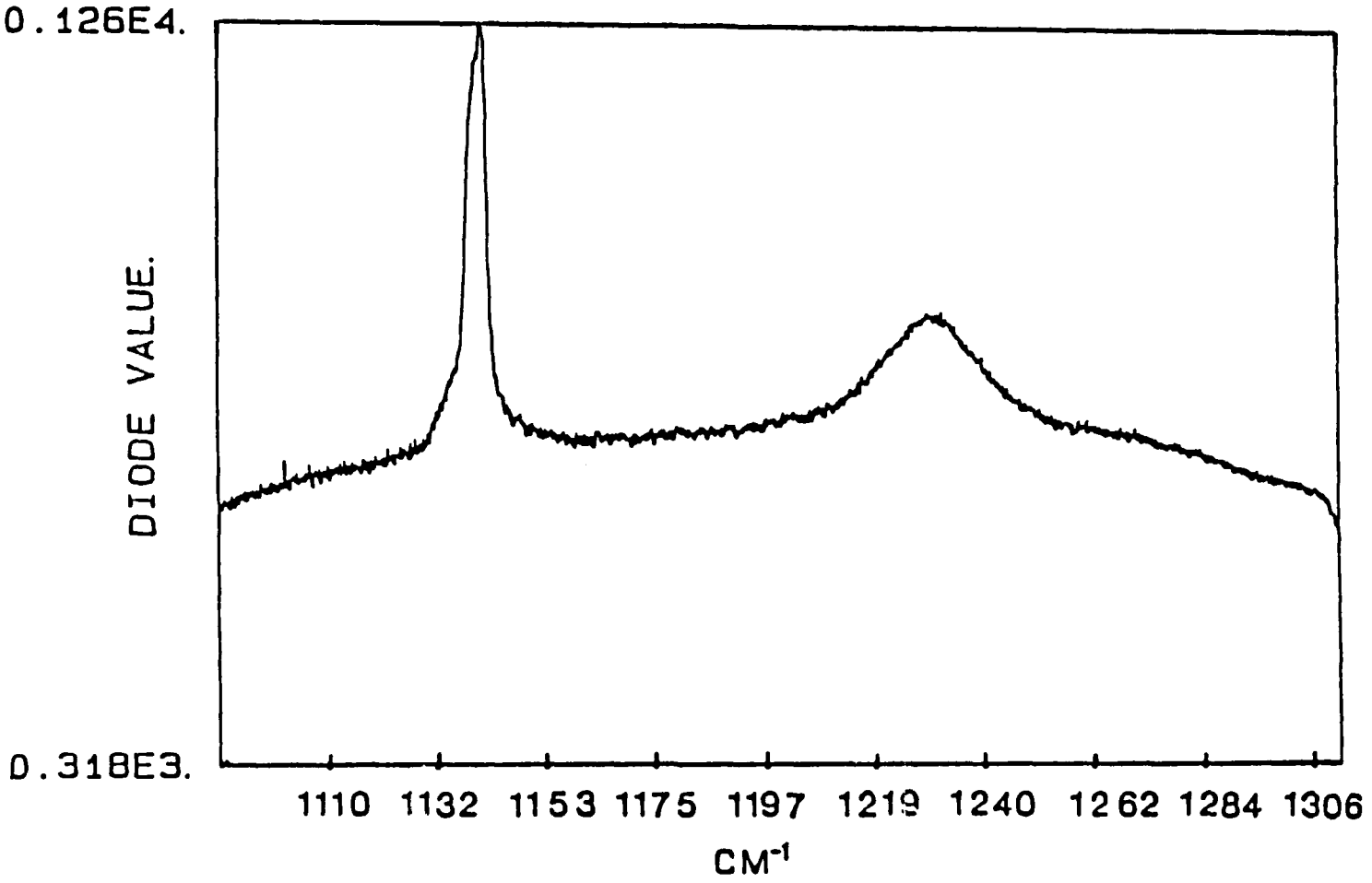

Fig. 11. Raman spectrum of TC-30% (v/v) SO_2. The peak at 1140 cm^{-1} is assigned to SO_2 and that at 1130 to TC.

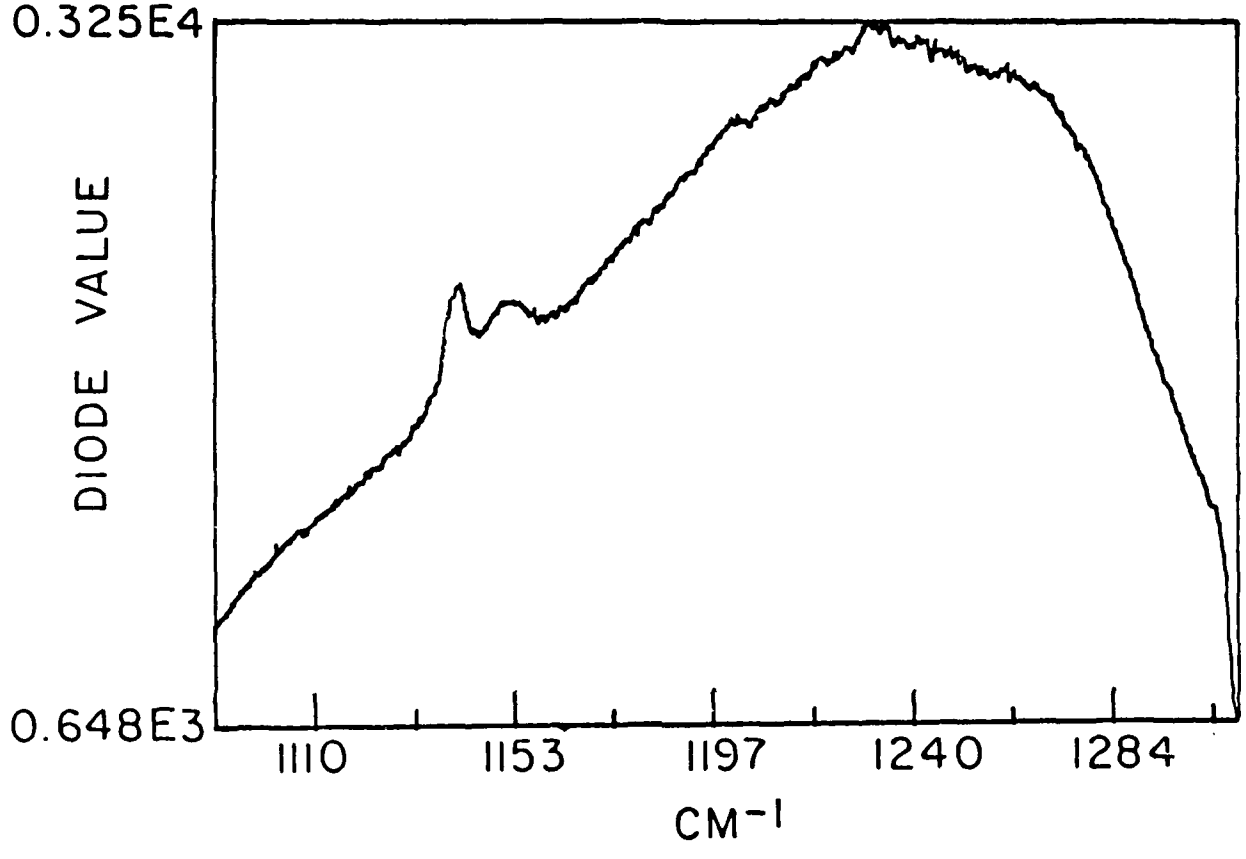

Fig. 12 . Raman spectrum of 1.3M CaX_2-TC 50% (v/v) SO_2 solution.

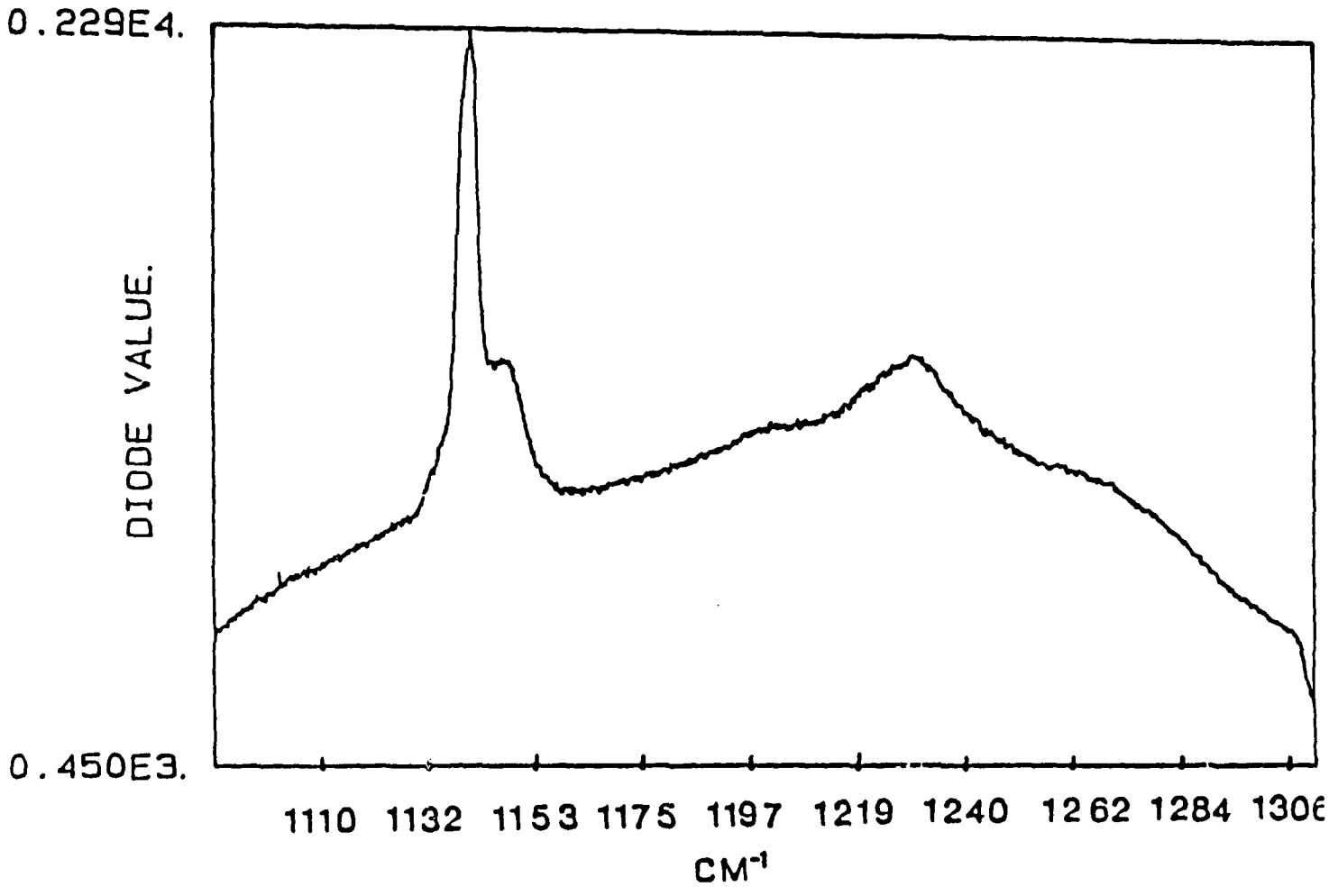

Fig. 13 . Raman spectrum of 0.84M SrX_2-TC 30% (v/v) SO_2 solution.

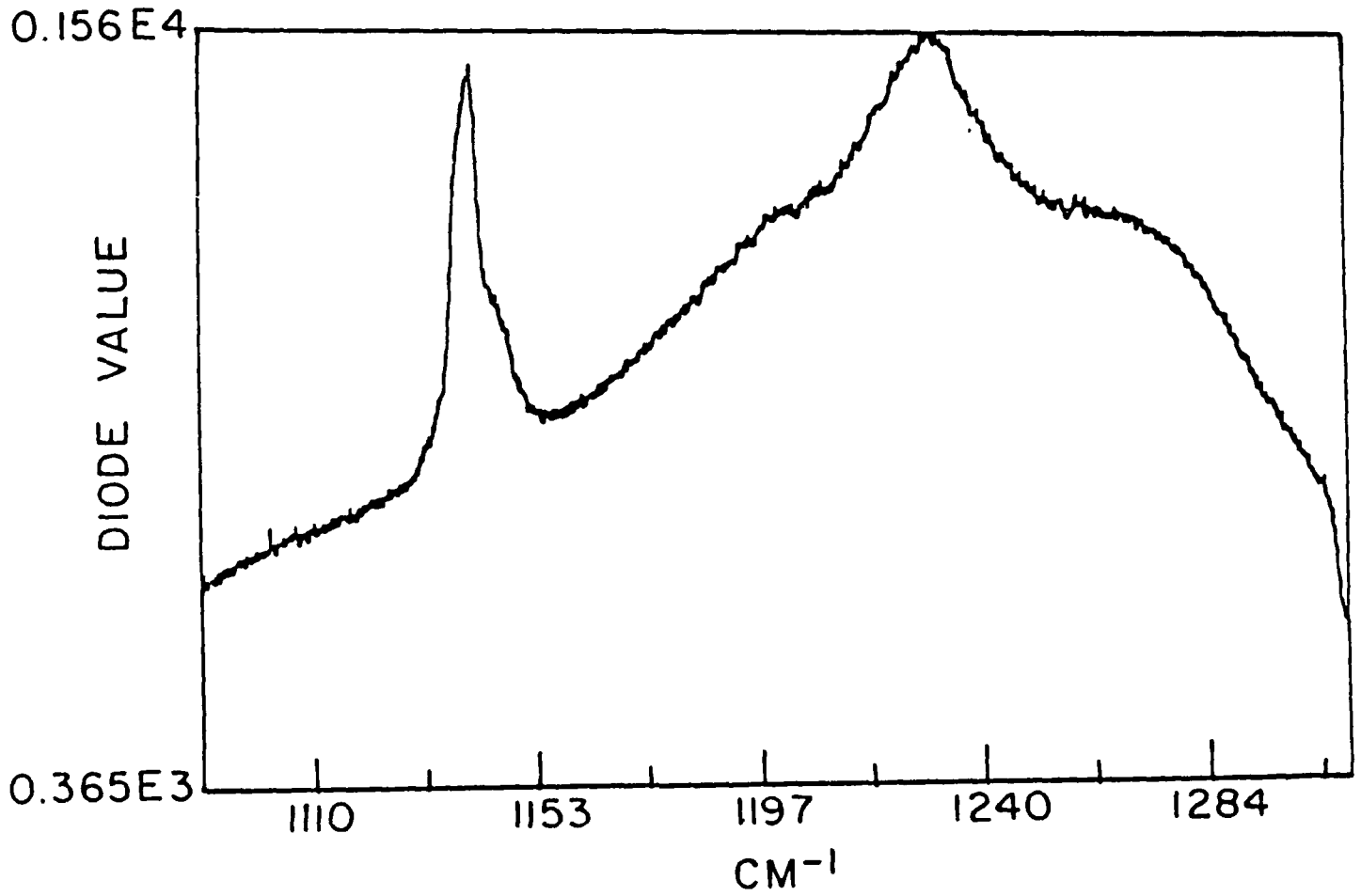

Fig. 14. Raman spectrum of 0.84M BaX_2-TC 30% (v/v) SO_2 solution.

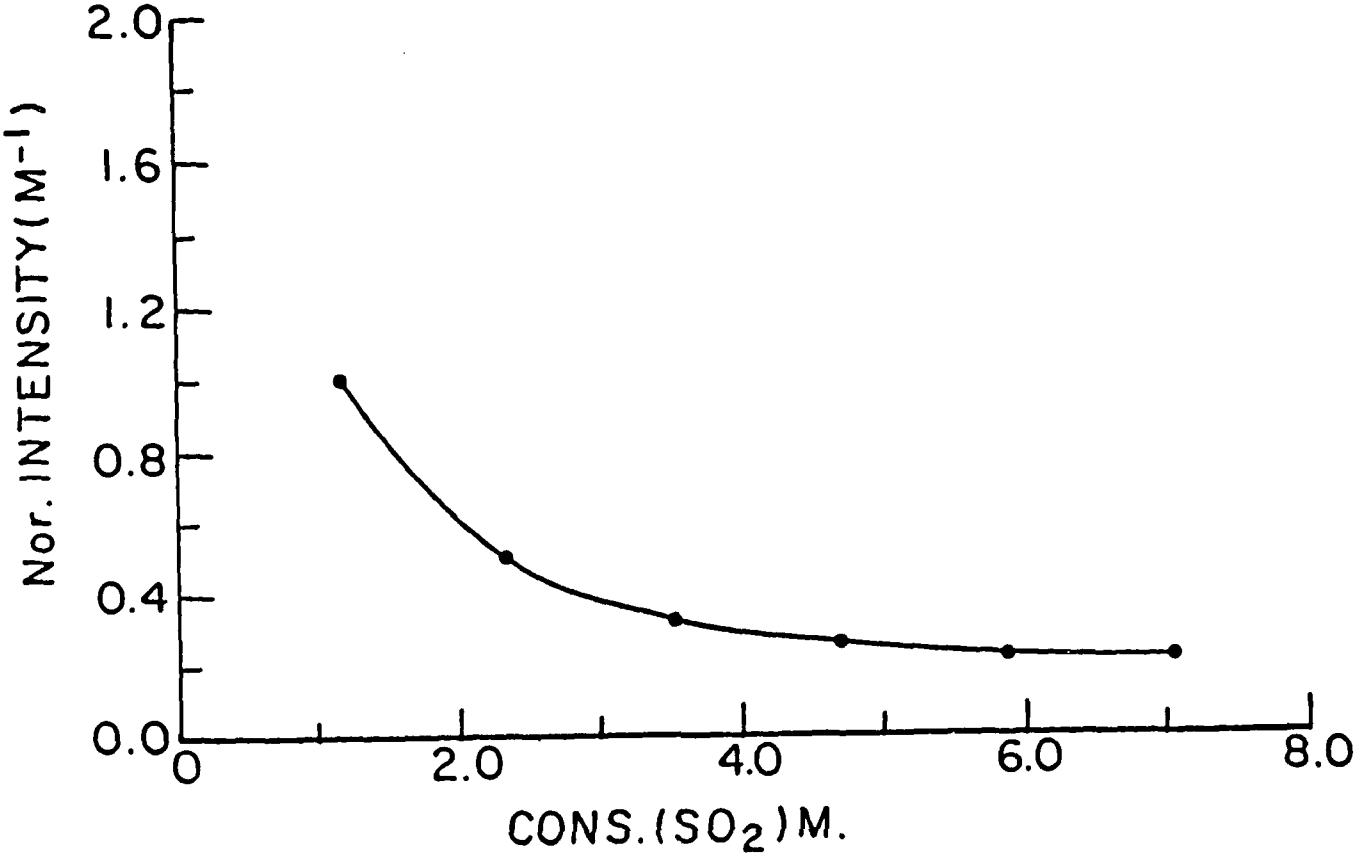

Fig.15. A plot of normalized intensity of the free SO_2 peak divided by the intensity of the bonded SO_2 peak vs SO_2 concentration.

$$\text{Nor.I} = \frac{\text{I (free } SO_2)}{[SO_2] \times \text{I(bonded } SO_2)}$$

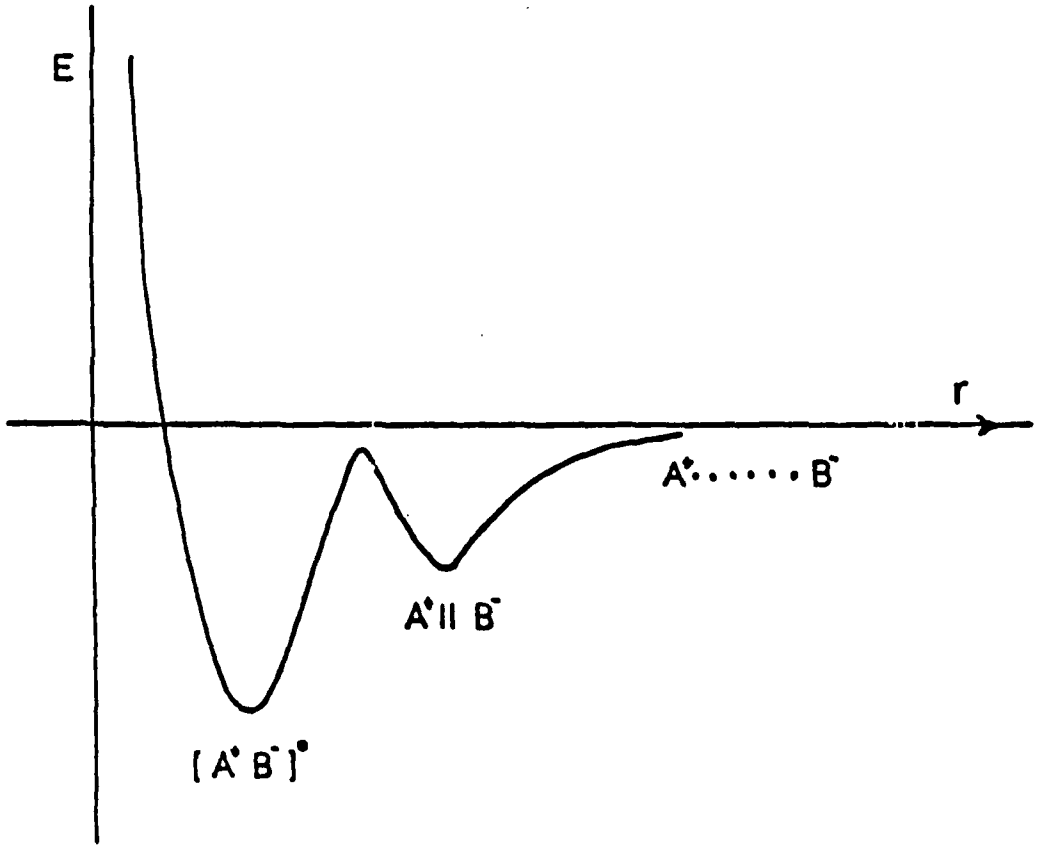

Fig. 16

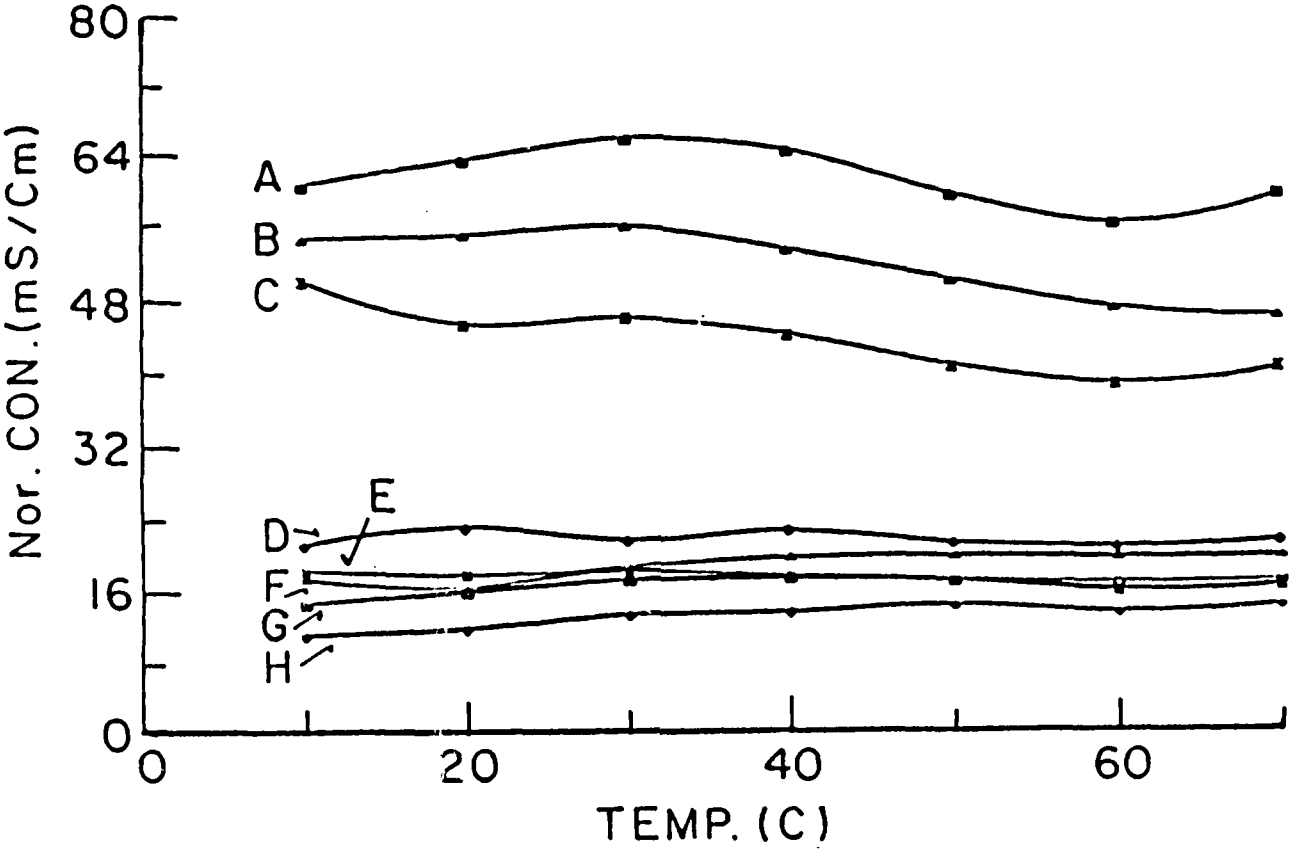

Fig. 17. Normalized conductivity of BaX_2-TC-SO_2 solutions vs temperature.

A to D 1.3M BaX_2, SO_2 percent: A-30; B-20; C-10; D-0.

E to H 0.84M BaX_2, SO_2 volume percent E-30; F-20; G-10; H-0.

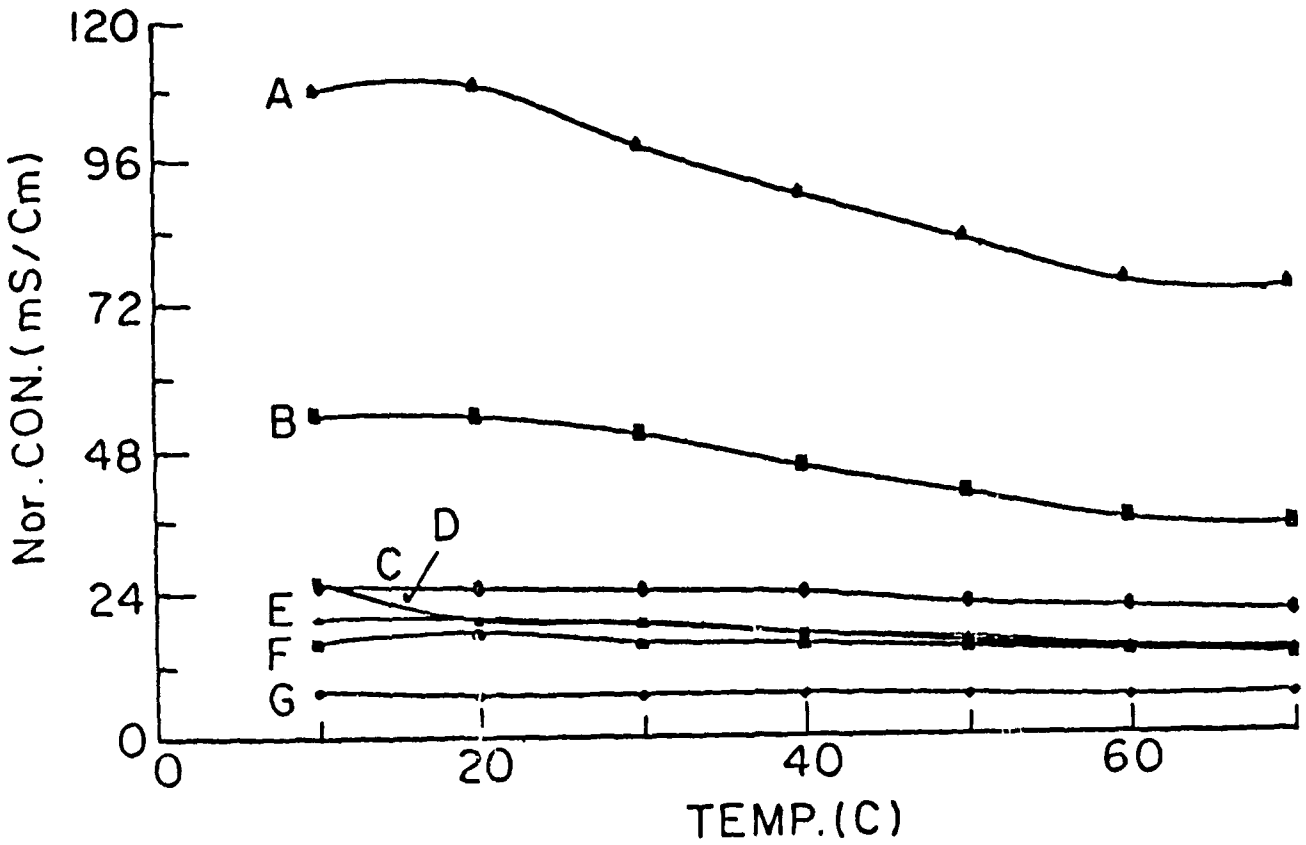

Fig. 18. Normalized conductivity of SrX_2-TC-SO_2 solutions vs temperature.

A to C 1.3M SrX_2, SO_2 volume percent: A-20; B-10; C-0.

D to G 0.84M SrX_2, SO_2 volume percent D-30; E-20; F-10; G-0.

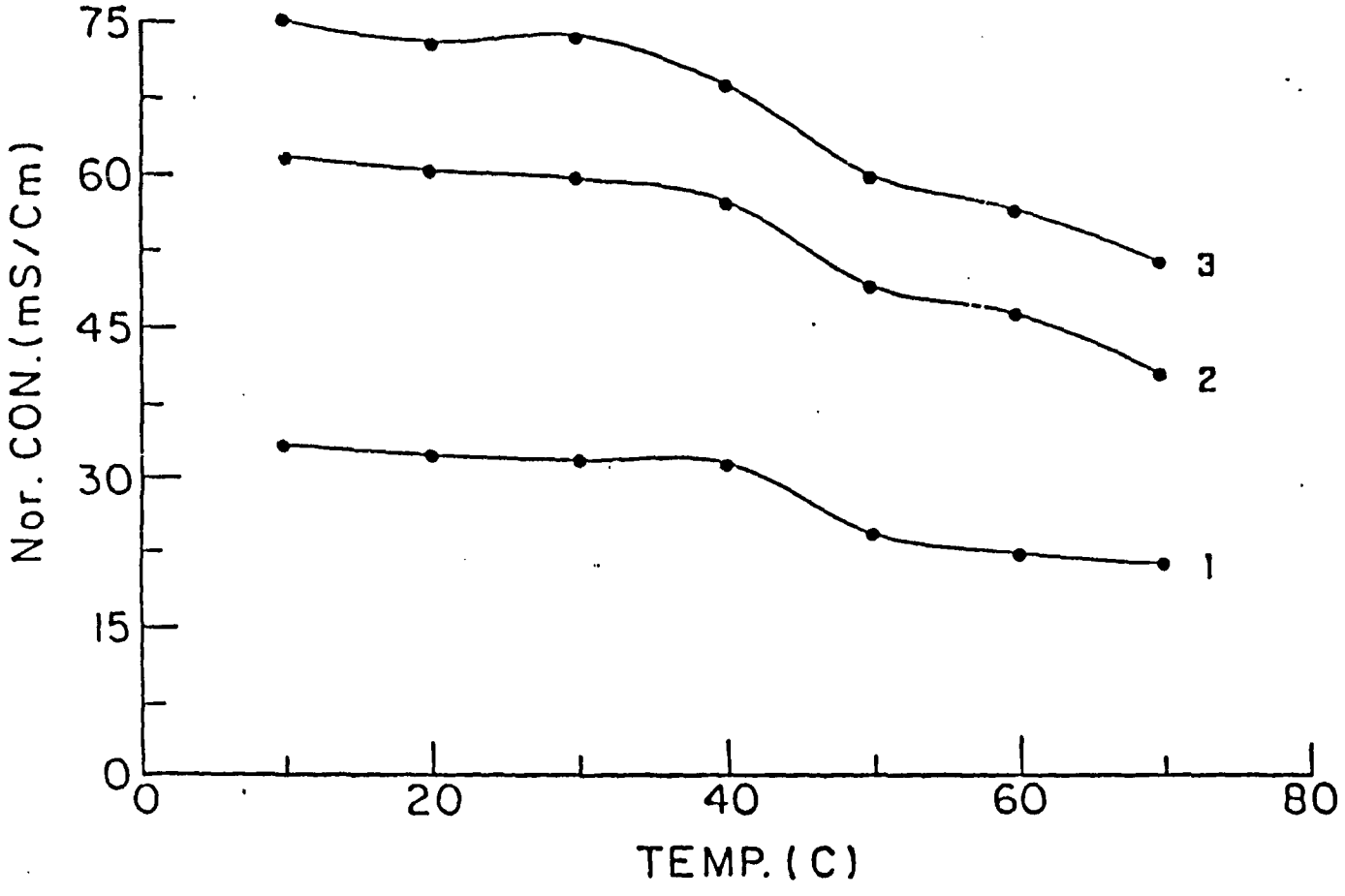

Fig. 19. Normalized conductivity of 1M CaX_2-TC-SO_2 solutions vs temperature. SO_2 volume percent: 1-0; 2-20; 3-30.

END

FILMED

6-89

DTIC